Design and Analysis of Switched Mode Power Converters for Renewable Based Telecom Supply

Submitted in

fulfillment of the requirements for the degree of

Doctor of Philosophy

by

Rajvir Kaur

ID: 2015REE9006

Under the Supervision of

Dr. Vijayakumar K.

DEPARTMENT OF ELECTRICAL ENGINEERING
MALAVIYA NATIONAL INSTITUTE OF TECHNOLOGY JAIPUR

December 2018

Declaration

I, **Rajvir Kaur**, declare that this dissertation titled, **"Design and analysis of switched mode power converters for renewable based telecom supply"** and the work presented in it, are my own. I confirm that:

- This work was done wholly or mainly while in candidature for a research degree at this university.
- Where any part of this thesis has previously been submitted for a degree or any other qualification at this university or any other institution, this has been clearly stated.
- Where I have consulted the published work of others, this is always clearly attributed.
- Where I have quoted from the work of others, the source is always given. With the exception of such quotations, this thesis is entirely my own work.
- I have acknowledged all main sources of help.
- Where the thesis is based on work done by myself, jointly with others, I have made clear exactly what was done by others and what I have contributed myself.

Place: Jaipur
Date:

Rajvir Kaur
(2015REE9006)

Certificate

This is to certify that the thesis entitled **"Design and analysis of switched mode power converters for renewable based telecom supply"** being submitted by **Rajvir Kaur (2015REE9006)** is a bonafide research work carried out under my supervision and guidance in fulfillment of the requirement for the award of the degree of **Doctor of Philosophy** in the Department of Electrical Engineering, Malaviya National Institute of Technology, Jaipur, India. The matter embodied in this thesis is original and has not been submitted to any other University or Institute for the award of any other degree.

Place: Jaipur
Date:

Dr. Vijayakumar K.
Assistant Professor
Department of Electrical Engineering
MNIT Jaipur

Acknowledgements

I take this opportunity to express my sincere and heartfelt gratitude to my research supervisor Dr. Vijayakumar K., Assistant Professor, Department of Electrical Engineering (EE), Malaviya National Institute of Technology (MNIT) Jaipur, for his constant guidance, regular interaction throughout my research work.

I extend my sincere thanks to the Director, MNIT, for offering all facilities for carrying out the research work. I express my sincere thanks to Prof. Rajesh Kumar, Professor and Head, EE, MNIT, for providing the facilities in the department throughout tenure of my research work.

I am grateful to Doctoral committee members, Prof. R.A. Gupta, Professor in EE, MNIT, Prof. H.P. Tiwari, Professor in EE, MNIT and Dr. Nitin Gupta, Assistant Professor in EE, MNIT for providing beneficial discussion to pursue this work.

I express my deep sense of gratitude to Dr. S. Neeli, Assistant Professor in EE, MNIT and Dr. C. Periasamy Assistant Professor, Department of Electronics and Communication, MNIT for their valuable suggestions towards this research work.

My sincere thanks are due to Dr. Nandha kumar Kandasamy, Senior Postdoctoral Fellow, iTrust Centre for Research in Cyber Security, Singapore University of Technology and Design, Singapore, who made valuable comments for the improvement of this research work.

I acknowledge my indebtedness to the fellow research scholars Mr. Saurabh Kumar, Mr. Soumyadeep Ray and other scholars of EE, MNIT. I acknowledge the support extended by M.Tech. students Mr. Ashok Bhupathi Kumar M., and Ms Khushboo Shah for their support during experimental work.

I owe my utmost gratitude to my parents, and friends for their encouragement and prayers to achieve this glorious mark. I further extend my thanks to those who have helped me in one or other way for carrying out this research work successfully.

Rajvir Kaur

Abstract

Telecommunication (telecom) plays a significant role in the socio-economic development of the nation. The telecom operators are bound to provide quality network services to subscribers, which require uninterrupted and reliable power supply to the base station (BS) of telecom towers. Conventionally, telecom operators have installed diesel generator (DGset) with battery banks at the BS site to ensure reliable operation during grid non-availability. The operation of DGset causes carbon emissions and increases the operating cost of BS. Accelerating growth of the telecom industry requires development of additional telecom towers to expand its network coverage to remote/rural areas. Thus, the share of telecom towers in poorly electrified remote/rural areas will increase which would result in more DGset powered BS.

Firstly, the issues with the conventional DGset power supply are studied in this thesis. The state of art is carried out for power supply topologies with different alternative resources to have continuous, uninterrupted, reliable, economical and environment friendly telecom power supply. This thesis is a step towards green telecom tower by eliminating the DGset from telecom power supply. In this context, the fuel cell based telecom tower power supply for remote/rural has been proposed to eliminate the operation of DGset. However, the challenge in integrating fuel cell to the telecom tower supply is that the resource has variable output voltage as function of environmental conditions and the load. On the other end, BS has the requirement of tight voltage regulation for reliable operation. Therefore, boost converter based intelligent interfacing unit has been proposed in conjunction with the fuel cell in order to achieve the required voltage profile. The efficient power conversion from fuel cell for telecom power supply could only be achieved if the dynamic behavior of the interfacing converter is properly tuned under varying load and source disturbances. Hence, intelligent hybrid controller having the best characteristics of linear and non-linear controller is proposed. Similar to linear controller, the proposed controller has simple structure, constant switching frequency, and easy implementation at low cost. The model free design procedure considering uncertainties of the system and robust response for a broad range of operation are inherited from intelligent controller. Modified adaptive real-value

coded genetic algorithm has been proposed to enhance the performance of the controller. The extensive analysis and simulation has been carried out to validate the performance of the intelligent hybrid controller for fuel cell based power supply to telecom towers.

Though, fuel cell based supply is environment-friendly but doesn't fulfill all the prerequisites of the BS power supply. The fuel cell has large time constant in order of minutes so, can't perform satisfactorily for fluctuating loads. Therefore, renewable based BS power supply topology is proposed. Integration of renewable resources to the DC bus also need interfacing unit. Thus, selection of switched mode power converter (SMPC) for the integration of renewable resources to the DC bus is discussed. Cuk converter is implemented for integration of renewable resources to DC bus due to its the wide range of operation, compactness and ripple free input and output current. The intelligent hybrid controller is implemented with Cuk converter based interfacing unit to enhance the dynamic response under load and source side disturbances. Further, the objective function to evaluate the fitness of the solution candidate in the optimization process is improved by considering the dynamic specification parameters (maximum overshooot, settling time and rise time) along with integral time absolute error (ITAE). Performance analysis of the Cuk converter with intelligent hybrid controller is validated by developing a laboratory prototype.

In hybrid renewable energy system (HRES), if renewable resources and battery bank are oversized; it will result in higher initial investment and underutilization of the resources. On the other hand, the undersized system would result in an energy deficit and less reliable system. Consequently, the quality of network and services to the subscribers degrade. Therefore, to have economical, practically viable, reliable and environment friendly alternative to the existing DGset based power supply, the proposed HRES supply should be an optimal mix of the renewable resources and storage. The optimal sizing problem is formulated for the minimization of cost of electricity (COE) along with loss of power supply probability (LPSP) and excess energy (EE). However, the nature of the objective functions (LPSP, COE, and EE) are contradictory in nature because, enhancement of reliability will result in an increase in excess energy that would increase the cost. Therefore, a multi-objective algorithm called as non-dominated sorting

genetic algorithm II (NSGA-II) is implemented to achieve a trade-off among the objectives.

Further, the uncertainties in wind speed and solar irradiation are incorporated using Weibull and Beta PDFs. Unlike, previous approaches which approximates capacity of wind turbine as continuous variable, the proposed approach considers the commercially available sizes of wind turbines which are discrete in nature. Hence, the continuous variable based optimization leads to a suboptimal solution, therefore, discrete multi-objective grey wolf optimization (DMGWO) is proposed. DMGWO utilizes the concept of the external archive to store the non dominated sorted solutions which enhances the convergence rate. The leader selection mechanism of DMGWO prevents premature termination of the algorithm. Further, a corrective algorithm is embedded in DMGWO to handle the discrete variable (capacity of wind turbine). The DMGWO finds the optimal energy mix of the proposed HRES by minimizing the three objective viz. LPSP, LCOE and excess energy.

Energy management of HRES supplied remote/rural telecom towers is proposed in this thesis to ensure high energy efficiency, reduced operational expenditure and enhanced reliability. Demand response management (DRM) concept is implemented by modelling the air conditioners as analogous to batteries to create virtual energy storage (VES). Similar to batteries, the VES also buffers the intermittency in the solar energy and enhances the reliability. The modelling of air conditioner does consider the cyclic turn on and off patterns along with the stochastic nature of the HRES. The VES based DRM enhances the life of battery energy storage (BESS) without installation of additional equipments to save energy in air conditioners.

Key words: Energy management, hybrid renewable energy system (HRES), intelligent hybrid controller, power converters, optimal sizing, virtual energy storage, voltage regulation.

Contents

List of Tables

List of Figures

List of Abbreviations

BB	Base band
BESS	Battery energy storage system
BS	Base station
COE	Cost of electricity
DGset	Diesel generator
DMGWO	Discrete multi-objective grey wolf optimization
DRM	Demand response management
EE	Excess energy
GA	Genetic algorithm
GSM	Global system for mobile communication
GWO	Grey wolf optimization
HRES	Hybrid renewable energy system
IC	Internal combustion
ITAE	Integral time absolute error
LCOE	Levelized cost of electricity
LPSP	Loss of power supply probability

LTE	Long-term evolution
MARCGA	Modified adaptive real coded genetic algorithm
MPPT	Maximum power point tracking
MPSO	Multi-objective particle swarm optimization
NSGA-II	Non-dominated sorting genetic algorithm II
OPEX	Operating expenditure
PA	Power amplifier
PDF	Probability distribution function
PEMFC	Proton exchange membrane fuel cell
PSO	Particle swarm optimization
PV	Photovoltaic
PW	Present worth
RF	Radio frequency
RHP	Right hand complex plane
SMPC	Switched mode power converter
Telecom	Telecommunication
TRX	Transceiver
UMTS	Universal mobile telecommunications system
VES	Virtual energy storage
VSC	Virtual storage capacity
WECS	Wind energy conversion system
ZN	Ziegler Nichols

Chapter 1

Introduction

Telecommunication (telecom) plays a significant role in the socio-economic development of the nation. Telecom fulfills the basic need of communication as well as the advanced data services. Advanced data services have brought a new dimension to the communication in areas such as multimedia communication, online gaming, and high-quality video streaming [1]. To ensure quality of service and network coverage to more than six billion subscribers worldwide, uninterrupted supply to base station (BS) are required. There are 3 billion telecom tower BS across the world, among them 3,20,100 BS are not connected to the grid (off-grid), and 7,01,000 BS do not have reliable and continuous supply (bad-grid) [2]. Thus, network services degrade in the poorly electrified remote/rural areas. Conventionally, telecom operators have installed diesel generator (DGset) with battery banks at the BS site to ensure reliable operation during grid non-availability. Consequently, telecom sector is responsible for the 2% of the total carbon emission contributing 3% of the total energy consumption across the world [3]. The accelerating growth of telecom industry demands additional infrastructure i.e. telecom towers to expand its network coverage and capacity especially in remote/rural areas. It is estimated that 15% more i.e. 1 million towers have to be installed worldwide in off-grid and bad-grid areas by 2020. Thus, by the year 2020, the share of the off-grid and bad-grid BSs will rise by 22% and 13% respectively, demanding more DGset powered BSs which would result in increase from present 170 metric tons to 235 metric tons of global carbon emission. Thirty percent of the expansion is estimated to happen

in African and Asian countries [4].

India is the second largest telecom market with 700 million subscribers. The government of India has launched Digital India campaign in July 2015 with a vision to digitally empower rural areas [5]. Implementing required infrastructure for the telecom services throughout the country especially in remote/rural areas is a prerequisite to modernize different sectors of the economy. Also, the remote/rural areas could avail government services electronically which otherwise are difficult to access or not accessible. Hence, telecom sector has to outreach the remote/rural areas aiming to achieve 100% rural teledensity. It demands the installation of 1,00,000 towers in remote/rural areas in India. The biggest barrier to the projected growth is the unavailability of adequate and reliable power supply to telecom towers. Currently, 40% of telecom towers do not receive uninterrupted and reliable power supply from the grid, and among them, 22% are off-grid towers [6]. The Fig. 1.1a gives the status of grid availability (in hours) per day in different states of India. The telecom towers could be classified on the basis of availability of grid as off-grid towers (central grid extension is not available), bad-grid towers (grid extension is available but has power outage of more than 8 hours) and on-grid towers (have reliable grid supply). The share of off-grid towers, bad-grid towers and on-grid towers as per Indian scenario is presented in Fig. 1.1b. The grid extension to power the remote/rural BS is not commercially viable option as load requirement is relatively low. Thus, telecom industry is heavily dependent on DGsets, to provide uninterrupted, reliable and quality power supply to BS.

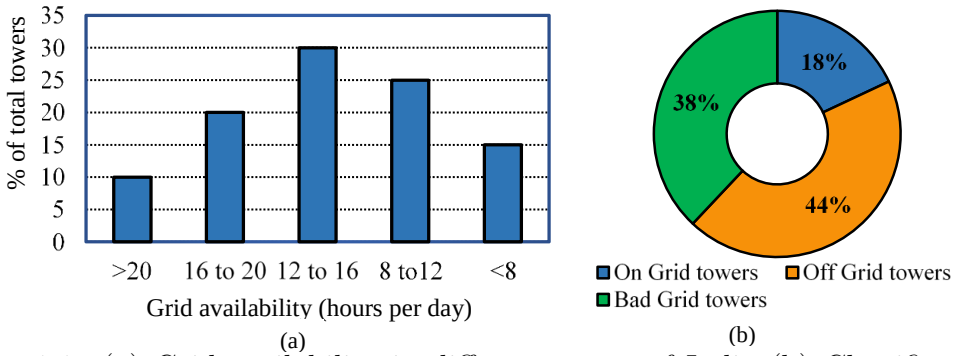

Figure 1.1: (a) Grid availability in different states of India (b) Classification of telecom towers in Indian scenario

1.1 Base station

In telecom terminology, a cell is defined geographical area with the communication/radio network coverage provided by a transceiver located at a fixed site known as base station. The geographical area forming a cell may have diameter in range of 2-50km and each has dedicated number of radio frequency channels. Generally, cellular networks consist of four types of cells which are macrocell, microcell, picocell, and femtocell which are shown in Fig. 1.2 [7]. Each cell has different diameter of network coverage provided by the antennas of corresponding corresponding strength at the BS. Thus, more the network coverage (larger the cell size), larger is the energy consumption at BS. Macro-cellular networks has largest coverage of the geographical area among all cells and typically, deployed in remote/rural areas and along the highways. The BS dedicated for the macro-cells has large power consumption and needs large footprints. The power consumption in BS corresponding to different cells is presented in table 1.1. Microcells concept is implemented in urban regions with high traffic demand. Pico-cellular networks are deployed in the residential areas. Femtocells which have short range and limited radio channels are designed for residential and small business.

Further, power consumption of BS vary with different cellular generations which are implemented so far with evolving cellular technology. Various cellular communication systems are global system for mobile communication (GSM) or second generation (2G), universal mobile telecommunications system (UMTS) or third

Table 1.1: Power consumption in different types of BS

BS Type	N_{TRX}	PA (W)	RF (W)	BB (W)	DC-DC (%)	Cooling (%)	Mains (%)	Total for N_{TRX}(W)
Macro	6	128.2	12.9	29.6	7.5	10.0	9.0	1350
Micro	2	6.3	54	2.6	39.0	0.0	9.0	144.6
Pico	2	0.13	6.8	4.0	4.3	0.0	11.0	14.7
Femto	2	1.1	0.6	2.5	9.0	0.0	11.0	10.4

generation (3G), the long-term evolution (LTE) or fourth generation (4G) and upcoming fifth generation (5G) which is expected to be more energy efficient than previous generations. Generally, a BS configuration follows the nomenclature n/n/n which denotes that a three sector site has 'n' antennas per sector. The different BS configurations such as GSM BS 2/2/2, GSM BS 4/4/4, GSM BS 6/6/6, UMTS node 2/2/2, and LTE eNode 2/2/2 has the approximate peak power requirement of 1.8kW, 2.3kW, 3.7kW, 1kW, and 965W receptively [8].

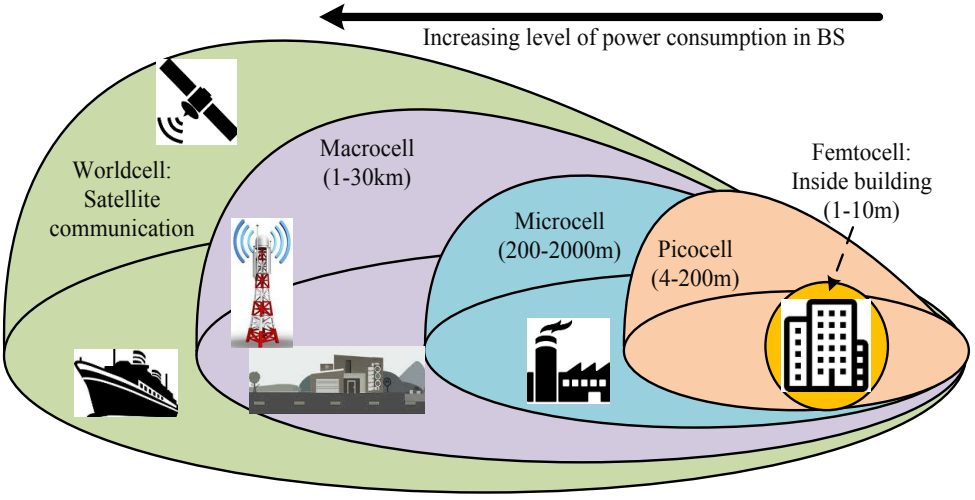

Figure 1.2: Different cellular networks

1.1.1 Conventional power supply for BS

A typical BS site consists of transceiver (TRX), power amplifier (PA), microwave/radio frequency (RF) equipment, base band (BB) processor, lighting load, heat exchanger or air conditioner. Critical load includes computer or network equipment which needs AC supply and switching equipments which needs DC supply. Since computer or network equipment can not support power outages greater than 3ms, are powered by redundant UPS with an average of 30 minutes battery backup. Switching equipment which are powered by DC power with N+1 redundant rectifiers having 2-6 hours battery reserve time. Non critical loads such as air conditioning and lighting loads can withstand short power outage. Conventionally, non critical loads are backed up by DGset.

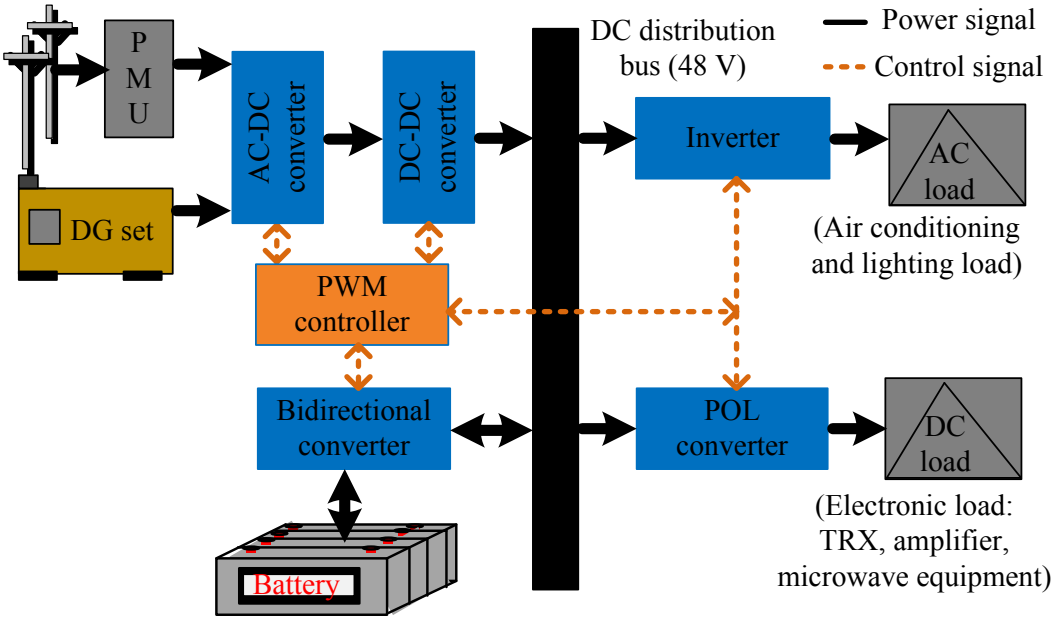

Figure 1.3: Architecture of conventional BS power supply

Generally, macrocell having a rating in the range of 1kW to 3kW, are deployed in the rural areas and along the highways. It consumes 60% of the overall energy consumption in the cellular networks. In conventional power supply architecture, BS is primarily provided by the grid with DGset and battery bank as back up as shown in Fig. 1.3. Total telecom load capacity depends on the number of the transceiver installed at the BS. Each transceiver has been rated as 160W approximately. The DC distribution bus system of 48V DC is adopted by considering the trade-off between the safety aspects and dissipation losses in the distribution system. As electronic equipment are rated for different voltage levels ranging from 3.3V to 48V therefore, the point of load converter is installed at the load end.

1.1.2 Issues in conventional BS power supply

There is an automatic switch that transfers the load between DG and the grid. The malfunction of the switch may result in the single point failure of the system [9]. Also, for the reliable start-up of DGset, two starters are operated simultaneously such that if one starter fails, the other will automatically start the system but with

extended time. The two starters preclude single failure that prevents DGset from starting [10]. Standby DGset in conventional BS supply dilutes the reliability of system as the most well maintained machines have a failure rate of 15% to start for 1% of the time when the grid fails for 24-hour missions [11]. Therefore, the requirement of battery banks with DGset for back-up is mandatory. The battery banks are the bulkiest part of the back-up supply requiring large footprint with special flooring which increases the operating expenditure (OPEX). As the lifespan of the battery is small in comparison to other equipment, it requires periodic maintenance making it the costliest part of the supply [12]. Further, routine maintenance visits of DGset, the transportation, and storage of diesel on the site along with volatile prices of diesel in the international market are adding to the OPEX of the telecom companies. Combined operation of battery and DGset increases the share of energy consumption expenditure to 70% in the overall OPEX of the telecom towers in remote/rural areas. Expansion of telecom industry to remote/rural areas will result in 10 times higher OPEX and results in increased dependency on DGset. The diesel consumption in telecom sector could be seen as 50% of Indian railways and 40% of industrial DGsets. Consequently, DGset operation is a grave threat to the environment as it causes noise and air pollution. Its operation adds to global carbon emission by producing greenhouse gas i.e. CO_2 [13]. Telecom sector has an average fuel consumption of 8760 litres diesel every year per tower considering 8 hours of operation by DGset. Carbon emission is approximately 2.68Kg/litre diesel consumption.

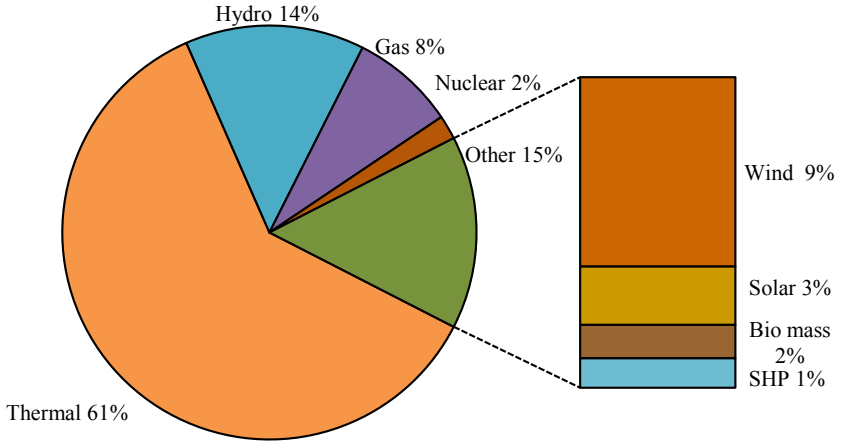

Figure 1.4: Total installed capacity of different resources in India

1.2 Challenges and research context

The conventional power supply for the remote/rural telecom towers results in increased OPEX, reliability and environmental issues. Thus, there is need for alternative resources for the BS power supply in remote/rural areas such that the cost of electricity is less, high power density, maintains DC distribution bus voltage, continuous, uninterrupted, and environment-friendly power supply to the BS.

1.2.1 Alternative resources

Different alternative resources are available to replace the DGset in the conventional power supply such as reciprocating internal combustion (IC) engine, microturbines, biomass energy, fuel cell, solar energy, and wind energy. Total installed capacity in India is 308GW and contribution of different resources is shown in Fig. 1.4 [14].

Reciprocating IC engine is a heat engine in which the intermittent combustion of fuel-oxidizer (air) takes place within the cylinder. The expansion of gases drives the piston linearly and crankshaft produces the rotating movement to rotate the shaft connecting the generator and hence, electricity is produced. Usually four stroke reciprocating IC engine is employed for electricity generation. A gas turbine is a continuous combustion heat engine which compresses the air to drive the turbine mounted on the shaft connecting the generator. Microturbines are small gas turbines for distributed generation that rotates at high-speed and acts as prime mover for an electrical generator. Microturbines are available in the range of 30-400kW. Electric power is produced as high frequency AC which is converted to high voltage DC and then inverted back to 60/50Hz, 480V AC by an inverter. Microturbine has capital and maintenance cost of \$700-\$1,100/kW and \$0.005-0.016/kW respectively. Efficiency without heat recovery is low in the range of 15-30%. However, with combined heat power application, efficiency of the overall

system is enhanced to 80%. The reciprocating IC engine (500kW), gas turbine (4.5MW), coal fired steam turbine (500MW) and microturbine (30kW) have NOx (ppm) emissions as 2100, 25, 200 and 9, CO (ppm) as 340, 50, n/a and 25, and THC(ppm) as 150, 10, n/a and 9 receptively [15].

Biomass is a dispatchable resource means controllable and available when needed, similar to fossil fuel electric generation systems. For electricity generation, woody biomass undergo direct combustion or gasification, agricultural, animal and human wastes are converted into gas in an anaerobic digester and other types of biomass is converted into bio-oil through pyrolysis. Biomass electricity systems has efficiency of approximately 20%. The disadvantage of biomass for electricity generation, is that the fuel needs to be procured, delivered, stored, and paid for. Also, biomass combustion produces emissions, which must be carefully monitored and controlled to comply with regulation.

A fuel cell is an electrochemical energy conversion device that produces electricity through chemical reaction without combustion (no undesirable emissions and noise). In fuel cell, the source fuel (hydrogen, methane or propane) are oxidized to generate electricity with water and heat as byproducts. Fuel cell combines the best features of engines and batteries: it can operate like an IC engine as long as fuel is available and it produces electricity directly from fuel.

Photovoltaic (PV) panels convert the solar energy to electricity. A 1 kW PV panel occupies 5 m^2 in area and the lifetime of is more than 25 years. The cost of PV panels is around $ 1000 for a PV panel with DC rating of 1 kW. The PV panel is array of PV cells connected in series and parallel combination. The PV panels are classified as mono-crystalline, poly-crystalline, thin film and hybrid PV technology has conversion efficiency of 16-18%, 14-15%, 8-12%, and 18-19% respectively. Dimension and specification of different PV panels is given table 1.2.

Wind energy conversion system (WECS) consists of wind turbine, gear box, and electric generator. A wind turbine obtains its power input by converting the force of the wind into a torque (turning force) acting on the rotor blades. Wind power generators which are attached to wind turbines, convert wind energy (mechanical energy) to electrical energy. The amount of energy which the wind transfers to the rotor depends on the density of the air, the rotor area, and the wind speed.

In other words, the "heavier" the air, the more energy is received by the turbine. The average capital investment for WECS is $2000 per kW.

Renewable resources of wind and solar energy are freely available in the abundant amount. Ideally, renewable sources are clean, green and maintenance free. If BS power supply topology constitutes reciprocating IC engine and microturbine, then that topology won't be environment friendly because consumption of either diesel or natural gas still there similar to conventional DGset power supply. Therefore, to have environment friendly topology for BS power supply, fuel cell and renewable resources (solar and wind energy) are considered in this thesis. Further, these topologies will be analyzed to have low OPEX.

1.2.2 Switched mode power converters

The output voltage of fuel cell and renewable resources (solar and wind energy) depends on load variations as well as on the environmental condition like temperature, atmospheric pressure, irradiation, wind speed and humidity. It varies from 10-30% above or below the rated voltage. On the other end, it is noteworthy that telecom load mostly constitutes electronic system which is sensitive to voltage variation. Therefore, an interfacing unit is necessary to integrate fuel cell or renewable resources (solar and wind energy) with telecom load in order to scale the voltage to level of distribution bus voltage (48V). The interfacing unit constitutes the switched mode power converter (SMPC) to match the voltage levels of source and the distribution bus, and the controller for voltage regulation. SMPC are DC-DC converters that regulates the voltage across DC loads. Converter plays

Table 1.2: Configuration of PV panels

Number of cells	36	60	72
Voltage at MPPT, V_{mp} (V)	18	30	36
Open circuit voltage, V_{OC} (V)	22	38	44
Nominal voltage, $V_{nominal}$ (V)	12	20	24
Power rating (W)	30	280	320
Cell arrangement	6× 6	10× 6	12× 6
Dimension (inches)	39× 39	65× 39	78×39

an important role to make power supply reliable, free from ripple and voltage fluctuations. Non-isolated DC-DC converters are preferable choice for low voltage and high current application like telecom site. Further, the selection of converter should be such that high power efficiency, low ripple current, compact, modular and most importantly the fast tuning performance during disturbances without the need of large passive storage components. The BS has the requirement of tight voltage regulation for reliable operation and need to incorporate the interfacing unit with suitable controller that maintains 48V at the DC bus. Therefore, efficient power conversion from fuel cell or renewable resources for BS supply is achieved if the dynamic behavior of the interfacing converter is properly tuned under varying load and source disturbances.

1.2.3 Controller for voltage regulation of DC distribution bus

Open loop analysis of converters suggests that DC-DC converter are non-linear time variant system. The output to control-input transfer function of the converters such as boost converter has a right hand complex plane (RHP) zero. The RHP zero makes the SMPC a non-minimum phase system which causes initial undershoot, zero crossing and overshoot [16] in the dynamic response of the system. Therefore, closed loop operation of the SMPC is a requisite for the satisfactory dynamic response. Conventionally, linear control techniques such as Ziegler-Nichols has been implemented to tune the PID/PI controller due to the simplicity of design and implementation [17]. However, the linear control techniques are designed by considering the small signal modeling in which linearization is done around the operating point. As a result, the model parameter varies with the changing operating conditions and results in poor large signal response. Detailed mathematical modelling of the system constituting the converter and fuel cell or renewable resources is required to obtain the transfer function of the overall system. Generally experimentally tunned PID controller is preferred for the SMPC integrating the renewable resources. However, this approach requires the experienced user, long processing time and doesn't ensure the optimal dynamic response of the SMPC. Thus, such a controller is required that ensures the fast dynamic response of the

SMPC under wide range of variation in input voltage and load, easy and inexpensive to implement.

1.2.4 Optimal sizing

Another challenge to integrate renewable resources to the BS power supply is the intermittency of the resources. To enhance the reliability, system tends to be oversized due to the requirement of large battery banks as PV power is not available during night and cloudy days. The oversized system results in an expensive power supply owing to high capital cost of PV panels, replacement cost of the batteries and higher rating of power converters. On the contrary, to achieve the low cost of electricity for the hybrid renewable energy system (HRES) based power supply the system, tends to be undersized which compromises the reliability. Therefore, optimal sizing analysis is essential to find the configuration of renewable resources and battery storage for economic and reliable power supply. The optimal sizing process should consider the non-linearity and intermittency of renewable resources.

1.2.5 Supervisory control for the BS supply

The futuristic BS power supply architecture is based on multi-sources, battery storages and integrating SMPCs. In this thesis, integration of renewable resources and battery storage to the BS power supply architecture using SMPCs will be proposed which would be environment friendly, reliable and provide low cost electricity. Thus, there is a need of controlling the performance of each resource and corresponding SMPC as well as the performance of the overall system which lead to a sustainable power supply topology. The multi-source BS power supply system is of few kilowatts with common goal to have efficient and sustainable power supply, therefore, centralized hierarchical control system is considered which would be implemented with low computational burden and communication. The Fig. 1.5 shows the different levels of control in the centralized hierarchical control. At primary level, control of local power, voltage and current happens to follow the

set points given by upper level controllers. Secondary level deals with voltage regulation of the DC distribution bus under the source and load side disturbances. The top level control system performs the overall monitoring of the individual controller and functions of supervisory control and data acquisition. The aim of supervisory control is to optimize the system operation, ensure load power sharing accurately and enhance the overall efficiency of the system. Therefore, supervisory control sometimes called as energy management of the system. The energy management of renewable based telecom power supply in remote/rural areas becomes critical due to the intermittent nature of the resources.

1.3 Research objectives

The research objectives pertaining to this thesis work can be stated as follows

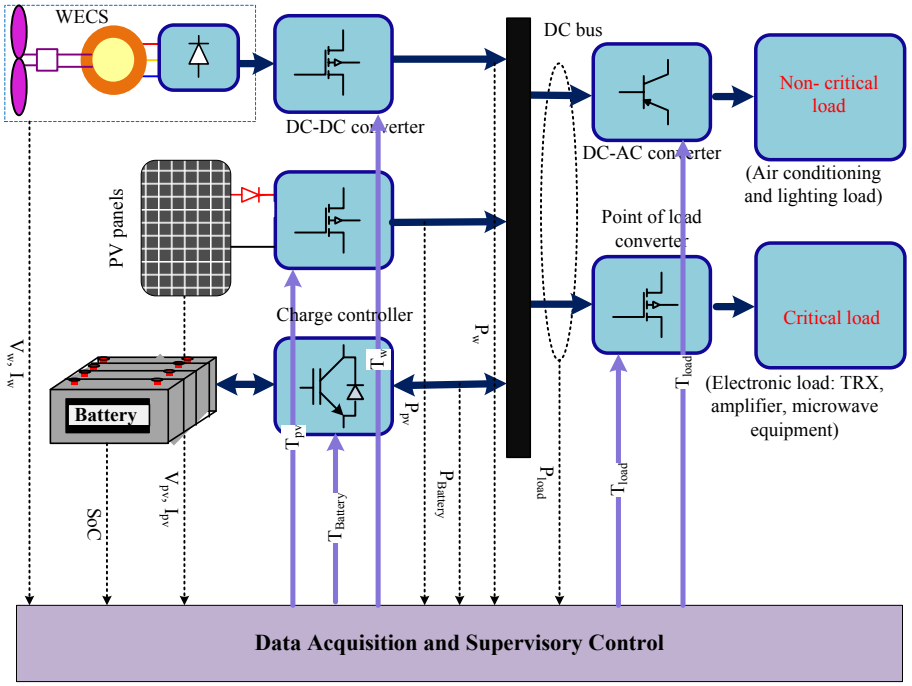

Figure 1.5: Hierarchical control for the BS power supply (Subscripts $_{pv}$, $_{w}$, $_{Battery}$, and $_{load}$, are for PV panel, WECS, battery storage, load; V, I, P, T, and SoC denotes the terminal voltage, current, power, switching signal and state of charge respectively)

1. To propose a hybrid power supply topology for the base transceiver station of telecom tower in remote and rural areas.

2. To ensure regulated DC distribution bus voltage of the base transceiver station of the telecom tower in the environment of renewable resources.

3. To carry out comparative study of proposed hybrid power supply topology for the BS with different SMPC in the environment of renewable resources.

4. To perform optimal sizing of power supply topology for BS to carry out cost effective analysis and energy management.

5. To propose a suitable and effective supervisory control for the base transceiver station power supply.

1.4 Thesis organization

The remaining thesis is organized as follows. The chapter 2 presents the detailed review of the different topologies presented so far in the literature for the BS to overcome the issues in conventional DGset based power supply. The chapter also reviews the state of art in the controller for the voltage regulation of the DC distribution bus and different SMPC for the implementation of those controllers. It also includes the section reviewing the literature about the different techniques to achieve optimal sizing of renewable based telecom power supply. Different criteria are summarized that have been considered by the researchers to formulate the optimization problem for optimal sizing. It also, reviews the methodologies to perform energy optimization in the BS.

Chapter 3 proposes a environment-friendly proton exchange membrane fuel cell (PEMFC) based power supply for BS in remote/rural areas is proposed. The terminal voltage of fuel cell varies with change in ambient temperature, pressure and humidity. Thus, an intelligent hybrid controller is proposed and implemented using boost converter. The proposed controller inherits the best features of the linear controller such as simplicity in implemention, fixed frequency operation and that of intelligent controller which have mode independent design, reduced mathematical

modelling, and wide range of operation. The performance of the intelligent hybrid controller is validated for three test conditions: i) input disturbance rejection, ii) output disturbance rejection, iii) reference tracking.

Chapter 4 proposes a hybrid renewable energy system based BS power supply that combines the complimentary natured PV and wind energy with battery storage to have environment friendly, reliable and low OPEX. The intelligent hybrid controller in chapter 3 is improved by proposing a modified adaptive real coded genetic algorithm (MARCGA) to tune the PID controller. The performance of the MARCGA assisted PID controller implemented using boost converter under different test conditions is compared with that of binary genetic algorithm (GA), particle swarm optimization (PSO) and grey wolf optimizer (GWO)-assisted controller. Further, Cuk converter is proposed as interfacing converter for integrating renewable resources (PV and WECS) with DC distribution bus. The Cuk converter which steps up and down the input voltage, allows the wide range of operation for renewable resources, ripple free input current and compactness in size. Thus, intelligent hybrid controller is implemented to Cuk converter for the voltage regulation of DC distribution bus under different test conditions. The successful implementation justifies the model free design of the controller as detailed mathematical modelling of the Cuk converter integrating the renewable resources in BS power supply architecture is not required. Further, the laboratory scale prototype for Cuk converter is developed to implement the intelligent hybrid controller using DSPIC33FJ128MC802 microcontroller. The extensive simulation and experimental studies are done in this chapter to analyze the performance of proposed intelligent hybrid controller.

The design of optimal configuration of PV-wind based power supply ensuring economical, reliable and green operation of the off-grid telecom towers is presented in Chapter 5. The detailed mathematical modeling of renewable resources is carried with consideration of the de-rating factor and maximum power point tracking (MPPT) factor. Hourly solar irradiation and wind speed data profile are used for long term analysis while considering peak load as the load profile. The cost of electricity (COE) is calculated after detailed economic analysis considering the investment cost of all the components of the HRES based BS supply, replacement, operational and maintenance cost of batteries. Reliability studies are based on

balancing the HRES power generation and load demand. Reliability studies are based on whether the generation can meet the demand which is represented in terms of loss of power supply probability (LPSP). However, it is equally essential for a standalone HRES to keep a check for excess power generation after meeting the load demand, as excess energy can not be sold to the grid. Therefore, an additional reliability index based on excess energy generated, along with LPSP, is introduced in this thesis for optimal sizing analysis of standalone HRES for BS. As the three objectives are not commensurate and contradictory in nature, therefore, multi-objective optimization problem is formulated to get the optimal configuration of HRES. Non-dominated sorting genetic algorithm (NSGA-II), a multi-objective optimization technique is implemented to minimize the objective function which includes LPSP, excess energy (EE) and COE. Extensive simulation study has been performed for different scenarios to analyze the feasibility of the proposed HRES based power supply.

In the chapter 6, detailed mathematical modelling of HRES to reflect the near practical behavior of the renewable resource is developed for the comprehensive cost analysis for optimal sizing. The BS load is modelled based on the long term evaluation model and the telecom traffic is modelled using poison probability distribution functions (PDF). The uncertainty in the renewable resources is incorporated using PDF in the optimal sizing optimization. The uncertainties in wind speed and solar irradiation are incorporated using Weibull and Beta PDFs. The leveled cost of electricity (LCOE) is considered for cost analysis of HRES which account for the capital, replacement, operation and maintenance costs. Similar to chapter 5, excess energy generation and LPSP are objective functions and formulated for the reliability analysis. In previous chapter, capacity of wind turbine is approximated to continuous variable. As commercially available sizes of wind turbines are discrete in nature and continuous variable based optimization leads to a suboptimal solution. As commercially available sizes of wind turbines are discrete in nature and continuous variable based optimization leads to a suboptimal solution. Therefore, a discrete multi-objective grey wolf optimization (DMGWO) is proposed in this chapter. Further, a corrective algorithm is embedded in DMGWO to handle the discrete variable (capacity of wind turbine). The DMGWO finds the optimal energy mix of the proposed PV-wind based HRES by minimizing the

three objective viz. LPSP, LCOE and EE.

The energy management technique for renewable based telecom supply in remote/rural areas is proposed in the chapter 7 which considers the intermittency and randomness in nature of renewable resources due to dependence on weather and geographical location of site. Demand response management (DRM) concept is implemented by modelling the air conditioners as analogous to batteries to create virtual energy storage (VES) to buffer the intermittency in the renewable energy without an actual battery. The modelling of air conditioner does consider the cyclic turn on and off patterns along with the stochastic nature of the HRES. The VES based DRM enhances the life of Battery energy storage system (BESS) without the installing new equipments to save energy in air conditioners.

The major conclusions of the thesis and scope for further work in this area are presented in chapter 8.

Chapter 2

Literature review

2.1 Introduction

The conventional way of supplying the BS of the telecom towers is discussed and the prerequisites of the BS power supply is stated in the previous chapter. This chapter presents the review of different topologies of architecture of power supply for telecom towers in remote/rural areas. Then, a survey of the literature is presented describing the optimal sizing of renewable based power supply for the BS in remote/rural areas. A summary of recent work reported in the literature has been provided through a comparative analysis of different SMPC for the renewable based power supply for BS. In the beginning of the chapter, different topologies of the BS power supply architecture is presented. For addressing the challenges of renewable resource integration in the BS power supply, role of SMPC is reviewed along with different control techniques. A dedicated section on the the optimal sizing of the renewable based BS power supply is included. This section also reviews different criteria and techniques considered for the optimal sizing of the renewable based BS power supply for the towers in remote/rural areas. In order to enhance the battery life and improve the performance of the BS power supply, the recently published work concerning the energy management is reviewed. The following paragraphs discuss topologies of BS power supply on remote/rural areas.

The telecom industry is expanding exponentially which require construction of

more towers especially in remote/rural areas. Most of the telecom tower sites in these areas are either off-grid or face long power outages thus, DGset along with battery bank form the conventional power supply for BS in remote/rural areas. The excessive use of conventional power supply has led to huge dependence on diesel as fuel and battery bank for reliable supply. This has not only increased the operating expenditure of telecom operators but also pose a threat to the environment. Also, the use of automatic switch is cause for single point failure in conventional power supply [18]. Thus, there is a need to find some alternative or renewable resource for the telecom tower power supply. Different alternative resources like microturbine, fuel cells, nuclear power plants, and renewable energy resources like solar PV, WECS, hydro-plants or biomass.

In comparison to DGset, microturbine has better energy conversion efficiency and lower noise level. Therefore, microturbine is proposed to replace the DGset with automatic switch for a grid connected BS which faces long power outage in [9]. The proposed topology reduces the battery reserve time upto 10 minutes which is sufficient to provide three chances to start the microturbine. The reduced battery size acquires less footprint at the site. Unlike, DGset, microturbine is more cleaner as it emits CO_2 only, not the nitrous and sulphurous compounds. Also, the microturbine is more efficient than DGset considering the higher energy density of natural gas than diesel [19]. However, microturbine operation is suitable for the base load operations because efficiency lowers at the reduced load operation. At reduced load cycles, overall system efficiency can be enhanced by utilizing the excess heat generation in a combined heat and power application [11]. Therefore, power supply using small microturbine coupled with solid-oxide fuel cell establishment is proposed to boost the thermal efficiency of the system [20, 21].

The fuel cell which produces electricity from direct energy conversion from chemical energy, combines the best features of reciprocating IC engines and batteries. Alike with engines, it operates as long as fuel is available and similar to battery, its operation is flexible and reliable due to modular design and absence of electromechanical rotating part [22]. Unlike batteries, where terminal voltage is a function of the rate of discharge current and requires several hours of recharging, fuel cell capacity doesn't degrade with time [23]. A fuel cell based back-up power supply without battery banks is proposed [11]. The author discusses the issues with bat-

tery bank in back-up supply. Battery bank is the expensive component with the shortest lifespan and requires special flooring infrastructure to have intrinsic weight bearing capacity. Battery disposal extends liability and adds to the maintenance cost. A fuel cell based back-up power supply without any auxiliary source suffers from the reliability issues. The fuel cell has large time constant in order of minutes and can not handle frequent large step loads and large inrush currents. Also, fuel cell technology is very expensive and requires large footprints. To buffer the large response time of the fuel cell, ultra-capacitor/super-capacitor based topologies are proposed to eliminate both battery and DGset [19, 22]. These topologies has longer payback time owing to the large capital cost of both fuel cell and super-capacitors. Also, energy density of super-capacitor is smaller than batteries by a factor of 10, therefore it is not suitable for long term energy storage as back-up source. Thus, battery bank cannot be eliminated completely from the back-up power supply. The fuel cell with start-up battery bank having short reserve time topology is proposed [24]. This configuration considers the slow dynamics of fuel cell during load transients and also on-site batteries with long reserve time is necessary as back-up when system run out of hydrogen supply. Thus, the concept of hybrid off-grid system which comprises of renewable resources and batteries supporting the integration of hydrogen technology is introduced [25]. Renewable resources are employed to generate the hydrogen from the on-site electrolysers. The topology is able to reduce the required battery size by 54%. However, the overall efficiency of the system is less considering that the indirect utilization of the renewable energy through fuel cell. The energy density of the three energy storage which are diesel as fuel, compressed hydrogen (200 bar) and lead acid battery is analysed in terms of total energy (kWh/kg) which are 12, 2 ,0.04 respectively and useful energy (kWh/kg) available from them are 2.4, 0.7, 0.036 respectively. Hence, the conversion efficiency of the diesel as fuel, compressed hydrogen (200 bar) and lead acid battery are 20%, 35% and 90% respectively.

India being a tropical country, has abundant potential of solar energy. Indian annual global solar radiation is approximately 5-7kWhr/sqm. per day with 300 days sunshine per year. Also, annual average wind speed of 5-6m/s makes wind energy an attractive solution to generate electricity [26]. Thus, renewable based BS power supply for telecom towers in remote/rural areas in India could be the

viable solutions. The standalone PV or WECS only system are not feasible due to the intermittent nature of the renewable resource. Thus, a energy storage back-up is a pre-requisite with renewable based power supply for BS of telecom towers in off-grid areas. An autonomous PV panels with battery as back-up power supply design is discussed in [27]. However, to meet the uninterrupted power supply for BS, the PV-battery system tends to be oversized due to the requirement of large battery banks as PV power is not available during night and cloudy days. The oversized system results in an expensive power supply owing to high capital cost of PV panels, replacement cost of the batteries and higher rating of power converters. Similarly, WECS with battery based standalone telecom power supply is studied in [28]. To overcome the wind intermittency, the battery is supplying the load all the time and being charged by the WECS. The proposed wind-battery system is also expensive as the battery is overused and increases the replacement cost of the batteries. The intermittency of the solar based power supply is balanced with the DGset and battery forming the back-up power supply for off-grid telecom towers [29]. During the solar power deficit DGset is run which results in reduction of size of PV panels and fuel consumption and prevents batteries from deep discharge. However, the objective to have environment friendly power supply for BS is not met. Pre-feasibility study of PV and WECS for BS in central India is carried out in [30]. The micro-sources are implemented in telecom sites to bring trade off between battery charging and DGset running by integrating PV panels [31]. A PV-wind-battery grid connected hybrid power supply for telecom equipment system is proposed to get the explore the complementary nature of renewable resources (solar and wind) [32].

In this thesis, a HRES formed by complementary PV and wind renewable resources along with battery back-up is proposed for the BS of telecom tower in remote/rural areas. Thus, optimal sizing based on detailed economic and reliability analysis should be done to find the optimal energy mix to meet the requirements of the telecom power supply. Also, integrating the renewable resources to BS power supply, necessitate the power converter interface to extract maximum power from the renewable resources considering their low conversion efficiency. Further, the renewable resources provide variable voltage which necessitate the power electronic interface for the voltage regulation at the distribution bus.

2.2 Voltage regulation of DC distribution bus

The need of environment friendly power supply necessitates the alternative resources (fuel cell and renewable resource) for BS power supply topology. However, there is challenge in integrating renewable resources to the BS of telecom tower is that the resources have variable output voltage as a function of environmental conditions and the load [33]. On the other end, BS has the requirement of tight voltage regulation of the DC distribution bus for reliable operation of different electronic components at the BS. Therefore, an interfacing unit is necessary to integrate alternative resources to the BS power supply. Since, alternative resources and distribution bus are DC natured, therefore, SMPC (DC-DC converter) becomes the part of interfacing unit to achieve the required voltage profile. The efficient power conversion from resources is obtained if the dynamic behavior of the interfacing converter is properly tuned under varying load and source disturbances [34]. The steady state requirement of the SMPC for BS power supply include good output voltage regulation, high efficiency and low ripple factor under varying load and input voltage condition. Whereas, the transient state of requirements include permissible undershoots and overshoots in the output voltage and inductor current, time taken by the output voltage to settle after the sudden disturbance and to rise after any input failure. It also includes the voltage and current stresses on the switching device and the saturation limit of the magnetic elements in the circuit [35, 36]. Different features of the SMPC are tabulated in table 2.1 which assist in the selection of the SMPC for the given topology of BS power supply.

Table 2.1: Performance characteristics comparison of DC-DC converter

Feature	Buck converter	Boost converter	Buck-boost converter	Cuk converter	Sepic converter
Input current	Pulsed	Continuous	Pulsed	Continuous	Continuous
Output current	Continuous	Pulsed	Pulsed	Continuous	Continuous
Voltage gain	≤ 1	≥ 1	$\leq 1, \geq 1$	$\leq 1, \geq 1$	$\leq 1, \geq 1$
Output voltage polarity	Non-inverted	Non-inverted	Inverted	Inverted	Non-inverted
$\frac{R_{in}}{R_o}$	D^2	$(1-D)^2$	$\frac{(1-D)^2}{D^2}$	$\frac{(1-D)^2}{D^2}$	$\frac{(1-D)^2}{D^2}$

Open loop analysis of converters suggests that it is a non-linear time variant system. The output to control-input transfer function of converters such as boost converter has a RHP zero. The system with RHP zero is known as a non-minimum phase system, has system response characterized with initial undershoot, zero crossing and overshoot [16]. Also, presence of RHP reduces the overall bandwidth reduces by 30 times the switching frequency [37]. The open loop converter operation for voltage regulation doesn't give satisfactory performance which necessitates closed loop operation. Conventionally, linear controllers has been used for the closed loop operation like Ziegler Nichols (ZN) method [38], root locus technique [39], circle based criteria [40], hysteresis method [41] and robust control [42]. These methods are based on small signal analysis of the boost converter which involves the linearization of the system using various mathematical modelling techniques [43, 44, 45, 46, 47, 48, 49] like state space averaging technique which is most popular [43]. The dynamic behavior of the DC-DC converter is improved by implementing type 3 compensation loop using transfer function approach [50]. Thus, a PI based current controller has been implemented for voltage regulation at load end in WECS supplying isolated DC loads [51]. The small signal model is applicable around the operating point which makes parameter of the model vary when operating point shifts. Hence, linear controller gives sluggish large signal response. The challenge of RHP zero complexity in control design could be tackled by operating boost converter in discontinuous mode of operation with reduced switching frequency will shifts the RHP zero to higher frequency which makes the system to behave as first order system having fast dynamic response [44, 52, 53]. At the same time, peak and ripple current increases that requires higher rating of device and additional filter. This increase in RMS current causes reduction in efficiency due to the presence of parasitic elements in the system. Another way to address the challenge of RHP zero is by eliminating it by using a capacitor of large equivalent series resistance value [16]. It is difficult to measure equivalent series resistance accurately because equivalent series resistance is a function of temperature. Moreover, the large value of equivalent series resistance becomes the source of ripple in output voltage. Elimination of RHP zero could be done by 'predictor' design by modelling it as a time delay [54]. Since predictor design approach is again based on small signal model of the converter and has difficulties in practical implementation. An extended window technique for digital controller to

calculate the duty ratio of the converter in advance is implemented to reduce the computational time delay in the process better reliable and stable operation [55]. Therefore, the controller design should be such that it addresses the non-linearity of the system.

Recently, researchers has implemented non-linear controllers for closed loop operation of DC-DC converter to meet challenges of its closed loop operation. These controllers could be broadly grouped into three groups. First group are of those controllers which adapts itself to the operating condition of the system i.e. adaptive controllers. An adaptive current mode controller is based on average current mode control for feedback in which slope of the compensating ramp is adaptively tuned as per the operating point [56] which has improved small signal transient response than the classical current mode controller but not the large signal dynamics. Another improved adaptive controller is adaptive model reference controller [57, 58] that boost up the small signal response with varying operating condition. But practical implementation require sensing of all state variables of the converter along with several OPAMPs and expensive ICs for implementing special functions (e.g. multiplication, division, logarithmic operation). Presence of too many components in higher order converters increases the cost.

Second group is of the controllers that don't require accurate model of the system like sliding mode controllers [59, 60]. The sliding mode controller gives superior dynamic performance of over PI controller for large variations in load resistance and supply voltage changes [61]. Though sliding mode controllers are known for their robustness but requires the knowledge of parameter variations for stabilization. It requires the sensing of all the state variables which increases the control complexity and cost of the system. Also, the variable frequency of operation and associated chattering problems make this controller less attractive. The methods of avoiding chattering problem add to the control complexity and realization of the controller. Another controller in this group is robust controller called $H\infty$ controller. The design of the controller is based on small-signal model at the operating point and includes the variations in the model as disturbances in line and load conditions [62, 63]. This approach maximize the closed-loop bandwidth of the nominal small-signal model but requires the sensing of input voltage.

Third group is of those controllers that are totally independent of the plant model known as intelligent control techniques which are fuzzy logic controller, artificial neural network and meta-heuristic algorithms. The non-linear nature and the ability of fuzzy logic controller to handle uncertain and imprecise inputs make the controller independent of system mathematical model to give good large signal transient response [64, 65, 66, 67, 68]. However due to increased cost, control complexity, the absence of systematic design and analysis procedure makes these controllers less attractive techniques in power supply industry. Meta-heuristic algorithms such as GA and PSO are based on global optimization random search procedure. Its best applicability is where traditional calculus based methods fails such as problems in which gradient calculation is a messy and difficult task, and the system is multi-modal or multi objective system [69, 70, 71, 72]. PSO is used as controller for the boost converter which uses the small signal model of the converter. The PSO finds the optimal value of duty cycle for the each sampling instant whenever the actual output voltage differs from the reference voltage [73]. However, the performance of the PSO algorithm is limited by the small signal modelling and the sampling time.

An analog feedback controller for a boost converter is designed by formulating optimization problem. The GA enhanced by queen-bee evolution algorithm is implemented to get the controller parameters [74, 75]. A modified-PSO is used to optimize the PID controller coefficients for Buck converter, which changes the ratio of proportional term and integral term during search process [76]. Different objective functions for the finding the PID parameters using meta-heuristic algorithm are studied and compared [77].

Hence, there is a need to redraft the design of voltage regulation controller for the DC-DC converter such that different specification of the dynamic response are met at the same which are rise time, settling time, maximum overshoot and steady state error. An appropriate fitness function for the meta-heuristic based optimization need to be developed that follows the trajectory of the dynamic response of the converter. The converter model shouldn't be the approximated and linearized small signal model which have been used all other previous techniques. The controller for the non-minimum phase system is such which is immune to internal and external disturbances and provides desired static and dynamic characteristics for

all operating point conditions.

2.3 Optimal sizing of renewable based BS power supply

In literature, several solar based BS has been proposed to reduce the diesel consumption of the BS in off-grid mode [29, 78]. Renewable powered BSs have reduced operating cost, environment friendly and has higher resistance to the disasters such as grid failures than the conventional DGset operated BS. However, a PV powered or wind powered BS are not reliable and economic owing to intermittency and high capital cost of renewable resources [79]. Optimal sizing analysis is essential to find the configuration of renewable resources and storage for economic and reliable power supply. The over-sized HRES results in higher reliability, but at higher capital expenditure and the undersized HRES gives economical system at the stake of reduced reliability of power supply. In this section, state of art of the different approaches towards the optimal sizing of renewable based BS power supply is presented. Various criteria considered in formulation of optimal sizing problem and techniques to get the solution are reviewed.

In literature, several factors are considered for the optimal sizing such as cost [80], reliability [81], environment [82] and social [83]. Different indices such as life cycle cost (LCC), annualized cost of the system (ACS) and LCOE are considered for cost analysis of HRES which account for the capital, replacement, operation and maintenance costs. Reliability studies are based on balancing the HRES power generation and load demand. Most of the studies in literature consider whether the generation can meet the demand. Hence, reliability indices such as LPSP, loss of load hours (LOLH) and demand not met (DNM) are used [84, 85]. However, it is equally essential for a standalone HRES to keep a check for excess power generation after meeting the load demand, as excess energy can not be sold to the grid. Therefore, an additional reliability index based on excess energy generated, along with LPSP, is introduced in this thesis for optimal sizing analysis of standalone HRES for BS.

Proper knowledge of renewable resource capability is necessary for the accurate planning of HRES. A detailed mathematical modelling of hybrid PV-biomass energy system to reflect the near practical behavior of the renewable is recommended for the comprehensive cost analysis for optimal sizing [80]. The high-resolution weather data taken every 10 seconds is used to find the trade-off between the cost, and demand not met by implementing multi-objective genetic algorithm for grid-tied HRES [85]. However, high-resolution data is not available for most of the sites of BS. The uncertainty in the renewable resources is incorporated using PDF in the optimal sizing optimization technique for residential microgrid [86]. However, capacity of wind turbine is approximated to continuous variable. As commercially available sizes of wind turbines are discrete in nature, continuous variable based optimization leads to a suboptimal solution. The 'average month' and 'worst month' techniques are implemented to perform a techno-economic analysis which may not fulfill the load demand in specific periods and lead to an over-sized system respectively [85, 87]. A long-term performance analysis for the standalone PV-battery system is done using analytical methods while considering the loading effects [88].

Most of the approaches consider cost as objective function to formulate the optimal sizing problem for minimization with other criteria as constraint or added to the cost after conversion to maintain unit consistency [80, 84, 89]. The single objective approach is not always practical as all the criteria cannot be converted to same unit as of cost. Moreover, the highly constraint optimization problem is challenging to reach optimal solution. LPSP is implemented as a constraint to minimize the ACS to find the optimal size of HRES components [80, 81]. A comparative study is done to analyze the effectiveness of different reliability indices such LPSP and LOLH to ensure the availability of HRES for the given time duration [84]. However, it is observed that to ensure 100% reliable system (LPSP=0), the larger size of HRES is selected. A multi-criteria decision analysis approach is presented to consider different criteria without the need of conversion for the unified unit based objective function to define the optimal sizing share between PV and wind power generations [90]. However, the indices for different criteria are incorporated as constraints in the optimization process. The conventional approaches such as weighted sum strategy or ϵ-constraint modeling are not efficient enough to solve

multiple-objective optimal sizing problem. The effect of one objective might influence the solution in a higher proportion. Dual objective problem based on capital cost and transport mobility is formulated for hybrid energy mix for emergency supply. The uncertainties in source and load demand is implemented using interval modelling. The multi-objective differential algorithm is implemented for the highly constrained, nonlinear, and discrete combinatorial optimization problem [79]. NSGA-II is implemented to get the optimal configuration of the renewable based power supply. The NSGA-II employs the fast non-dominated sorting and parameterless niching operator to group the individuals in the population after selection, recombination and mutation [91]. Multi-objective particle swarm optimization (MPSO) also implemented for optimal sizing. However, the fast convergence of the algorithm may leads to the local minimum stagnation and results in a pseudo Pareto front (sub-optimal solution).

Thus there is a need to formulate a multi-objective optimization problem to get the configuration of HRES taking into consideration economics, reliability and excess energy generation criteria. The renewable resources should modelled to incorporate the intermittency. The telecom load should be modelled for its variability and randomness instead of considering a constant load as done in literature. Unlike literature where capacity of the WECS is assumed continuous variable, the optimal sizing problem formulation should consider it as discrete variable.. Thus, such a multi-objective algorithm is required which is able to handle both continuous and discrete variables, and avoids local minima.

2.4 Power management approaches in base station power supply

The distribution of power consumption averages of the various components of BS is recapitulated in [92]. It shows the power consumption by component in a BS; the largest energy consumer in BSs is the radio frequency equipment (power amplifier plus the transceivers and cables), which consumes approximately 65% of the total energy. Among the other components of the BS, the important energy consumers are air conditioning (17.5%), digital signal processor (10%), and

the AC-DC converter (7.5%). Energy consumption optimization in a BS includes three approaches: energy optimization of the network and radio frequency connection, energy optimization of the site sheltering the BS, and optimization of energy consumption of BS. Reduction in energy consumption at network level is achieved by implementing dynamic management of network resource such as transitional states of sleep (progressive commutation of BS) and dynamic allocation of the spectrum of frequencies as a function of the traffic load [93, 94]. Energy optimization of the site sheltering the BS can be obtained by adopting distributed architecture of BS and optimally placing the equipments near to each other to minimize the losses in cable [95]. Optimization of energy consumption of BS focuses on the improvement of energy efficiency of different components of BS. The power amplifier are redesigned using special high frequency materials like Si, GaAs to refine its behavior near linearization. The efficiency and linearity of power amplifier is enhanced by implementing numerical techniques for energy distortion cancellation [96]. The architectures like ASIC, FPGA, or DSP are implemented in integrated circuits for digital signal processor to reduce the power consumption [97]. Selecting the high efficiency power electronic converter for interfacing is another step to enhance BS efficiency. Lastly, power consumption in air conditioning can be reduced by lowering the operational temperature of BS to the minimum or by using additional elements such as heat exchangers, membrane filters, and smart fans or heat modules [98].

Power consumption in the BS components is reduced by implementing the concept of DRM. In DRM algorithms, interruptible loads are shed based on market conditions and demand limits to modify the instantaneous power demand during periods of peak demand [99, 100, 101]. Few DRM algorithms take into account the variations in the load demand as well as source (renewable resources) [102, 103]. However, the load are modelled as constant power loads operating at the rated power without any cycling or variations. The research is conducted on air conditioners and refrigerators with time constant above 30minutes and demonstrated that such loads such have a distinct cyclic turn on period and turn off period [104]. The concept of VES is implemented in multi-story buildings to use the refrigerators and air-conditioners as alternative energy storage devices to enhance the efficiency of renewable based power supply [105]. VES based DRM enhances the

life of BESS without the installing new equipments to save energy in air conditioners. Application of VES in grid management services such as voltage regulation and load management are also getting attention in recent studies [106, 107].

Considering the fact that individual energy consumption and carbon emission of a telecom BS is less. However, the collective energy consumption of the global telecom BS is 3% of the global energy consumption. Thus, making individual BS energy efficient would result in global impact. The futuristic power supplies for BS are renewable based therefore conventional energy management strategies are incapable . Thus energy management algorithm for the renewable based telecom supplies should incorporate the DRM concept in the BS power supply which prevalent is smart grids.

2.5 Summary

This chapter has explained the issues with conventional power supply for the BS in remote/rural areas. With the predicted expansion of telecom towers to remote/rural areas, the need for environment friendly, reliable, economical OPEX, high power density, and energy efficient power supply has emerged. Therefore, different topologies for BS power supply with alternative resources and back-up supply has been reviewed based on the pre-requisite of the BS power supply in remote/rural areas. The state of art for different controllers for the voltage regulation of DC distribution bus is presented considering the futuristic power supply based on fuel cell or renewable resources for the BS. Further, the performance of the renewable based BS power supply is based on its optimal configuration. Therefore, the detailed literature review is presented on the optimal sizing of renewable based power supply. The different approaches to formulate the optimization problem along with different criteria considered for objective function formulation has been discussed in this chapter. The need for the multi-objective problem formulation for optimal sizing is stressed upon to ensure the reliability and economics. It is observed that several assumptions has been made in literature to simplify the optimization process for sizing. However, it deviates the system from its practical behaviour. Therefore, the WECS capacity variable needed to be treated as dis-

crete variable which generates the requirement of such a multi-objective algorithm that can handle continuous as well as discrete variables simultaneously. Further, renewable resources should be modelled considering the intermittent nature as well as load should be modelled with its randomness and variability to have a more practical representation of the system. Lastly, latest research articles are reviewed that recommend to bring the concept of energy efficiency at the individual BS level. Therefore, the prevailing concept of DRM should be incorporated in the BS power supply to perform the energy management.

Chapter 3

PEMFC based base station supply with genetic algorithm assisted interfacing converter

3.1 Introduction

In India, the telecom industry has grown exponentially to emerge as world's second largest telecom market in past two decades with more than 944.01 million mobile phone users facilitated by 700,000 telecom towers across the country. As telecom industry is already at the boom and with the roadmap laid by the policies of the department of telecommunication would continue to expand in near future with deep penetration in remote rural areas [26]. The current status of rural teledensity is approximately 46.14%, and national telecom policy has set the target to achieve 100% by the year 2020 [6]. In this path of growth and projection of telecom industry, the foremost challenge is to provide the supply to BS of telecom tower in remote rural areas where around 5% villages are not electrified. Since, telecom industry requires an uninterrupted reliable power supply to provide quality service to the customer without rolling out of services. At present scenario, around 70% of the telecom towers don't get the continuous, reliable supply from state electricity boards. The excessive use of conventional power supply having DGset and battery bank increased the OPEX of telecom companies which includes cost

of diesel as fuel, transportation, regular maintenance visit and replacement of batteries (have shorter lifespan). Further, massive dependence on conventional supply pose threat to environment as its operation adds to global carbon emission by producing greenhouse gas i.e. CO_2. Thus, a PEMFC based clean and reliable power supply for BS of telecom tower is proposed in this chapter to eliminate the operation of DGset and to meet the targets set by national telecom policy.

PEMFC is preferred because of its low operating temperature which leads to less warm up time and less thermal stress on components in comparison to other types of fuel cells. Moreover, PEMFC based supply would have modular, flexible in its operation and reliable due to modularity in its design and absence of an electromechanical rotating part. Since, fuel cell operates like an engine i.e. as long as hydrogen supply is available. The continuity of hydrogen as fuel for PEMFC based supply for remotely located telecom site is maintained by feeding reformer with natural gas or bio-fuels. Availability of natural gas could be made from nearby gas pipeline route. Alternatively, hydrogen is produced on site by electrolysers powered by PV or WECS or both. The output of fuel cell varies during load variations and telecom tower has wide and frequent load variations as function of communication signal traffic. However, BS consists of electronic equipment sensitive to voltage fluctuations therefore, supply requires tightly regulated DC voltage at distribution bus at all operating conditions that includes load as well as source side disturbances. Thus, an interfacing unit between fuel cell and the BS load is required. As the PEMFC is a variable DC voltage source, therefore, DC-DC converter is the appropriate choice for the low voltage, high current BS power supply. In this chapter, an intelligent interfacing unit based on boost converter is proposed which scales the variable DC output voltage of PEMFC to the level of DC distribution bus and performs the voltage regulation which is pre-requisite of the telecom BS power supply.

When the boost converter implemented in open loop, it doesn't give regulated output voltage. Conventionally, linear controllers have been used for the closed loop operation such as ZN method based on small signal analysis which involves the linearization of the system. Further, the applicability of the small signal model is around the operating point which varies the parameter of the model when operating point shifts. Hence, the linear controllers give a sluggish large signal re-

sponse. A non-linear adaptive current mode controller based on adaptive tuning of slope using compensating ramp has been implemented in literature. Its practical implementation requires several OPAMPs and expensive ICs for realizing the special functions (multiplication, division, logarithmic operation). Next, sliding mode controller gives the superior dynamic performance over PI controller for large variations in load and supply voltage changes. But, it requires the knowledge of parameter variations for reachability and stabilization and the variable frequency of operation causes chattering problems. The controllers which are wholly independent of the plant model i.e. intelligent control techniques such as fuzzy logic controller, artificial neural network and meta-heuristic algorithms. Meta-heuristic algorithm such as GA which have been applied to various engineering problems. It finds the global solution to the optimal control problems which are non-linear, discontinuous, multi-modal, multi-objective and multi-variable without involving messy and complicated calculation of gradient. The non-linear nature and the ability of controller to handle uncertain and imprecise inputs make the controller independent of system mathematical model to give a good large signal transient response. Thus, efforts have been put towards improving the performance of the converter by proposing a GA-assisted intelligent hybrid controller.

The chapter is organized as follows: Section 3.2 describes the structure of the proposed PEMFC supply system for BS. Further, the description of intelligent interfacing unit consisting of the boost converter is given along with the modelling of fuel cell and boost converter. Afterwards, the problem formulation along with proposed GA-assisted controller is also explained in section 3.3. Section 3.4 presents the analysis and discussion on the robustness of proposed intelligent interfacing unit with GA-assisted controller for various input, output disturbance rejection, and reference tracking capability. Concluded remarks of the chapter are presented in section 3.5.

3.2 Base station power supply architecture

The architecture of conventional power supply for BS of telecom towers in remote/rural as shown in the Fig. 3.1. A 48V DC distribution system in BS have

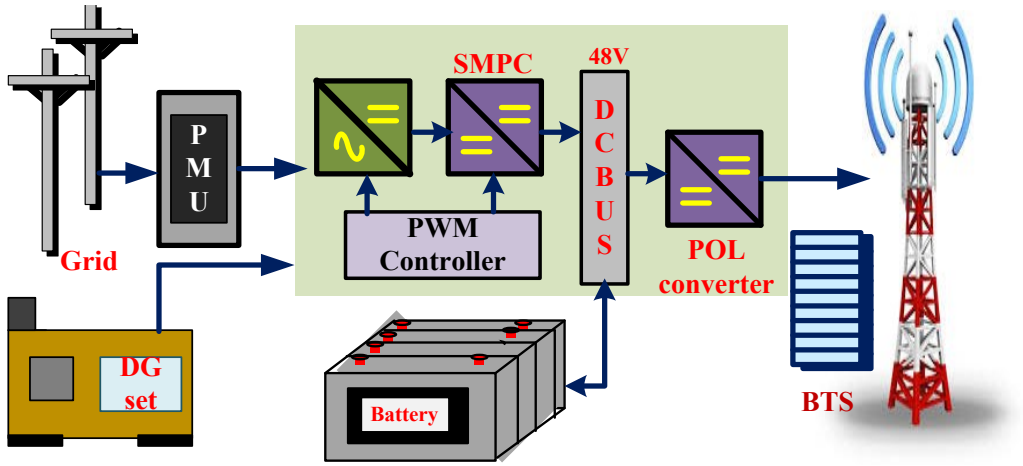

Figure 3.1: Architecture of conventional power supply for BS

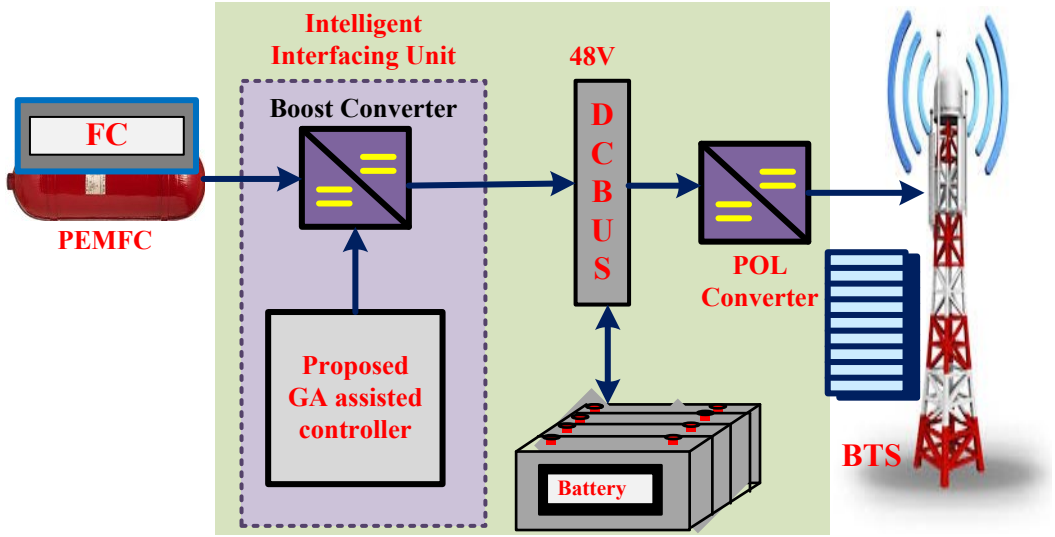

Figure 3.2: Architecture of the proposed PEMFC based power supply for BS

adopted taking safety aspects associated with high DC voltage into the consideration. From DC distribution bus, load end electronic equipment are powered through the point of load (POL) converters. The grid supply is interfaced to the BS DC distribution bus using SMPC. The purpose of the interfacing system constituting SMPC is to act as a buffer for the telecom load variations and input supply fluctuations so that a tight voltage regulation will be maintained at DC bus. It is to be noted that the telecom load mostly constitutes electronic equipments which are very sensitive to voltage variation.

3.2.1 Proposed PEMFC based power supply architecture

Architecture of the proposed PEMFC based power supply to the BS is shown in Fig. 3.2. The PEMFC of 2.5kW is chosen as a clean resource for powering the BS which takes hydrogen and oxygen as fuel to generate electricity by chemical reaction and produces water vapor as a by-product. PEMFC does not require any frequent maintenance visits. Thus, OPEX is reduced for telecom operators. The output voltage of the PEMFC depends on load variations as well as on the environmental condition like temperature, atmospheric pressure, and humidity. It varies from 15-30% above or below the rated voltage and thus, necessitates incorporating the interfacing unit that maintains 48V at the DC bus. The proposed intelligent interfacing unit constitutes a boost converter and associated controller for regulating the output voltage of the converter. The boost converter steps up the variable voltage of PEMFC to 48V, the distribution bus voltage of BS. The proposed intelligent controller in this chapter maintains the tight regulation of the DC bus voltage under PEMFC voltage fluctuations and load variation of BS of telecom tower based on communication signal traffic. Moreover, the proposed controller will provide a fast response, so that the overall system should not become sluggish due to the presence of the converter.

3.2.1.1 Modelling of fuel cell

Fuel cell converts the chemical energy of fuel (hydrogen and oxygen) to electrical energy and water as byproduct. The mathematical modelling of the fuel cell based on the principle of thermodynamics is presented in this section [108, 109].The potential developed across each cell is given by

$$Enerst = 1.229 - 0.0085(T_{cell} - 298.15) + 4.3085 \times 10^{(-5)} T \ln(\rho_{H_2}\sqrt{\rho_{O_2}}) \quad (3.1)$$

Where, T_{cell} is the cell temperature (K), and partial pressure of hydrogen and oxygen are given by

$$P_{H_2} = RH_c\rho^{st}_{H_2O}\left(\frac{1}{\frac{RH_c\rho^{st}_{H_2O}}{\rho_c}e^{\frac{4.192(i/A)}{T^{1.334}}}} - 1\right) \tag{3.2}$$

$$P_{H_2} = 0.5RH_a\rho^{st}_{H_2O}\left(\frac{1}{\frac{RH_a\rho^{st}_{H_2O}}{\rho_a}e^{\frac{1.635(i/A)}{T^{1.334}}}} - 1\right) \tag{3.3}$$

Saturation pressure of water vapor can be calculated by

$$\log_{10}(\rho^{st}_{H_2O}) = 0.0295(T_{cell} - 273.15) - 9.19 \times 10^{-5}(T_{cell} - 273.15)^2 + 1.44 \times 10^{-7}(T_{cell} - 273.15)^3 - 2.18 \tag{3.4}$$

The terminal voltage of the single cell is obtained by subtracting the losses occurring inside the fuel cell which are activation loss, mass transfer loss and ohmic loss.

$$V_{cell} = E_{nernst} - \eta_{act} - \eta_{ohm} - \eta mt \tag{3.5}$$

Activation loss occurs due to delay caused by chemical process taking inside the cell and calculated by

$$\eta_{act} = -[Y_1 + Y_2T_{cell} + Y_3T_{cell}\ln(C_{O_2}) + Y_4T_{cell}\ln(i)] \tag{3.6}$$

$$C_{O_2} = \frac{\rho_{O_2}}{5.08 \times 10^6 e^{-498/T}} \tag{3.7}$$

As electrodes and polymer membrane have some electrical resistance along the conducting of the path connecting membrane and electrode lead to ohmic losses given by

$$\eta_{ohm} = i(R_M + R_c), \qquad R_M = \frac{\rho M^l}{A} \tag{3.8}$$

$$\rho_M = \frac{181.6 \left\{ 1 + 0.03 \left(\frac{i}{A} \right) + 0.062 \left(\frac{T_{cell}}{303} \right) \left(\frac{i}{A} \right)^{2.5} \right\}}{\left\{ \lambda - 0.634 - 3 \left(\frac{i}{A} \right) \right\} + exp \left(4.18 \left(\frac{T_{cell} - 303}{T_{cell}} \right) \right)} \tag{3.9}$$

The change in concentration of reactants at the electrode surface causes concentration loss given by

$$\eta_{mt} = -\beta \ln \left[1 - \frac{i_{den}}{i_{limit,den}} \right] \tag{3.10}$$

The unknown parameters could be calculated using global optimization technique as suggested in [108, 109].

3.2.2 Intelligent interfacing unit

The proposed intelligent interfacing unit consists of the boost converter and GA-assisted controller. The boost converter makes the source and load voltages compatible by stepping up the voltage level as a function of the duty ratio. Further,

BS DC distribution bus requires reliable, uninterrupted and well-regulated DC supply of 48V. Hence, boost converter should provide a well-regulated voltage with fewer ripples at the output. Also, it should settle to steady state after any sudden disturbance and rise after any input failure, in minimum time with permissible undershoots and overshoots in the output voltage. Therefore, it is often operated in a closed loop which is shown in Fig. 3.3 to meet the requirements of the interfacing unit. In a closed loop configuration, the output voltage (i.e. DC distribution bus voltage) is sensed with the help of voltage sensors and compared with a reference voltage in a comparator which generates the error signal ($e(t)$). Then, $e(t)$ is fed to the proportional-integral (PI) controller which produces the control signal ($u(t)$) as a function of its parameters i.e. proportional gain (K_P) and integral gain (K_I). Based on the PWM control law, the modulator generates the firing pulses for the gate driver of the semiconductor switch i.e. MOSFET by comparing it with a carrier signal of switching frequency. For output voltage regulation, the optimal switching of MOSFET is required that is dependent on the optimal selection of K_P and K_I. In the following section, modelling of the boost converter has been carried out to analyse the dynamic response of the boost converter, and the controller is designed for closed loop operation to meet the requirements of the interfacing unit.

3.2.2.1 Modelling of the boost converter

The boost converter with MOSFET as semiconductor switching device is presented in Fig. 3.3 The design parameters of the boost converter are input voltage (V_{in}) = 26-39V, output voltage (V_o) = 48V, inductor (L) = 0.01mH, capacitor (C) = 21.6 mF, load resistance (R) = 1.20, and switching frequency (f_s) = 20kHz. State space averaging techniques is used to describe the dynamics of the system. The two states considered here are inductor current and capacitor voltage. Further, a large signal model of the boost converter is presented by following state space equations. During the interval DT_S (i.e. 'ON' state of switch), behavior of the system is described as

$$\dot{x} = Ax + BV_{in},\ y = Ex \tag{3.11}$$

$$A = \begin{bmatrix} \frac{-r_L}{L} & 0 \\ 0 & \frac{-1}{C(R+r_C)} \end{bmatrix}, B = \begin{bmatrix} \frac{1}{L} \\ 0 \end{bmatrix}, E = \begin{bmatrix} 0 & \frac{R}{(R+r_C)} \end{bmatrix} \tag{3.12}$$

During the interval $(1 - DT_S)$ (i.e. 'OFF' state of switch), behavior of the system is described as

$$A = \begin{bmatrix} \frac{-r_L + \frac{Rr_C}{(R+r_C)}}{L} & \frac{-R}{C(R+r_C)} \\ \frac{R}{C(R+r_C)} & \frac{-1}{C(R+r_C)} \end{bmatrix}, B = \begin{bmatrix} \frac{1}{L} \\ 0 \end{bmatrix}, \tag{3.13a}$$

$$E = \begin{bmatrix} \frac{Rr_C}{(R+r_C)} & \frac{R}{(R+r_C)} \end{bmatrix} \tag{3.13b}$$

Averaged large signal model is obtained by averaging the circuit during DT_S interval and (1-DT_S) interval over the one cycle is given by

$$\dot{x} = \begin{bmatrix} \frac{-r_L}{L}D + (1-D)\frac{r_L + \frac{Rr_C}{(R+r_C)}}{L} & (1-D)\frac{-R}{C(R+r_C)} \\ (1-D)\frac{R}{C(R+r_C)} & \frac{-1}{C(R+r_C)} \end{bmatrix} x + \begin{bmatrix} \frac{1}{L} \\ 0 \end{bmatrix} \tag{3.14a}$$

$$y = \begin{bmatrix} (1-D)\frac{Rr_C}{(R+r_C)} & \frac{R}{(R+r_C)} \end{bmatrix} x \tag{3.14b}$$

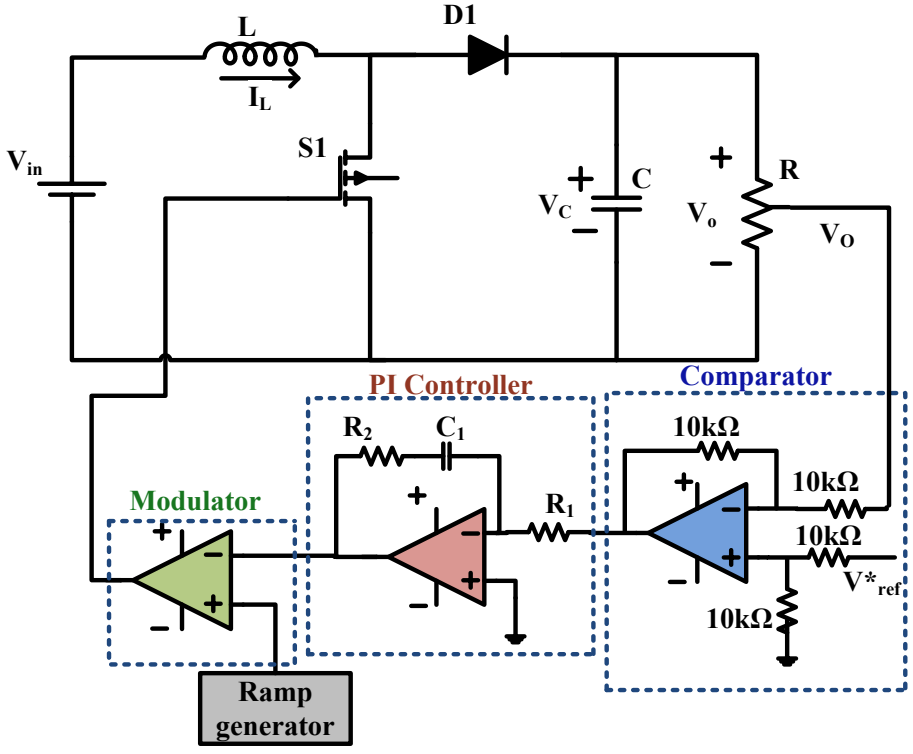

Figure 3.3: Closed loop operation of boost converter

3.3 Problem formulation

The schematic of boost converter along with closed loop controller is presented in the Fig. 3.3. In PWM control law, the feedback signal of V_o is compared with the reference voltage (V_{ref}) and the error signal is generated as

$$e(t) = V_{ref} - V_o(t) \tag{3.15}$$

Further, the error is fed into the PI controller that gives control output to generate gate pulses to the converter.

$$u(t) = K_P - K_I \int e(t) \tag{3.16}$$

In this chapter, the parameters of the controller are obtained by using proposed GA based optimization for the boost converter based intelligent interface system for PEMFC powered BS system. The proposed GA-assisted controller considered the voltage regulation using boost converter at the DC distribution bus of the BS as an optimal control problem. A suitable fitness function is formulated for GA based on which it provides optimal values of K_P and K_I parameters. The proposed controller provides well-regulated output as well as fast robust, dynamic response of the interfacing system for the PEMFC. In addition, the performance characteristics of the proposed GA-assisted controller for intelligent interfacing unit is compared with conventional ZN tuning method of PI controller.

3.3.1 Ziegler and Nichols control technique

The conventional ZN method is used to tune PI controller for the proposed boost converter based interfacing system of PEMFC supplied BS. In this approach, the proportional controller gain is increased till closed loop system becomes critically stable. Proportional gain corresponding to this point is called as ultimate gain and the corresponding time period of oscillation is called as the ultimate time period. The K_P and K_I are calculated as 0.45 times ultimate gain and 0.83 times ultimate time period respectively.

3.3.2 Proposed genetic algorithm-assisted controller

Genetic algorithm mimics the adjustability, robustness, and efficiency of natural genetics and natural selection. It doesn't require any derivative information of the problem. This reduces the computational burden as well as search time to find the global optimum solution. The objective function is formulated so as to minimize error $e(t)$ using the performance indices given below:

$$\text{Performance index} \quad \text{ITAE} = \int_{t}^{t_{\text{sim}}} |e(t)|\, d(t) \tag{3.17}$$

$$\text{Minimize} \quad \text{F}(\phi) = \text{ITAE} \tag{3.18}$$

$$\text{Subjected to } \phi_{min} \leq \phi \leq \phi_{max}, \tag{3.19}$$

Where, $\phi = f(K_P, K_I)$ and indicates the boundary conditions for controller parameters. The different steps involved in GA-assisted controller design the GA are shown by flowchart in Fig. 3.4. As analysed from literature, population size

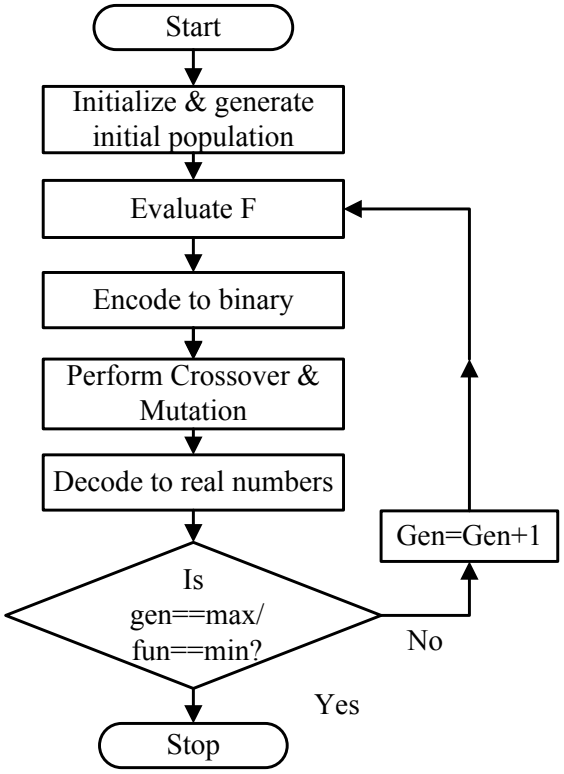

Figure 3.4: Flowchart of GA

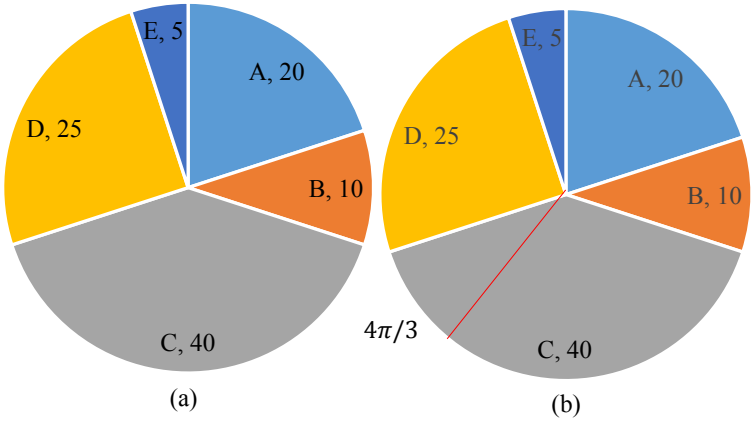

Figure 3.5: Roulette wheel procedure for chromosome selection

could be in the range of 10-30 for single objective function. In this chapter, the population size of 15 is chosen to have a trade-off between population diversity and convergence for a problem having many objectives formulated as a single linear function. New chromosome i.e. offspring is produced through the process of reproduction which includes the selection of parent population and applying

crossover and mutation operators. After the computation of fitness level for each chromosome, fittest are selected using roulette wheel method as parent population to form the mating pool. This process mimics Darwins concept of survival of the fittest. In roulette wheel selection method, a virtual wheel is created in which chromosome is assigned a sector proportional to its fitness function value. The procedure is explained in Fig. 3.5(a) with five chromosomes namely A, B, C D and E. Now, generate an angle randomly, and the chromosome corresponding to generated angle was selected. In Fig. 3.5(b), a randomly generated angle of 4/3 rad. is shown. Thus, chromosome C gets selected. In the present problem, the multi-point crossover is chosen which increases the efficiency as two solution variables are rooted in one chromosome. Another genetic operator is a mutation in which any bit of the chromosome is toggled depending upon the probability of occurrence of mutation. Stop the program when generations reach maximum defined limit or function value reaches minimum tolerance value ('min') i.e. stagnation condition is reached.

3.4 Results and discussion

As the roadmap of national telecom policy 2012, the telecom industry would penetrate deep into remote rural areas which don't have a quality and reliable supply from the grid. Telecom companies have to ensure reliable and uninterrupted supply to BS of the telecom tower as they are bound to provide quality service to customers without any rolling out. Due to which the dependency of telecom industry on the DGset has increased which has increased the OPEX and carbon emissions of the telecom sector. Hence, a PEMFC based renewable hybrid supply architecture for BS is proposed under the green initiative taken in national telecom policy 2012 by department of telecommunication to address this issue. The proposed PEMFC based power supply to BS not only provides a green solution for telecom by eliminating DGset but also reduces the battery bank size which is the bulkiest and expensive part regarding maintenance. For interfacing PEMFC with BS load, a boost converter based intelligent interfacing unit is proposed with a robust genetic algorithm based fast dynamic response controller. The proposed controller regulates the 48V at DC distribution bus of the BS under the load

variations and input supply fluctuations. The performance characteristics of proposed GA-assisted controller are compared with ZN based PI controller for boost converter interface for PEMFC supplied BS. PEMFC provide 30V DC supply to 1.8kW of BS telecom load under standard conditions. But, under varying load condition and environmental conditions like humidity, temperature, and pressure the output of PEMFC may range from 26V to 39V. The telecom load also may vary from 500W to 2.2kW depending on the number of transceivers operating as per the communication signal traffic. Thus, the proposed boost converter with GA-assisted controller as the interfacing system for PEMFC supply acts as a buffer between the load and supply. The proposed GA-assisted controller ensures 48V DC at the DC distribution bus of the BS system.

The proposed GA based control technique is tested for the following conditions to ensure 48V DC regulation at the distribution bus for the all possible conditions of operation of the system.

- Input disturbance rejection: This is simulated as testing the control technique for a step increase in input voltage (V_{in}) of boost converter from 26V to 39V and as step decrease in input from 39V to 26V.
- Output disturbance rejection: It tests the performance of controller for 22% of overloading i.e. 2.2kW during the peak traffic of communication signals and 72% of under loading condition i.e. 0.5kW load when only one transceiver is in operation.
- Reference tracking: The capability of the proposed control technique to able to track V_{ref} is tested for $\pm$10% of the distribution bus voltage i.e. 53V and 43V.

The performance of the proposed GA-assisted control technique is weighed against the conventional method of regulating the output of boost converter i.e. ZN based tuned PI controller. The K_P and K_I parameters of PI controller calculated from ZN method are 0.0406 and 8.12 respectively. A dedicated program for GA is developed in Matlab and executed for 50 generations to find the optimal global values of PI controller as 5 for K_P and 53.1281 for K_I. The V_{in} is increased from 0 to 30V (output voltage of PEMFC under normal operating conditions) for given

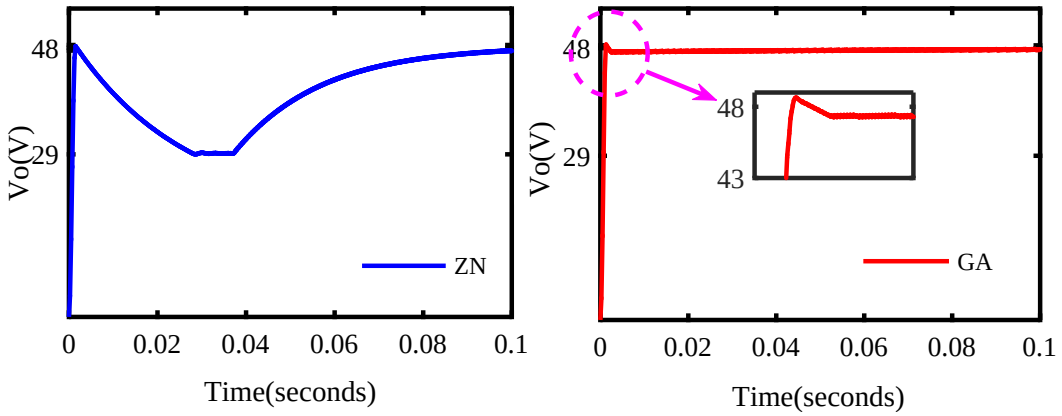

Figure 3.6: V_o of interfacing unit using ZN and GA-assisted controller when V_{in} is increased from 0 to 30V at time=0s.

Table 3.1: Dynamic response of interfacing unit with ZN and GA-assisted controllers

Specifications	ZN tuned controller	GA-assisted controller
Rise time (ms)	1.14	1.00
Peak Time (ms)	22.50	1.30
Overshoot (+) /undershoot (-) (%)	38.50 (-)	0.00
Settling time (ms)	98.42	30.0

load of 1.8kW to track the given reference voltage of 48V. The dynamic response of the interfacing unit with ZN controller as well with GA-assisted controller for the above-stated conditions is shown in Fig.3.6. The response of interfacing unit with ZN controller indicates that converter response undergoes an undershoot of 38.50% reaching the value of 29V and settles to steady state value in 98.42ms. The response of the interfacing unit with GA-assisted controller does not exhibit any undershoot or overshoots. Moreover, it takes settling time of 30ms only. The detailed analysis of dynamic response obtained from both the techniques is tabulated in table 3.1. The proposed GA-based controller is around 85% faster than ZN based PI controller. Also, the rise time for GA-assisted controller is improved by 14%.

Further, the robustness of GA and ZN based controller against fluctuations in PEMFC output voltage are carried out as input disturbance. In Fig. 3.7a, input voltage undergoes a step increase from 26V to 39V at 0.5s, GA-assisted controller

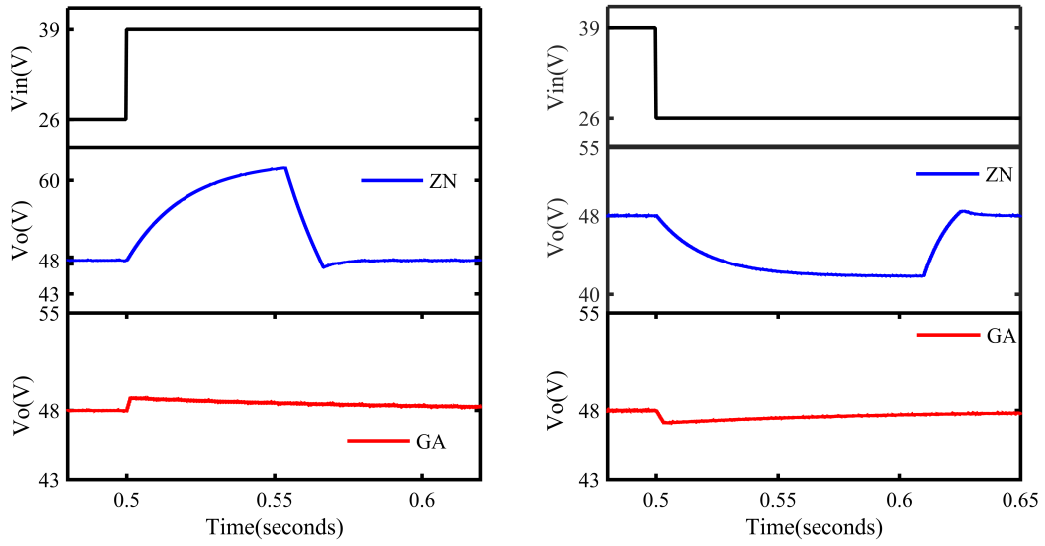

Figure 3.7: V_o of interfacing unit using ZN and GA-assisted controller for input disturbance rejection, change in V_{in} from (a) 26V to 39V at time=0.5s (b) 39V to 26V at time=0.5s.

settles quickly in 40ms with less overshoot of 0.88%. Whereas, ZN based controller takes a long time of 66.6ms to settle with overshoot of 28% and undershoot of 1.3%. In Fig. 3.7b, a step decrease in input voltage from 39V to 26V is introduced at 0.5s. The proposed GA-assisted controller settles in only 65.5ms with less than 1% undershoot. While using ZN based controller, the response of boost converter is poor with settling time of 121.8ms and undershoot of 11.47%. Thus, the results confirm the working of GA-assisted controller and superior tracking capability during input disturbance. In Fig. 3.8, the robustness of the proposed GA-assisted controller is tested on load variations. The Fig. 3.8a shows the response of the interfacing unit with GA-assisted controller and ZN controller for load variation from minimum load to rated load. It is observed that decrease in load leads to reduction in load current for maintaining a constant voltage of 48V at the distribution bus. The response curve of the converter with ZN controller shows a huge undershoot of 38.86% reaching a value of 29V in 26.6ms and settles to steady state in 101.70ms. Comparatively, GA-assisted controller smoothly settles to the steady-state value within 72.40ms. The Fig. 3.8b, shows the response curve of both controllers with a boost converter. The ZN based controller takes a dip of 12.13% in 35.70ms and settles to steady state in 47.10ms. However, the GA-

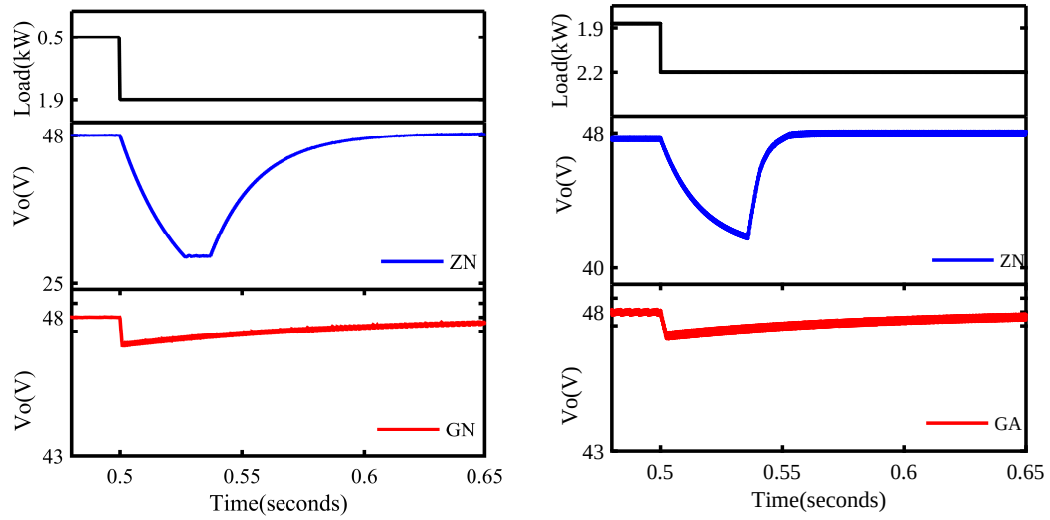

Figure 3.8: V_o of interfacing unit using ZN and GA-assisted controller for output disturbance rejection (a) under loading condition current at time=0.5s (b) overloading condition at time=0.5s.

assisted controller smoothly and quickly reaches the steady state value in 34ms. It is evident from the results that the GA-assisted controller performed superior to the conventional controller.

In Fig. 3.9, the reference voltage step change of ±10% is introduced at 0.5s. The ZN based controller suffers from a delayed response as shown in Fig. 3.9. It takes a delay of 25ms to respond to change in reference from 48V to 43V. Further, the output reaches the steady state value without any overshoots and undershoots taking an overall time of 48ms. It is noted from the Fig. 3.9b that the proposed GA-based controller quickly tracks the reference change in 3.5ms. Similar response of GA-assisted controller is shown in Fig. 3.9a, where it follows the change in reference voltage of 53V to 48V introduced at 0.5s in 2.40ms only. Whereas conventional ZN based controller takes long settling time 71.10ms to track the reference change triggered at 0.5s shown in Fig. 3.9b.

A detailed comparison of proposed GA-assisted controller with conventional ZN based controller for robustness on input, output disturbances and the reference tracking capability is summarized in table 3.2. It could be noted that for input disturbance rejection, a step increase in Vin from 26V to 39V with GA-assisted

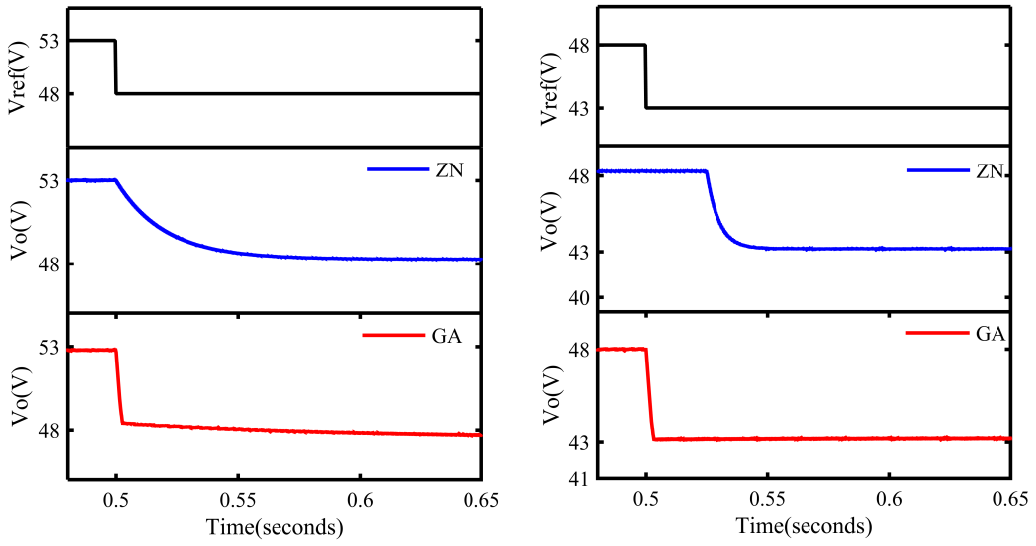

Figure 3.9: V_o of interfacing unit using ZN and GA-assisted controller for reference tracking, V_{ref} changes from (a) 53V to 48V at time=0.5s (b) 48V to 53V at time=0.5s.

controller the overshoot or undershoot reduces by 96.41% while the settling time improved by 50.28%. Similarly, for a step decrease in V_{in} from 39V to 26V, GA-assisted controller outperformed the conventional controller by reducing undershoot or overshoot by 91.37% and settling to steady state 46.22% faster. Further, for output disturbance rejection, a step decrease in load, has reduction in undershoot by 96.86% with the use of GA-assisted controller as compared to the conventional controller. It improves the settling time by 28.81%. In step increase in load, overshoot reduces from the value of 12.13% as with conventional controller to 0.947% and settles in 34 ms only as in the case of GA-assisted controller. For validating the performance of proposed controller for reference tracking capability, a step increase in V_{ref} from 48V to 53V is triggered. The system with GA-assisted controller settles in 2.40ms which is 96.47% faster than a conventional controller. A similar response of the system with GA-assisted controller is noted for the step decrease in V_{ref} 48V to 43.2V is triggered. The system settling time improves by 92.54% with GA-assisted controller.

Table 3.2: Comparative analysis of dynamic response of proposed hybrid controller

Test cases	Mp (%)		Ts (ms)	
	ZN	GA	ZN	GA
Step increase (28-43)V	27.6(+)	0.99(+)	71.8	35.7
Step decrease (43-28)V	11.47(-)	0.99(-)	121.8	65.5
Step increase (12-50)A	38.86(-)	1.22(-)	101.7	72.4
Step decrease (50-12)A	12.13(+)	0.947(+)	47.1	34
Step increase (48-53)V	0	0	68	2.4
Step decrease (53-48)V	0	0	36.2	2.7

3.5 Summary

In this chapter, a PEMFC based power supply for the BS of remote/rural telecom towers is proposed for enhancing the performance and reduce OPEX of the system. The reliable, continuous and quality of power supply to the loads is ensured by matching the voltage level of PEMFC with DC distribution bus, regulating the voltage at the bus and providing a buffer between the load and supply. These features are incorporated into the interfacing unit by the proposed GA-assisted controller. The GA-assisted controller has made the response of the interfacing unit much faster as 85% than the conventional system. The controller ensures the tight regulation of the DC bus voltage during the load variations at BS and voltage fluctuations in the source. Further, the proposed interfacing unit with GA-assisted controller facilitates easy, frequent and smooth switching of the telecom tower load without degrading the transient responses of the overall system. This feature allows the optimal load sharing among the towers without loss of efficiency, time lag and no risk of system failure is involved. A clean, green, modular and flexible PEMFC based telecom supply has been proposed and implemented to facilitate the telecom industry's expansion while addressing all the issues regarding conventional way. Thus, the proposed PEMFC supply system including intelligent interfacing unit is a promising solution for achieving the 'green telecom' targets laid by national telecom policy 2012.

Chapter 4

HRES powered BS with modified adaptive real coded genetic algorithm-assisted interfacing converter

4.1 Introduction

India is the second largest telecom market in the world with 700 million subscribers. Nearly 50% of towers are situated in rural areas which are either off-grid or faces long hours of load shedding. Moreover, the reliable start-up of DGset is questionable, due to which it is equipped with two starters which make the starting slow and DGset operation expensive. Further, the replacement and maintenance cost of batteries adds to the OPEX of telecom towers. In off-grid and bad grid regions, energy consumption contributes to the 70% of the overall OPEX [26]. Thus, there is need to find the alternative resources to supply the BS such that BS power supply has high power density, high efficiency, low operating cost, regulated DC bus voltage, uninterrupted, reliable and environment-friendly.

In previous chapter, PEMFC based power supply is proposed for the BS in remote/rural areas. Also, regulated DC bus voltage is ensured by the proposed

interfacing unit consisting of boost converter with intelligent hybrid controller. The proposed controller is easy to implement similar to linear controller and has robust dynamic response against load, source and reference disturbances. Though PEMFC based supply is environment-friendly but doesn't fulfill all the prerequisites of the BS power supply. The fuel cell has large time constant in order of minutes so, can't perform satisfactorily for fluctuating loads. Therefore, in the present chapter, renewable based BS power supply topology is proposed. Integration of renewable resources to the DC bus also need interfacing unit. Thus, selection of SMPC for the integration of renewable resources to the DC bus is discussed. Cuk converter is implemented in this chapter for integration of renewable resources to DC bus. The choice Cuk converter provides the wide range of operation, compactness and ripple free input and output current.

The intelligent hybrid controller concept which is proposed in previous chapter, inherits the best features of linear controllers and meta-heuristic techniques. The controller is a fixed frequency controller with smooth implementation and robust against load and source disturbances. Additionally in this chapter, the intelligent hybrid controller is improved by proposing a modified adaptive real-coded genetic algorithm (MARCGA) to tune the PID parameters. Unlike the binary GA, MARCGA handles the real numbers, has similarity check and enhanced diversity in the population. The various algorithms such as binary GA, PSO, MARCGA and, GWO are used for the tuning of PID controller parameters. Further, the objective function to evaluate the fitness of the solution candidate in the optimization process is improved by considering the dynamic specification parameters ($M_P, T_s,$ and T_r) along with ITAE. The performance of intelligent controller tuned with each algorithm is compared by the dynamic performance characteristics of the interfacing converter. Performance analysis of the Cuk converter with intelligent hybrid controller is validated by developing a laboratory prototype.

The chapter organization is as follows. The intelligent hybrid controller with meta-heuristic algorithms and problem formulation are explained in section 4.2 and 4.3. Performance of the the controller implemented with boost converter is discussed in section 4.4. Then, the architecture of the proposed HRES BS power supply is explained along with selection of SMPC for the HRES in section 4.5. It is followed by mathematical modelling of renewable resources in section 4.6. After-

wards the same controller is implemented with Cuk converter. Section 4.7 gives the modelling of Cuk converter. The detailed simulation are carried to analyze the performance the controller with Cuk converter for reference tracking, source and load disturbance rejection capabilities in section 4.8. Later, the laboratory prototype is developed in section 4.9 and concluding remarks in section 4.10

4.2 Intelligent hybrid controller

The proposed controller has the best features of both PID controller and meta-heuristic optimization control algorithms. The industry has been using PID controllers for many decades for simple, inexpensive implementation, fairly robust performance and fixed frequency operation. Controller does not cause any control complexity associated with variable frequency operations like chattering or sub-harmonic oscillation. The performance of PID controller hugely depends on how well the parameters (K_P, K_I, and K_D) are tuned for the plant. Conventionally, PID parameter tuning has been done based on the small signal model of the plant linearized around the operating point. If the averaged model is used, the switched behavior of the converter is not captured. Hence, the parameter tuning should be done for such a model of the converter that includes the non-linearity with time varying nature of the converter. The uncertainties on load or source along with parameter variation should also be considered. It is known that designing the parameters for the continuous time model of the converter would be best tuned. Thus, the meta-heuristic algorithm is the best option for tuning of the parameters of PID as it looks on the system as a black box. Further, the trade-offs among different performance specifications of the dynamic response of the interfacing converter with PID controller tabulated in table 4.1 are satisfied by the algorithms by using improved objective function presented in this chapter. The MARCGA is proposed to find the optimal tuning of the PID controller. The potential of the proposed algorithm is compared with controller tuned by existing GA, PSO and GWO. According to no free lunch theorem, one algorithm is not best suited for all the engineering problems. The present chapter explores the potential of GA, MARCGA, PSO and recently developed GWO for proper tuning of the PID which would result in the robust controller.

Table 4.1: Effect of PID parameters on dynamic response

Parameter	Rise time	Overshoot	Settling time	Steady state error
K_P	Reduce	Increase	Less effect	Reduce
K_I	Reduce	Increase	Increase	Eliminate
K_D	less effect	Reduce	Reduce	No effect

4.2.1 Genetic algorithm

GA is a meta-heuristic algorithm based on population genetics implementing Darwin's concept of 'survival of the fittest'. The initial population of the solution variable is generated which is encoded to binary form. The size of chromosome decides the accuracy and the amount of quantization error during the conversion from real numbers to binary number.The objective function F is evaluated to estimate fitness of each chromosome. Then the parent was selected by a selection process like a roulette wheel or tournament selection which is analogous to natural selection. Parent population recombines through the genetic operator i.e. crossover to generate offspring. Based on mutation probability, offspring undergo mutation to sustain the divergence in population to aid the exploration of the solution search space. Figure 4.1a illustrates the different steps of the algorithm in the form of a flowchart. In this study binary-coded chromosome of length 14 and population size of 100 is considered. Parent population is selected using roulette wheel selection procedure, and offspring are reproduced using probabilistic crossover and mutation. The offspring are produced by process of roulette wheel selection,probabilistic crossover and mutation.

4.2.2 Particle swarm optimization

PSO is an optimization algorithm inspired by the cooperative social behavior of the groups. It imitates the concept that how birds find their food in the confined area. It uses real number coding to represent the swarm population particles. In this study swarm size of 30 is chosen. The position of the particles with their velocity is initialized. Then fitness of each particle is calculated by evaluating the objective function. Each particle keeps the record of its best position (L_b)

and accordingly global best (G_b)for the whole swarm is updated in each iteration. The velocity (V_p) and position (P_p) are maintained using (4.1). The flowchart describing the steps in the algorithm is shown in Fig. 4.1b. For $(k+1)^{th}$ iteration,

$$V_p(k+1) = w\,V_p + c_1 r_1(L_b - P_p) + c_2 r_2(G_b - P_p) \tag{4.1a}$$

$$P_p(k+1) = P_p(k) + V_p(k+1) \tag{4.1b}$$

where, c_1, c_2 are constants having the value of 2 and w is weight matrix.

4.2.3 Modified adaptive real coded genetic algorithm

In binary GA, all the genetic operators are performed on the binary represented the population, though the boost converter has continuous variables. With large population size and high degree precision, binary GA requires substantial computational time. Therefore, MARCGA is proposed in this chapter. In RCGA, genetic operators are applied to the real numbers directly that reduce the computation time. Further, a weighted similarity check is implemented on the population to replace the similar individuals by a random individual. The implemented similarity check reduces with the increasing number of generations which ensure the proper diverse explorability of the algorithm in the starting generations and aids exploitability in later generations. The systematic account of the proposed MARCGA algorithm is given in the Fig. 4.1c. The parent population is selected using roulette wheel selection procedure, and offspring population are generated by parent-centric crossover and non-uniform mutation.

4.2.4 Grey wolf optimization

GWO simulates the hunting mechanism and leadership hierarchy in apex predators of food chain i.e. a pack of grey wolves. There are four types of wolves in the pack, alpha (α) the leader, beta (β) the subordinators, omega (ω) the scapegoats and the remaining are delta (δ).

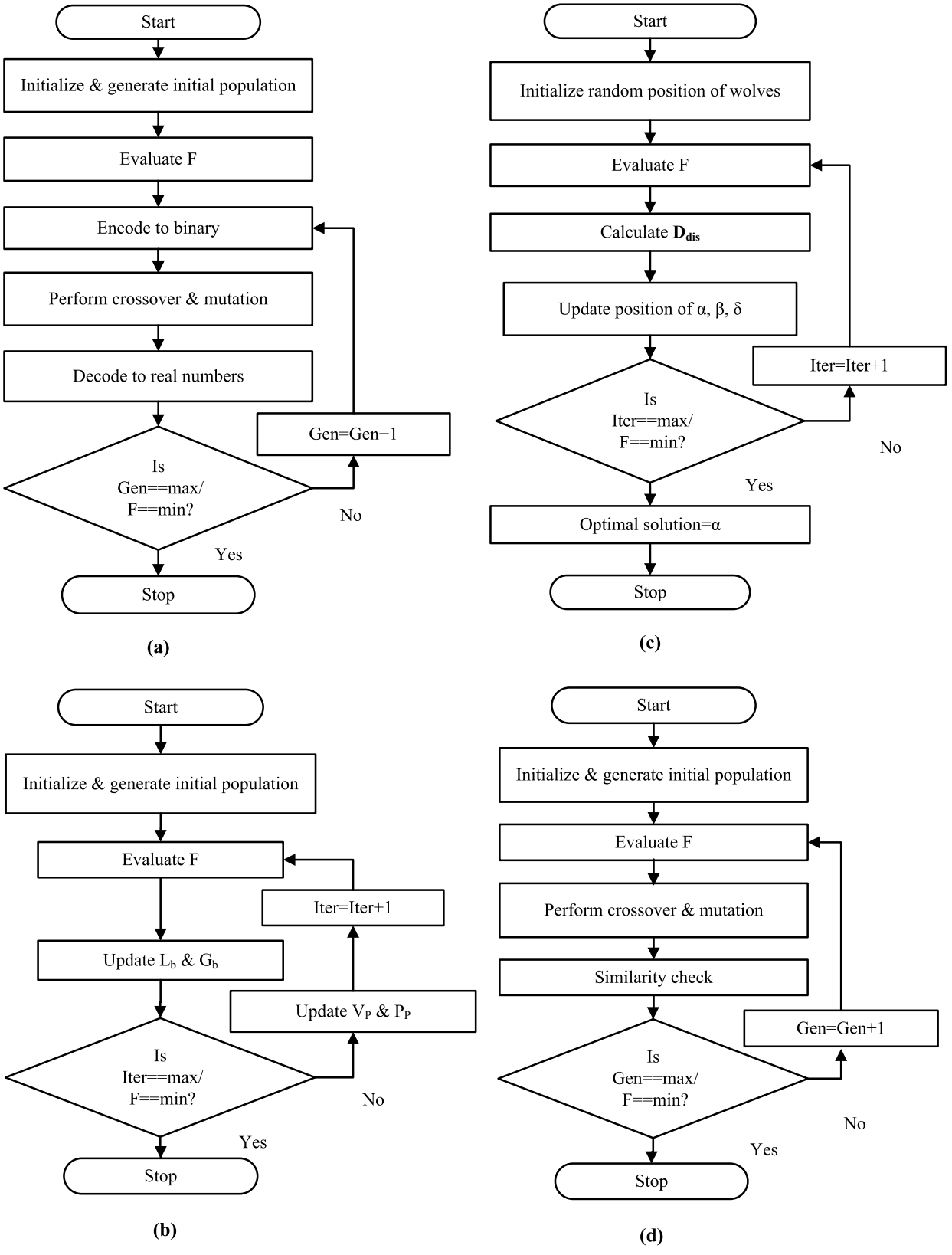

Figure 4.1: (a)Binary GA (b)PSO (c)GWO (d)MARCGA

These together in the pack of 5-12 perform the three steps of hunting: searching which aids in exploring the search space, encircling and attacking the prey supports the exploitation of the space. In the mathematical model of the algorithm, it keeps track of top four best solutions in the order as best assigned to the α, then to β, ω, and δ. The encircling is modeled for iteration k_{th} as

$$\vec{X}(k+1) = \left|\vec{X_p}(k) - \vec{A}\vec{D_{dis}}\right| \tag{4.2a}$$

$$\vec{D_{dis}} = \left|\vec{C}\vec{X_p}(k) - \vec{A}\vec{X}(k)\right| \tag{4.2b}$$

where, $\vec{A} = 2\vec{a}r_1 - \vec{a}$, $\vec{C} = 2r_2$, $\vec{a}$ varies linearly from 2 to 0. r_1 and r_2 are random variables in the range [0,1]. The flowchart of GWO algorithm is given in the Fig. 4.1d.

4.3 Problem formulation

An optimal control problem subjected to constraints having continuous and non-linear variables is formulated to achieve the desired performance of interfacing converter with the controller for the hybrid power supply for BS. The algorithm finds the minimum value of the objective function. Thus, proposed objective function F is stated in (4.3) considers the system dynamic specifications: settling time (T_S), rise time (T_R) and maximum overshoot (M_P) along with integral of absolute time error (ITAE).It is subjected to lower and upper limits of the PID parameters.

$$F = (T_S + T_R)e^{-1.5} + (M_P + \text{ITAE})(1 - e^{-1.5}) \tag{4.3}$$

where, $\text{ITAE} = \int_t^{t_{\text{sim}}} |V_{\text{ref}} - V_o|\, d(t)$
subject to: $C_{\min} \leq C \leq C_{\max}$, where, $C = f(K_P, K_I, K_D)$

4.4 Performance analysis of intelligent hybrid controller for boost converter in PEMFC power supply

The improved intelligent hybrid controller is first implemented on the boost converter for the PEMFC based BS power supply proposed in chapter 3. A dedicated computer program for the algorithms is developed in Matlab and executed for the maximum of 500 generations on the same machine with same initial conditions to ensure a similar platform for each algorithm. A graph is plotted for the variation of objective function value as the function of number of generation, to evaluate the capability of each meta-heuristic algorithm for tuning of PID controller parameters is shown in Fig. 4.2. The figure depicts that GWO has the fastest convergence rate as compared to other algorithms. It reaches the optimal solution within 20 iterations. Similar to GWO, PSO is also a swarm based optimization algorithm and converges fast within 31 iterations unlike population-based algorithm such as binary GA and MARCGA which take 234 and 456 iterations respectively. It is noted from Fig. 4.2 that PSO get trapped in local minima. As expected, MARCGA finds an optimal solution due to the modification introduced in classic binary GA such as similarity check and constraint real code population. The enhancement in diversification of the population has resulted in the accuracy to find the optimal solution. Therefore, MARCGA has a better exploration of the search space and attains the minimum value of the objective function among other algorithms, giving optimal solution. At the end of the iterative process for each meta-heuristic algorithm, the tuned parameters of the hybrid controller are tabulated in table 4.2. The robustness of the intelligent hybrid controller tuned with four different meta-heuristic techniques is checked for all the possible variations in the source or load side. The output of fuel cell is 36V under normal condition for 1.92kW load of the BS. The telecom load could vary from 0.6 kW when only one transceiver is working to 125% overloading condition i.e. 2.5kW load. The DC bus voltage tolerance limitation could be 10% of 48V. Thus, three different cases are formulated to analyze the dynamic performance of the intelligent converter with the proposed hybrid controller: (a) source side variations, (b) load side variations, and (c) reference tracking capability.

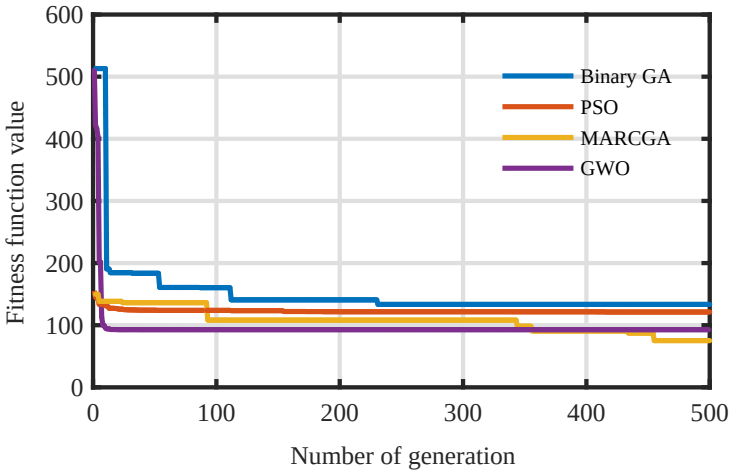

Figure 4.2: Convergence curve

Table 4.2: Dynamic response of the system for black start-up with tuned intelligent hybrid controller

Parameter→ Algorithm ↓	K_P	K_I	K_D	M_p (%)	T_r (ms)	T_s (ms)
Binary GA	0.5190	11.046	0.0037	1.98	28.32	159.34
PSO	0.3369	18.598	0.0038	3.02	18.95	118.68
GWO	0.7116	25.721	0.0006	2.48	6.90	89.60
MARCGA	0.5911	22.781	0.0009	2.17	6.45	86.16

4.4.1 Dynamic performance of the system due to source side variations

Variation in V_{in} to the interfacing converter is due to the variable output of the fuel cell may differ in the range of 28V to 43V depending on load or environmental conditions. Therefore, a maximum possible step increase from the lowest limit of output voltage of fuel cell to maximum limit i.e. 28V to 43V is introduced at t_1=0.4s, and a similar maximum step decrease in V_{in} from 43V to 28V is introduced at t_2= 0.65s. Figure 4.3 shows the dynamic response of the intelligent interfacing converter with intelligent hybrid controller tuned with binary GA, PSO, GWO,

and MARCGA. The V_o and I_o of the converter with binary GA-assisted controller settle to the steady-state value in 155.2ms after having an overshoot of 13.58% for a step increase in V_{in}. The settling time and undershoot are 179.7ms and 7.71% respectively for a step decrease in V_{in} as shown in Fig. 4.3a. In Fig. 4.3b dynamic response for V_o and I_o of the converter with PSO-assisted controller is presented. During step increase change in input, the V_o and I_o shoots up to 55.58V and 46.3A respectively and settles to 48V and 40A respectively in 84.3ms. Again, during step decrease of input, the V_o and I_o settles in 107.3ms after having undershoot of 7.92%. Figure 4.3c and 4.3d presents the V_o and I_o of the converter with the GWO and MARCGA-assisted controller takes a settling time of 81.8ms and 79.4ms respectively with an overshoot of 15.83% and 12.86% respectively when subjected to input disturbance at t_1=0.4s. Similarly, when converter with the GWO and MARCGA-assisted controller subjected to step decrease in V_{in}, the settling time is 81.8ms and 79.4ms respectively and overshoot is 15.83% and

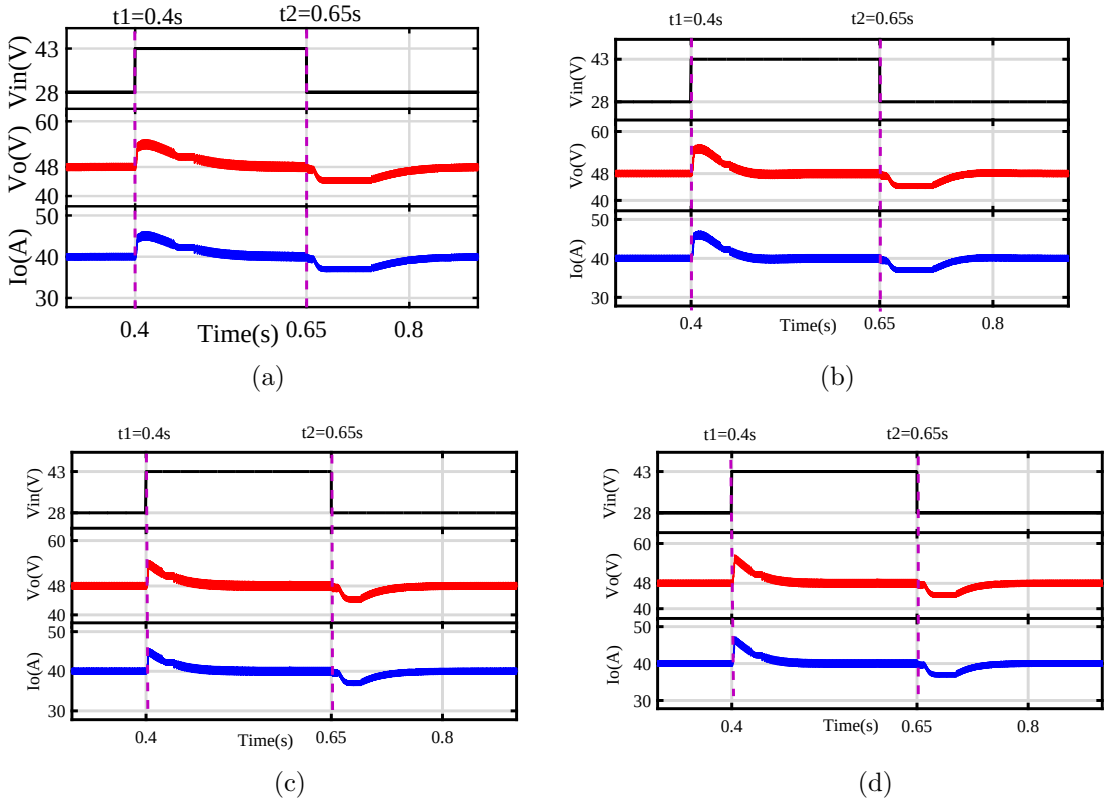

Figure 4.3: Dynamic response of the system during step change in V_{in} from 28V to 43V at t_1=0.4s and from 43V to 28V at t_2=0.65s using controller assisted by (a)GA (b)PSO (c)GWO (d)MARCGA

12.86% respectively.

4.4.2 Dynamic performance of the system due to load side variation

The telecom load varies as the function of traffic of communication signals. During very light traffic, only one transceiver works hence the telecom load is calculated as 0.6 kW and load current (I_o) as 12A. During heavy traffic, telecom load is calculated as 2.4kW and I_o as 50A. The interfacing converter is simulated for maximum possible variation in load condition, and dynamic response of the converter is given in Fig. 4.4. If the connected load is increased from 0.6kW to 2.4kW at t_1=0.4s, the

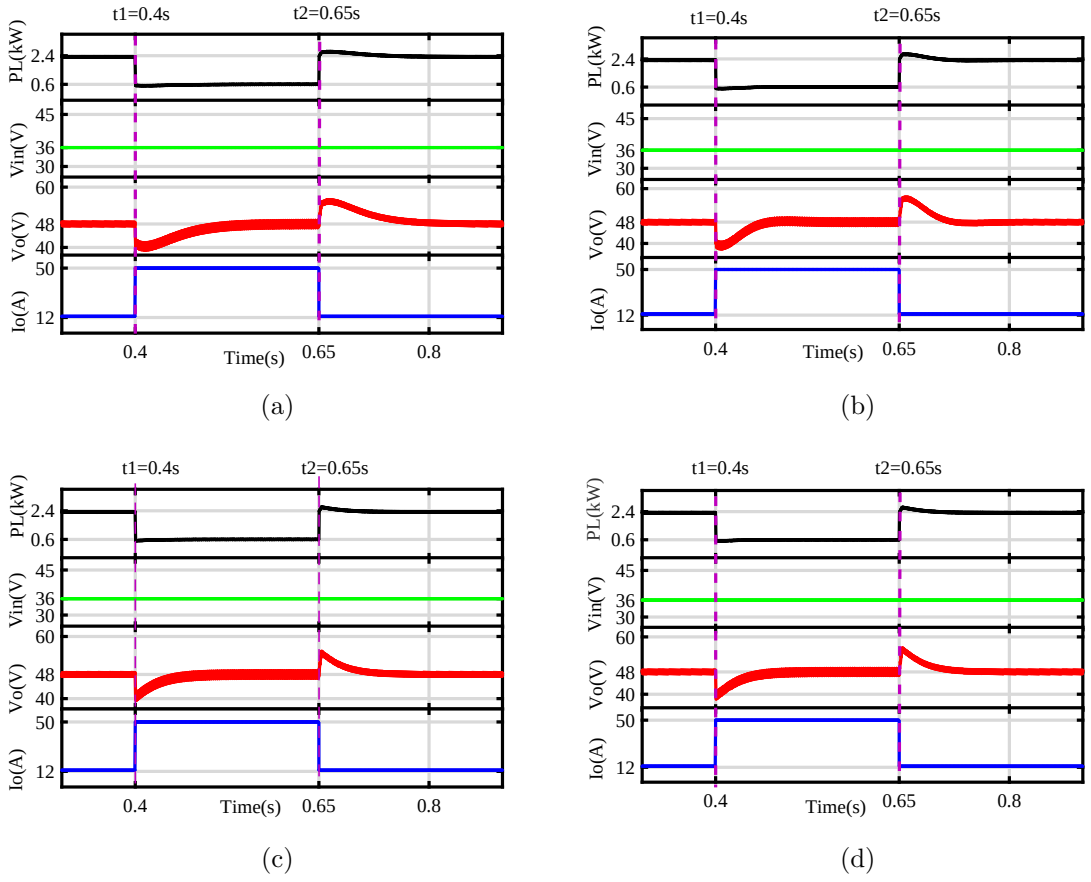

Figure 4.4: Dynamic response of the system during step change in load from 2.4kW to 0.6kW at t_1=0.4s and from 0.6kW to 2.4kW at t_2=0.65s using controller assisted by (a)GA (b)PSO (c)GWO (d)MARCGA

binary GA-assisted controller has undershoot of 16.35% and settles in 123ms. Now, the system is unloaded at t_2=0.65s, the V_o shoots by 15.10% and attains steady state value in 147ms. The PSO-assisted controller is employed during overloading of the system at t_1=0.4s, the system settles in 76.6ms but achieving a maximum undershoot of 18.40%. During unloading at t_2=0.65s, the system has a settling time of 83ms and maximum overshoot of 17.21%. The maximum undershoot with GWO and MARCGA-assisted controllers are 17.79% and 15.67% respectively with settling time of 98.1ms and 90.5ms respectively. A similar response is observed when the unloading of the system happens at t_2=0.65s. Maximum overshoot with GWO and MARCGA-assisted controllers are 16.50% and 14.00% respectively with settling time of 77ms and 75ms respectively.

4.4.3 Dynamic performance of the system due to reference tracking capability

The reference tracking capability is tested in the proposed system as by triggering a step increase in V_{ref} from 43V to 53V at t_1= 0.4s, and V_{ref} is decreased by same step size i.e. from 53V to 43V at t_2=0.65s. The dynamic response of the interfacing converter with proposed hybrid controller tuned with different meta-heuristic techniques is shown in Fig. 4.5. The dynamic response of interfacing converter with hybrid controller tuned with four meta-heuristic algorithms indicates the excellent reference tracking capability with each algorithm without any overshoot or undershoot. The binary GA-assisted and PSO-assisted controller settles in 1.2ms and 1.4ms respectively for a step increase and a decrease in V_{ref}. Similarly, GWO and MARCGA-assisted controller settles in 1.6ms while tracking the reference at t_1=0.4s and t_2=0.65s.

4.4.4 Comparative study of dynamic performance of the proposed hybrid intelligent controller

The performance of the proposed controller is tested for black start up of the fuel cell at 0.05s, and V_{in} attains the nominal value of 36V for rated load condi-

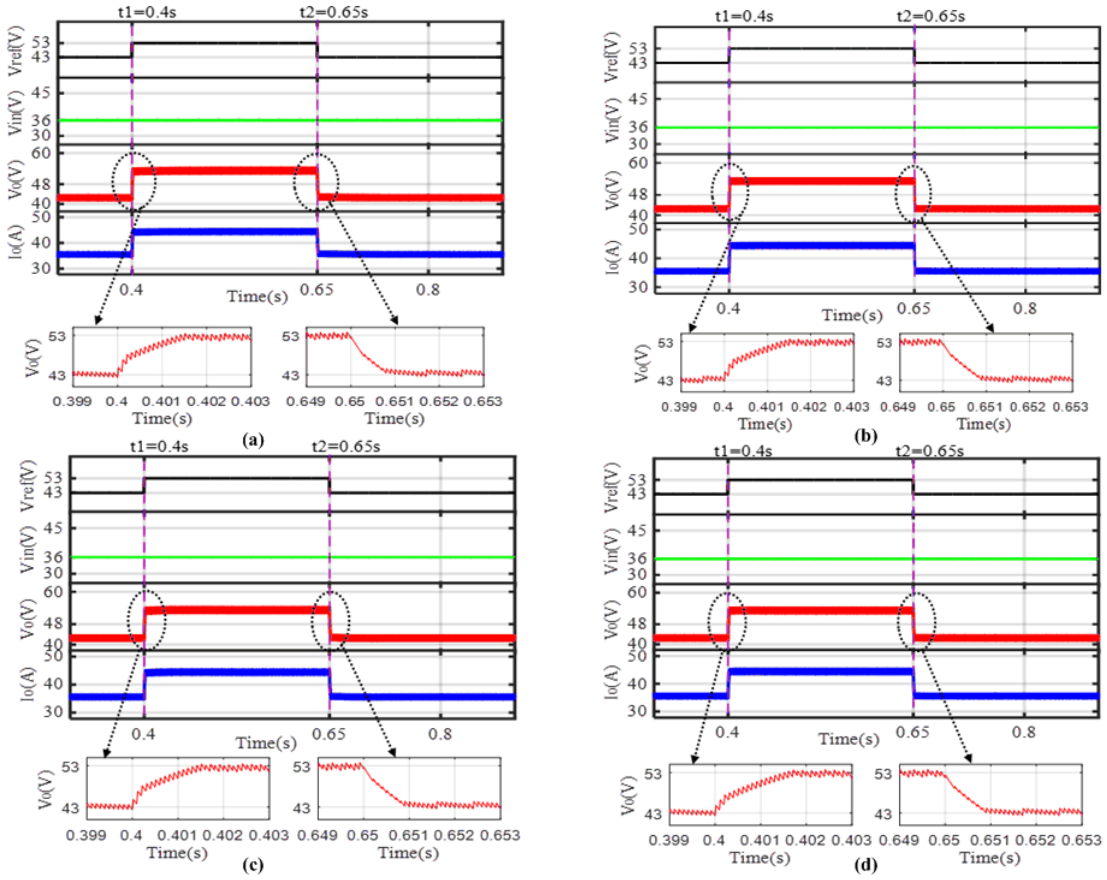

Figure 4.5: Dynamic response of the system during step decrease in connected load from V_{ref} from 43V to 53V at t_1=0.4s and step decrease in V_{ref} from 53V to 43V at t_2=0.65s using controller assisted by (a)GA (b)PSO (c)GWO (d)MARCGA

tions. The Fig. 4.6a shows the dynamic response curve of interfacing converter with the hybrid controller-assisted with binary GA, PSO, GWO, and MARCGA. The PSO tuned controller has the overshoot of 3.02% while binary GA-assisted controller response has minimum overshoot of 1.98%. The overshoot seen in the response curve with GWO and MARCGA are 2.48% and 2.17% respectively. The MARCGA-assisted controller dynamic response curve rises to 90% of the steady state value i.e. 43V in 6.45ms while binary GA-assisted controller has the slowest rise time of 28.3ms. The rise time of interfacing converter with a GWO-assisted controller is closer to that of MARCGA-assisted controller i.e. 6.9ms. The rise time of PSO-assisted controller is 18.95ms. The MARCGA-assisted controller settles to the steady-state value of 48V quickly in 86.16ms. Similar to rise time,

settling time is also closer to that of MARCGA tuned controller i.e. 89.6ms. The dynamic response curve of binary GA shows slow response with settling time of 159.34ms while settling time of PSO tuned controller is 118.68ms. The dynamic response specifications of interfacing converter tuned with all four algorithms are summarized in table 4.3. The comparative response of the proposed hybrid intelligent controller using different algorithms under input disturbance is presented in Fig. 4.6b. The interfacing converter with MARCGA-assisted controller is the fastest to settle after overcoming the input disturbance introduced at t_1=0.4s and t_2=0.65s.

The comparative analysis of the proposed hybrid intelligent controller using different algorithms under load disturbance is presented in Fig. 4.6c. The connected load is increased from the minimum load (0.6kW) to maximum load (2.4kW) at t_1=0.4s; the GA-assisted controller has undershoot of 16.35% which is minimum among all controllers while PSO-assisted controller has maximum undershoot of 18.40%. During overloading condition at t_2=0.65s, the MARCGA-assisted controller has the least overshoot of 14% and maximum when the PSO-assisted controller is employed. The binary GA-assisted controller shows a sluggish response during unloading and overloading conditions with settling time of 123ms and 147ms respectively. However, improvement in the settling time is observed in GWO-assisted and MARCGA-assisted controller for output rejection. However, the MARCGA-assisted controller was outperformed and having the minimum settling time among other controllers. The dynamic response of interfacing converter with hybrid controller tuned with four meta-heuristic algorithms indicates the excellent reference tracking capability with each algorithm without any overshoot or undershoot and settles to steady state value in less than 2ms.

As observed from the convergence curve shown in Fig. 4.2, MARCGA has reached the minimum value of the objective function. The response of the MARCGA-assisted controller for input and output disturbance rejection is best among all the controllers which is summarized in the table 4.3.

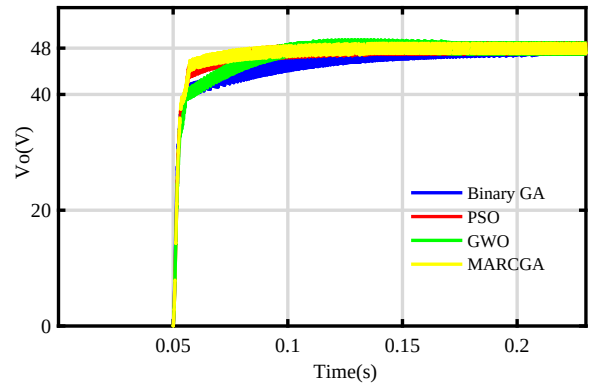

(a)

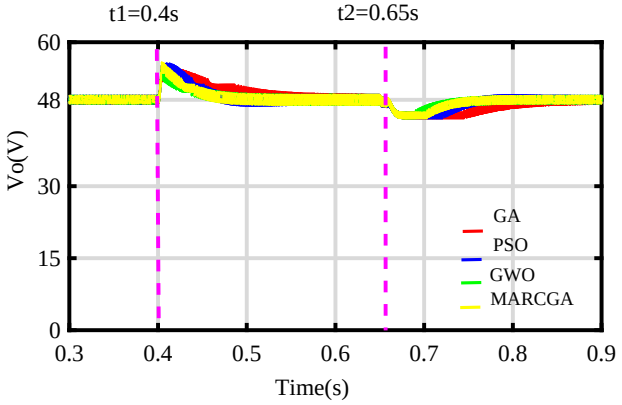

(b)

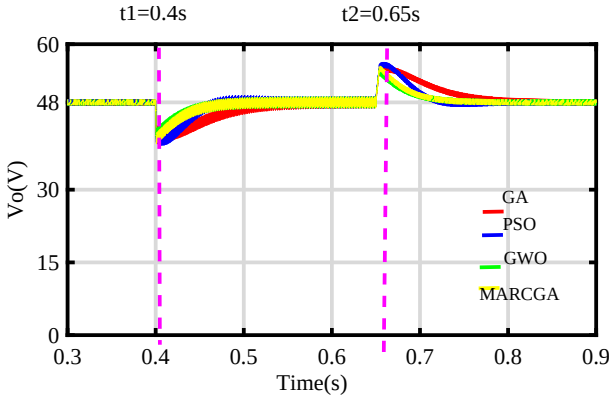

(c)

Figure 4.6: Comparative analysis of dynamic response of intelligent hybrid controller tuned with binary GA, PSO, GWO and MARCGA during (a)black start-up at t=0.05s (b)source side variation at t_1=0.4s and t_2=0.65s (c)load side variation at t_1=0.4s and t_2=0.65s

Table 4.3: Comparative analysis of dynamic response of proposed hybrid controller

	Overshoot (+)/ Undershoot (-)(%)				Settling Time (ms)			
	GA	PSO	GWO	MARCGA	GA	PSO	GWO	MARCGA
Step increase (28-43)V	13.58 (+)	15.63 (+)	15.83 (+)	12.86 (+)	155.2	84.3	81.8	79.4
Step decrease (43-28)V	7.71 (+)	7.92 (+)	7.71 (+)	7.50 (+)	179.7	107.3	98.1	90.5
Step increase (12-50)A	16.35 (+)	18.40 (+)	17.79 (+)	15.67 (+)	123	76.6	70	68
Step decrease (50-12)A	15.10 (+)	17.21 (+)	16.50 (+)	14.00 (+)	147	83	77	75
Step increase (48-53)V	0	0	0	0	1.2	1.4	1.6	1.6
Step decrease (53-48)V	0	0	0	0	1.2	1.4	1.6	1.6

4.5 Hybrid renewable energy system

Different alternative resources are implemented in literature to replace the DGset and automatic switch in the conventional power supply for the BS. Microturbine is more efficient than DGset considering the higher energy density of natural gas than diesel. Microturbine is proposed to replace DGset with automatic switch for a grid connected BS which faces long power outage in [9]. Unlike, DGset, microturbine is more cleaner as it emits CO_2 only, not the nitrous and sulphurous compounds [15]. However, microturbine operation is suitable for the base load operations because efficiency lowers at the reduced load operation. At reduced load cycles, overall system efficiency can be enhanced by utilizing the excess heat generation in a CHP [11]. Small microturbine coupled with solid-oxide fuel cell establishment is proposed to boost the thermal efficiency of the system [21]. A back-up solution using fuel cell without battery is proposed in [11]. Fuel cell operation is flexible, reliable and capacity doesn't degrade with time [23]. However, fuel cell has large time constant in order of minutes and can not handle frequent large step loads, large inrush currents, expensive and requires footprint. To buffer the large response time of the fuel cell, ultra-capacitor/super-capacitor based topologies are proposed to eliminate both battery and DGset [22]. This configuration considers the slow dynamics of fuel cell during load transients and also on-site batteries with long reserve time is necessary as back-up when system run out of hydrogen supply. Renewable resources and batteries supporting the integration of hydrogen technology is introduced [25].

India being a tropical country, has abundant potential of solar energy. Also, annual average wind speed of 5-6m/s makes wind energy an attractive solution to generate electricity [26]. Autonomous PV panels or WECS based BS power supply fails to provide the continuous supply to the telecom load considering the intermittent

Table 4.4: Energy density of energy storage elements

	Diesel	Compressed hydrogen	Lead-acid battery
Total energy (kWh/kg)	12	2	0.04
Useful energy (kWh/kg)	2.4	0.7	0.036
Conversion efficiency	0.2	0.35	0.9

nature of renewable resources due to seasonal and climatic periodic variations. Hence, the quality of network and services by the telecom tower degrades. There is a need of the back-up power supply to ensure the reliable and uninterrupted supply to the BS load. The energy density of the three energy storages which are diesel as fuel, compressed hydrogen (200 bar) and lead acid battery is presented in table 4.4. The battery has highest conversion efficiency among the energy storages given in table 4.4. Stand-alone PV with battery as back-up power supply design is discussed in [27]. The electricity generation from PV is available during day hours results in the need of long reserve hours for battery back-up which increases the OPEX of telecom operators due to the replacement cost of batteries. Similarly, WECS with battery based stand-alone telecom power supply is studied in [28]. To overcome the wind intermittency, the battery is supplying the load all the time and being charged by the WECS which increases the replacement cost of the batteries. It is noteworthy that solar and wind nature have complementary nature in daily, annual and regional basis. Therefore, a multi-source PV-wind based power supply will be a more effective alternative to mitigate the generation-demand power fluctuations and reduced the battery bank size. A PV-wind-battery grid connected hybrid power supply for telecom equipment system is proposed to get the benefits the complementary nature of renewable resources (solar and wind) [32].

To bring down high OPEX as well as the public and regulatory pressure to reduce the pollution from telecom towers powered by conventional power supply are driving telecom operators to adopt greener solutions for BS supply [6]. If only 2.5 lakh telecom towers in India are shifted to renewable resources based power supply, it is estimated that 944 million USD would be saved annually. In this thesis work, HRES formed by complementary PV and wind energy along with battery back-up is proposed for the BS of telecom tower in remote/rural areas. Figure 4.7 presents the proposed HRES based power supply for BS.

4.5.1 Architecture of HRES for BS

The architecture of HRES based power supply for BS in remote/rural areas is shown in Fig. 4.7. The HRES based power supply consists of renewable resources

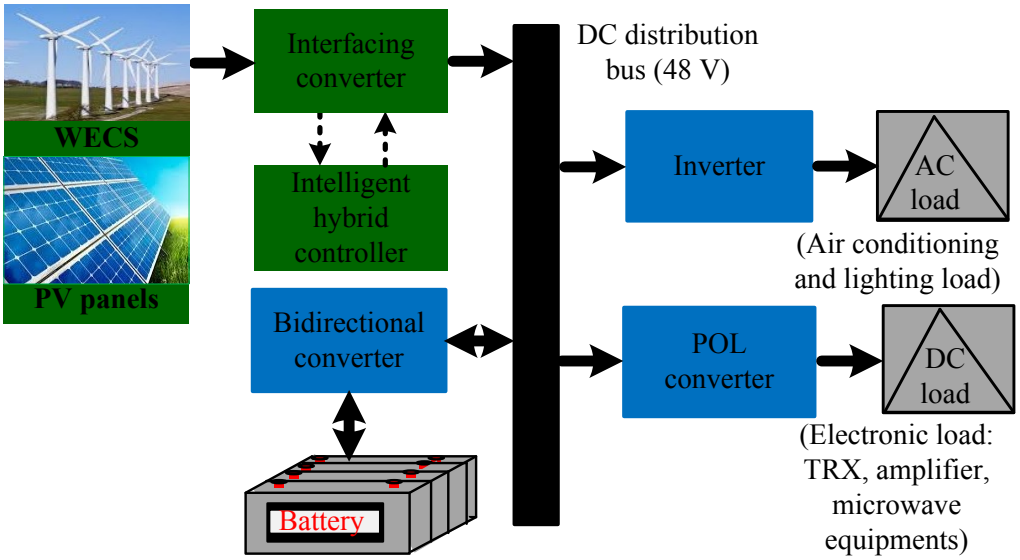

Figure 4.7: Architecture of renewable based BS power supply

(PV and WECS) interfaced to the DC distribution bus using SMPC. A 48V DC distribution system in BS have adopted taking safety aspects associated with high DC voltage into the consideration. From DC distribution bus, load end electronic equipment are powered through the POL converters. The output voltage of the renewable resources (PV and WECS) is function of load variations as well as environmental condition like temperature, atmospheric pressure, irradiation, wind speed and humidity. It varies from 10-30% above or below the rated voltage. Therefore, renewable resources cannot be directly interfaced with DC distribution bus. It is to be noted that the telecom load mostly constitutes electronic system which is sensitive to voltage variation. Therefore, it is necessary to incorporate the interfacing unit that maintains 48V at the DC bus. The proposed intelligent interfacing unit constitutes SMPC and associated controller for regulating the output voltage of the converter. The converter matches the variable voltage of renewable resources to 48V, the distribution bus voltage of BS. The proposed intelligent controller in this chapter maintains the tight regulation of the DC bus voltage under source voltage fluctuations and load variation of BS of telecom tower based on communication signal traffic. Moreover, the proposed controller will provide a fast response, so that the overall system should not become sluggish due to the presence of the converter.

4.5.2 Selection of Switched mode power converter topology for HRES

The integration of PV and WECS in proposed HRES based BS power supply to the DC distribution bus requires an interfacing unit. The interfacing unit should match the voltage level of the source to that of the DC distribution bus. The output voltage of PV and the rectified output voltage of wind generator are DC in nature, therefore, DC-DC converters (SMPC) are required. The open circuit voltage of PV array is a function of the ambient temperature which varies ±10% of the rated voltage of the array throughout the year. PV array with 48V is installed as a part of HRES based telecom supply which is a low voltage and high current supply system. Thus, to maintain 48V at the DC bus, both buck and boost operation is required in the SMPC. The performance requirements of the converter: i) operate at desired voltage level, ii) minimum voltage or current ripple, iii) fast dynamic response to load or source disturbances. Cuk converter which can step up and down the input DC voltage is selected for interfacing renewable resources to the DC distribution bus. Comparative analysis of the Cuk converter with the buck-boost converter is shown in table 4.5

Table 4.5: Comparative analysis of Cuk converter and buck-boost converter

Feature	Buck-boost converter	Cuk converter
Voltage ripple (ΔV)	Load current dependent $\Delta V \propto \frac{1}{f_s}$	Load current independent $\Delta V \propto \frac{1}{f_s^2}$
Current ripple	More	Less
Switching loss	Higher	Less
Dissipation in ESR	more	Less
Dc gain and efficiency	Lower	Higher for real components
Size and weight	Bulky	Significantly reduced
Energy transferring element	Inductor	Capacitor

4.5.3 Voltage regulation for HRES

However, the biggest challenge for integrating PV or WECS to the BS supply is that the resources have variable output voltage as a function of environmental conditions and the load [110]. On the other end, BS has the requirement of tight voltage regulation for reliable operation. Therefore, an interfacing unit consisting of SMPC with controller is necessary to integrate renewable resources with telecom load. The dynamic behavior of the SMPC is improved by implementing the intelligent hybrid controller as proposed in Chapter 3. The proposed hybrid controller utilizes the best features of the linear controller and meta-heuristic control algorithms. The proposed controller is artificial intelligence assisted PID controller for the HRES based BS supply. The controller has simple structure without any variable switching frequency issues, easy to implement at low cost are similar to the linear controller. The model free design procedure considering uncertainties of the system and robust response for a broad range of operation are inherited from intelligent controller. As PI or PID controllers tuned using conventional linear methods are based on using small signal modelling of the system which involves linearization around the operating point [48]. The small signal model is applicable around the operating point which makes parameter of the model vary when operating point shifts. Hence, linear controller gives sluggish large signal response. Extensive computational process required to model the complete HRES based power supply which includes renewable resources and SMPC [111]. Then, meta-heuristic optimization techniques are implemented for power electronics applications in [112]. These control algorithms do not require state space averaging or any other modeling of the converter. The system can be treated as a black box and consider it as optimal control problem for finding the optimal global solution. According to no free lunch theorem, one meta-heuristic algorithm does not solve the entire optimization problem with the same accuracy. It may give the best performance for a particular set of the problem or may perform poorly for another set of optimization problem [113]. Thus, different meta-heuristic algorithms which are GA [114], PSO [115], proposed MARCGA with large population diversity and GWO [116] are considered in this thesis to find the best suited for the proposed intelligent hybrid controller.

4.6 Renewable resource modelling

The PV module consists of several cells in series and parallel combination which will generate the rated power under nominal conditions. The generated power depends upon the irradiation and ambient temperature. Thus, PV cell is mathematically modeled in (4.4)-(4.6).

$$I_{PV} = I_{ph} - I_o \left[e^{\frac{qV_{PV}}{\chi KT} - 1} \right] \tag{4.4}$$

$$I_o = I_{rr} \left[\frac{T}{T_{ref}} \right]^3 e^{qE_{go}\left[\frac{1}{T_{ref}} - \frac{1}{T}\right]} \tag{4.5}$$

$$I_{ph} = \left[I_{sc} + K_T (T - T_{ref}) \right] \frac{G}{1000} \tag{4.6}$$

The variable speed wind turbine based WECS is considered. The output of the turbine is function of wind speed and follows the cube law in (4.7). The power output of the WECS for each hour is given by:

$$P_{w,t} = \begin{cases} 0, & \text{if } v_{ci} < v_t > v_{co} \\ v_t^3 \frac{C_w}{v_t^3 - v_{ci}^3} - C_w \frac{v_{ci}^3}{v_t^3 - v_{ci}^3}, & \text{if } v_{ci} < v_t < v_r \\ C_w, & \text{if } v_r < v_t < v_{co} \end{cases}$$

$$C_w = 0.5 \eta_{WT} C_p A \rho v_r^3 \tag{4.7}$$

where, $C_p = 0.22(\frac{116}{\lambda_i} - 0.4\theta - 5)e^{\frac{-12.5}{\lambda_i}}$, $\lambda = \frac{\omega_r R}{v_r}$, $\frac{1}{\lambda_i} = \frac{1}{\lambda + 0.08\theta} - \frac{0.035}{1+\theta^3}$

4.7 Cuk converter modelling

Cuk converter is a step up/down DC-DC converter. It acts as voltage regulator while interfacing proposed HRES with the BS. It combines the good characteristics of both buck converter and boost converter. The Cuk converter inherently has ripple free input and output current, hence proper choice of converter topology. Figure 4.8a shows the power circuit diagram of Cuk converter

with the intelligent hybrid controller. The pole zero plot with step response is presented in Fig. 4.8b obtained from open loop analysis. The design parameters of the interfacing converter are specified as input voltage (V_{in})= 40-100V, output voltage(V_o)= 48V, inductor(L)=(L_o)= 0.0028mH, capacitor(C)= 0.38mF, (C_o)=1mF, load resistance(R)= 1.22Ω and switching frequency (f_s)= 20kHz.

When switch 'S' is 'ON', for duration of DT_s ,

$$\frac{di_L}{dt} = \frac{1}{L} v_{in} \tag{4.8a}$$

$$\frac{di_{L_o}}{dt} = \frac{1}{L_o} \left(v_C - v_{C_o}\right) \tag{4.8b}$$

$$\frac{di_C}{dt} = \frac{1}{C} \left(-i_{L_o}\right) \tag{4.8c}$$

$$\frac{di_{C_o}}{dt} = \frac{1}{C_o} \left(i_{L_o} - \frac{v_{C_o}}{R}\right) \tag{4.8d}$$

When switch 'S' is 'OFF', for duration of $(1-D)T_s$,

$$\frac{di_L}{dt} = \frac{1}{L} \left(v_{in} - v_C\right) \tag{4.9a}$$

$$\frac{di_{L_o}}{dt} = \frac{1}{L_o} \left(v_{C_o}\right) \tag{4.9b}$$

$$\frac{di_C}{dt} = \frac{1}{C} \left(i_L\right) \tag{4.9c}$$

$$\frac{di_{C_o}}{dt} = \frac{1}{C_o} \left(i_{L_o} - \frac{v_{C_o}}{R}\right) \tag{4.9d}$$

Cuk converter is a fourth order system having four left half-plane poles and two RHP zeros as depicted from the averaged state space equations

$$\begin{bmatrix} \frac{\hat{v}_C}{dt} \\ \frac{\hat{v}_{C_o}}{dt} \\ \frac{\hat{i}_L}{dt} \\ \frac{\hat{i}_{L_o}}{dt} \end{bmatrix} = \begin{bmatrix} 0 & 0 & \frac{1-D}{C} & \frac{-D}{C} \\ 0 & \frac{-1}{RC_2} & 0 & \frac{1}{C_o} \\ \frac{-(1-D)}{L} & 0 & 0 & 0 \\ \frac{D}{L_o} & \frac{-1}{L_o} & 0 & 0 \end{bmatrix} \begin{bmatrix} \hat{v}_C \\ \hat{v}_{C_o} \\ \hat{i}_L \\ \hat{v}_{L1} \end{bmatrix} + \begin{bmatrix} 0 \\ 0 \\ \frac{1}{L_1} \\ 0 \end{bmatrix} \hat{v}_{in} + \begin{bmatrix} \frac{I_{L_o} - I_L}{C_1} \\ 0 \\ \frac{v_C}{L} \\ \frac{v_C}{L_o} \end{bmatrix} \hat{d} \tag{4.10}$$

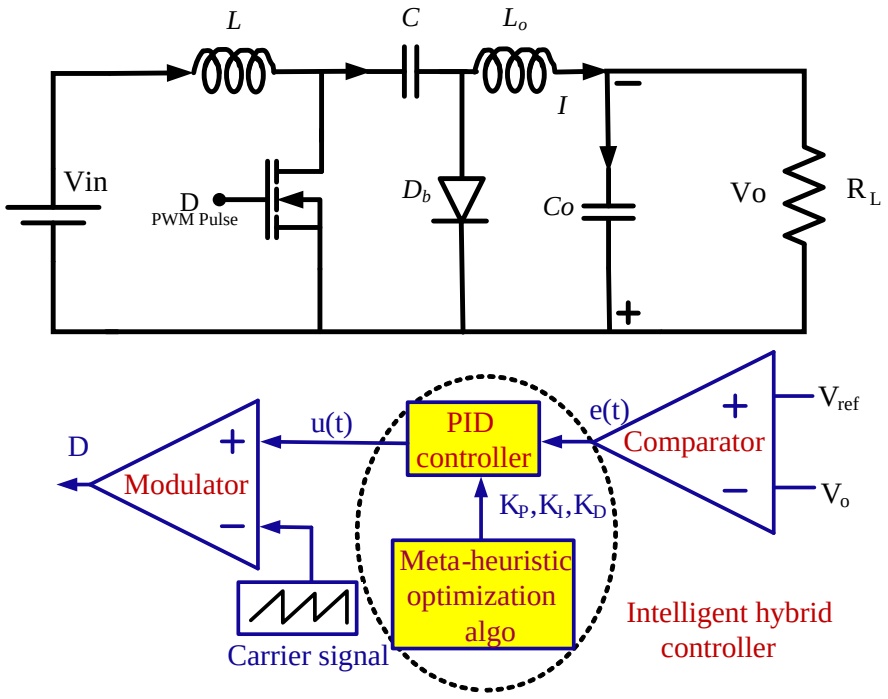

(a)

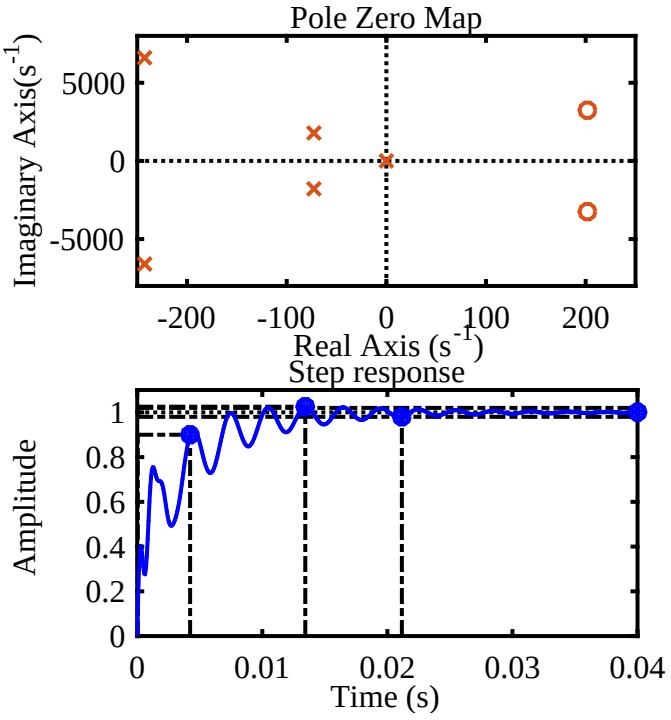

(b)

Figure 4.8: (a) Cuk converter with intelligent hybrid controller (b)Dynamic response of Cuk converter

4.8 Performance analysis of intelligent hybrid controller implemented with Cuk converter

The improved intelligent hybrid controller implemented with Cuk converter for the voltage regulation of the DC bus of the proposed HRES based BS power supply. The tuned parameter of intelligent hybrid controller assisted with binary GA, PSO, GWO and MARCGA are obtained using the programs developed as explained in section 4.4. At the end of the iterative process for each meta-heuristic algorithm, the tuned parameters of the hybrid controller are tabulated in table 4.6. The robustness of the intelligent hybrid controller tuned with four different meta-heuristic techniques is checked for all the possible variations in the source or load side. The output PV is 48V under normal condition for 1.92kW load of the BTS. The telecom load could vary from 0.6kW when only one transceiver is working to 125% overloading condition i.e. 2.5kW load. The DC bus voltage tolerance limitation could be ±10% of 48V. Thus, three different cases are formulated to analyze the dynamic performance of the intelligent converter with the proposed hybrid controller: (a) source side variations, (b) load side variations, and (c) reference tracking capability.

4.8.1 Dynamic performance of the system due to source side variations

Variation in V_{in} to the interfacing converter is due to the variable output of the wind-PV may differ in the range of 40V to 100V depending on load or environmen-

Table 4.6: Parameters of tuned intelligent hybrid controller

Parameter→ Algorithm ↓	K_P	K_I	K_D
Binary GA	0.0206	17.139	0.0037
PSO	0.0300	13.795	0.0038
GWO	0.0175	16.851	0.0006
MARCGA	0.0206	16.316	0.0009

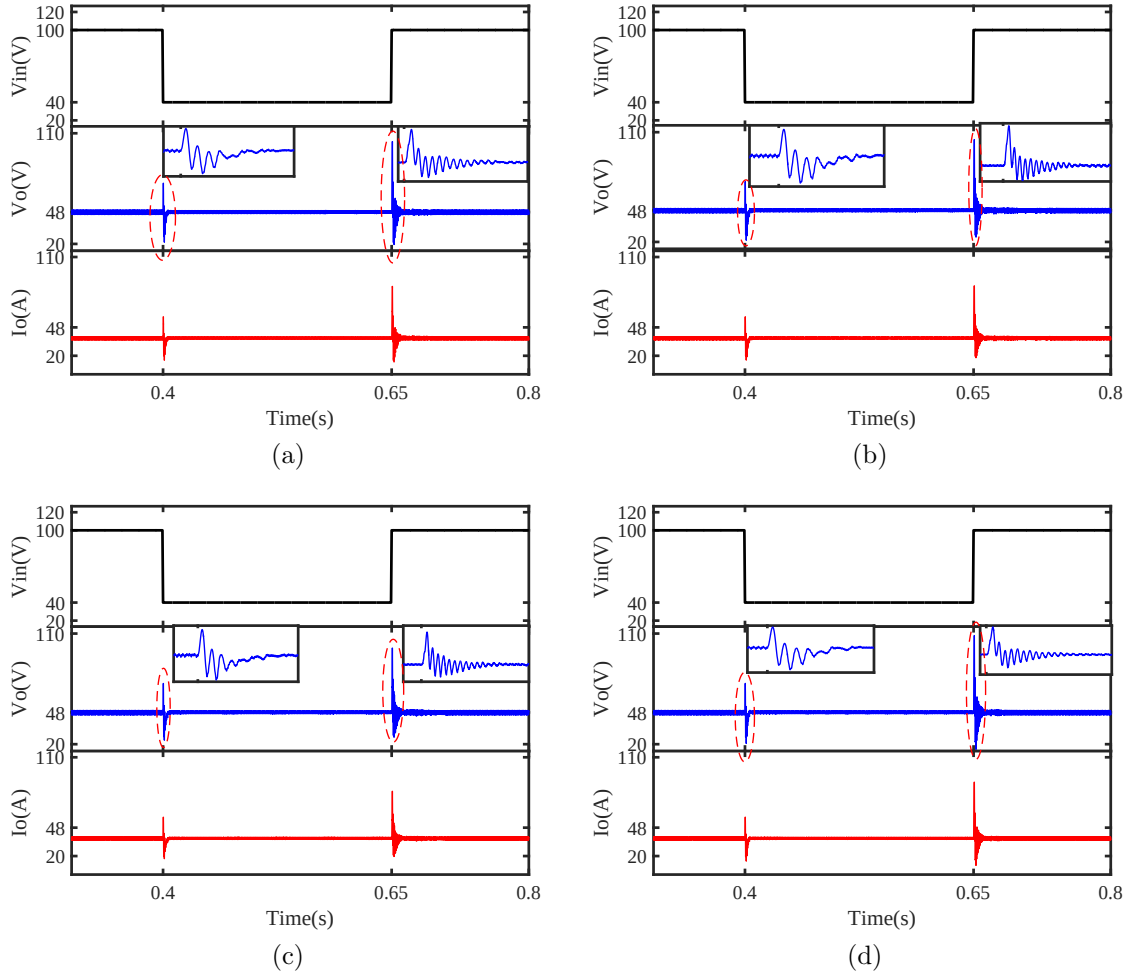

Figure 4.9: Dynamic response of the system during step change in V_{in} from 40V to 100V at t_1=0.4s and from 100V to 40V at t_2=0.65s using intelligent hybrid controller assisted with (a)Binary GA (b)PSO (c)GWO (d)MARCGA

tal conditions. Therefore, a maximum possible step decrease from 100V to 40V is introduced at t_1=0.4s, and a similar maximum step increase in V_{in} from 40V to 100V is introduced at t_2= 0.65s. Figure 4.9a shows the dynamic response of the intelligent interfacing converter with hybrid controller tuned with binary GA, PSO, GWO, and MARCGA. The V_o and I_o of the converter with binary GA-assisted controller settle to the steady-state value in 6.4ms after having an undershoot of 43.57% for a step decrease in V_{in} and 11ms with undershoot of 106.25% for a step decrease in V_{in} as shown in Fig. 4.9a. In Fig. 4.9b dynamic response for V_o and I_o of the converter with PSO assisted controller is presented. During step increase in input, the V_o and I_o shoots up to 115V and 46.3A respectively and settles to

48V and 40A respectively in 14.1ms. Again, during step decrease of input, the V_o and I_o settles in 7.4ms after having undershoot of 42.56%. Figure 4.9c and 4.9d presents the V_o and I_o of converter with the GWO and MARCGA-assisted controller takes a settling time of 13ms and 13.5ms respectively when subjected to input disturbance at t_2=0.65s. At the same time, overshoot in V_o of converter with the GWO and MARCGA-assisted controller are 96% and 115% respectively. Similarly, when converter with the GWO and MARCGA-assisted controller subjected to step decrease in V_{in}, the settling time is 7.1ms and 6ms respectively and undershoot is 43.58% and 43.69% respectively.

4.8.2 Dynamic performance of the system due to load side variations

The telecom load may vary in the range of few watt to kW in islanded mode of operation. Minimum load of 0.6 kW and load current (I_o) as 12A. During peak hours, the load may go to 2.4kW and I_o as 50A. The interfacing converter is simulated for maximum possible variation in load condition, and dynamic response of the converter is given in Fig. 4.10. If the connected load is decreased from 2.4kW to 0.6kW at t_1=0.4s, the binary GA-assisted controller has undershoot of 19.82% and settles in 5.5ms. Now, the system is loaded at t_2=0.65s, the V_o overshoots by 18.59% and attains steady state value in 7ms. The PSO-assisted controller is employed during under loading of the system at t_1=0.4s, the system settles in 6.7ms but achieving a maximum undershoot of 23.21%. During overloading at t_2=0.65s, the system has a settling time of 8.20ms and maximum overshoot of 21.67%. The maximum undershoot with GWO and MARCGA-assisted controllers are 19.45% and 22.12% respectively with settling time of 4.65ms and 7.20ms respectively. A similar response is observed when the overloading of the system happens at t_2=0.65s. Maximum overshoot with GWO and MARCGA-assisted controllers are 17.96% and 20.96% respectively with settling time of 7.2ms and 7.3ms respectively.

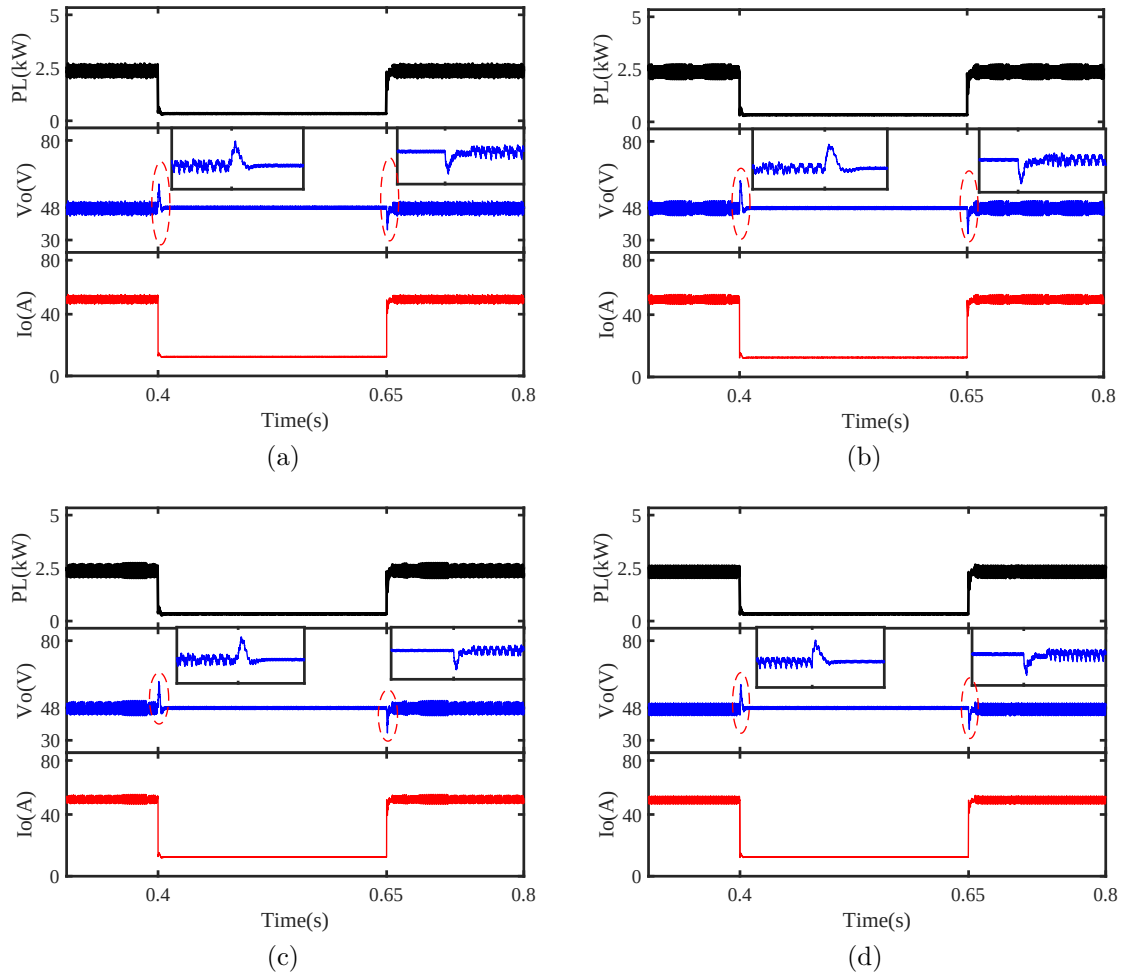

Figure 4.10: Dynamic response of the system during step change in load from 2.4kW to 0.6kW at t_1=0.4s and from 0.6kW to 2.4kW at t_2=0.65s using intelligent hybrid controller assisted with (a)Binary GA (b)PSO (c)GWO (d)MARCGA

4.8.3 Dynamic performance of the system for reference tracking capability

The reference tracking capability is tested in the proposed system as by triggering a step decrease in V_{ref} from 53V to 43V at t_1= 0.4s, and V_{ref} was increased by same step size i.e. from 43V to 53V at t_2=0.65s. The dynamic response of the interfacing converter with proposed hybrid controller tuned with different meta-heuristic techniques is shown in Fig. 4.11. The dynamic response of interfacing converter with hybrid controller tuned with four meta-heuristic algorithms indicates the excellent reference tracking capability with each algorithm without any overshoot or

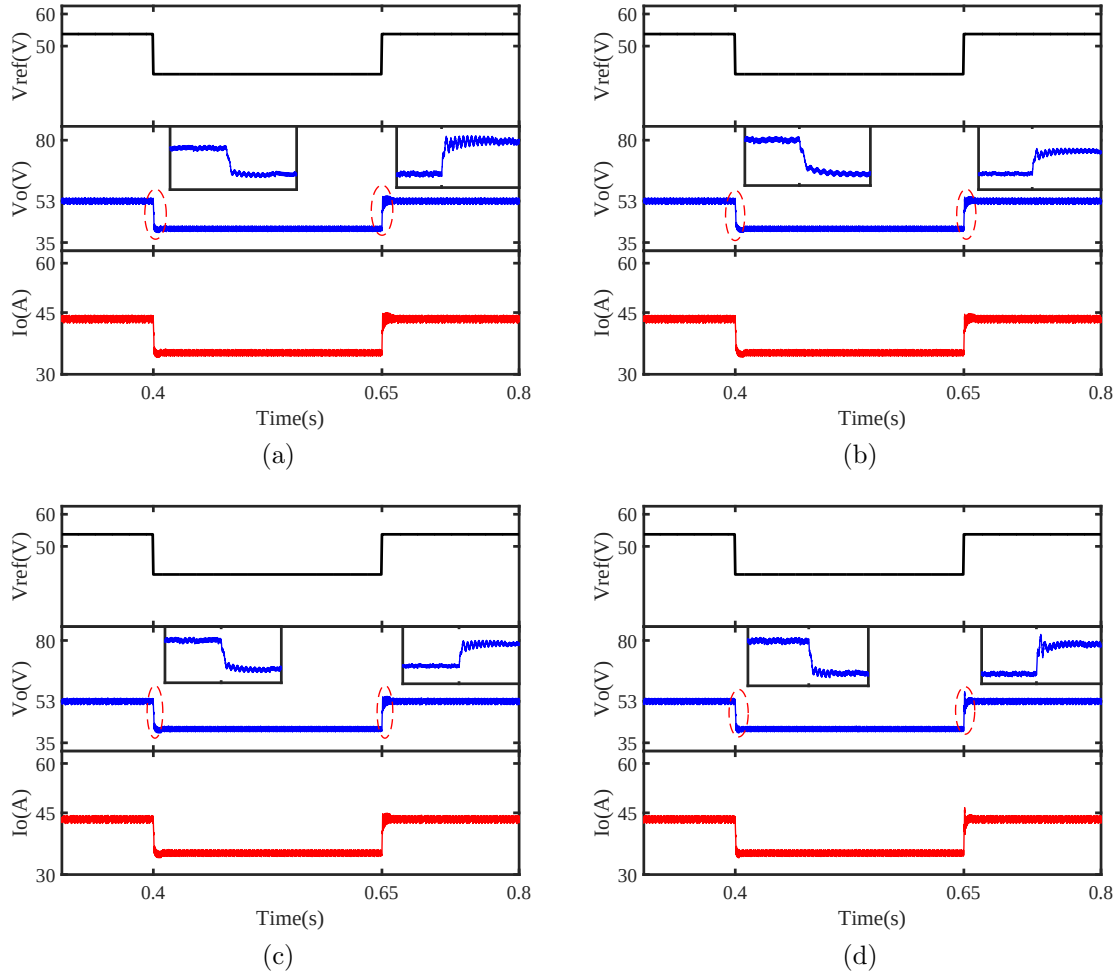

Figure 4.11: Dynamic response of the system during step decrease in connected load from V_{ref} from 43V to 53V at t_1=0.4s and step decrease in V_{ref} from 53V to 43V at t_2=0.65s using controller assisted with (a)Binary GA (b)PSO (c)GWO (d)MARCGA

undershoot. The binary GA-assisted and PSO-assisted controller settles in 1.2ms and 1.4ms respectively for a step decrease and a increase in V_{ref}. Similarly, GWO and MARCGA-assisted controller settles in 1.6ms while tracking the reference.

Comparative analysis of dynamic response of proposed intelligent hybrid controller is summarized in table 4.7

Table 4.7: Comparative analysis of dynamic response of proposed intelligent hybrid controller

	T_s(s)	M_p(%)	ΔV (%)	V_s(V)	T_s(s)	M_p(%)	ΔV (%)	V_s (V)
	V_{in} change: 100V to 40V				V_{in} change: 40V to 100V			
GA	6.40	43.57	2.51	48.37	11.00	106.25	3.91	47.26
PSO	7.40	42.56	2.68	48.14	14.10	115.05	4.50	47.43
GWO	7.10	43.58	4.47	48.07	13.00	96.92	2.92	47.80
MARCGA	6.00	43.69	4.31	48.42	13.50	115.42	4.46	47.42
	P_L change: 50A to 12.5A				P_L change: 12.5A to 50A			
GA	5.50	19.82	1.79	47.77	7.00	18.59	10.21	47.67
PSO	6.70	23.21	1.57	47.98	8.20	21.6	1 11.75	48.18
GWO	7.20	22.12	2.13	47.82	7.30	20.96	10.51	47.82
MARCGA	4.65	19.45	1.98	47.77	7.20	17.96	10.61	47.42
	V_{ref} change: 53V to 43V				V_{ref} change: 43V to 53V			
GA	1.60	-	2.86	42.75	11.00	-	0.94	51.56
PSO	10.00	-	4.12	42.85	12.00	2.64	3.2	53.10
GWO	10.50	-	4.21	42.91	9.80	3.37	2.97	52.94
MARCGA	4.50	-	4.11	42.88	10.00	6.6	2.83	53.00

4.9 Experimental verification

The prototype of Cuk converter is designed and fabricated in laboratory to validate the performance of the proposed intelligent hybrid controller assisted by GA, PSO, GWO and MRCGA to perform the voltage regulation at the DC distribution bus. The converter prototype is of 100W with output voltage 48V and the V_{in} may vary in the range 40-100V. The controller is implemented using DSPIC33FJ128MC802 microcontroller which generates the gate pulse to drive the MOSFET switch (IRFP460) in the converter power circuit. Feedback signals are measured with isolated voltage (BESTEKX VSLV205C) and current transducers (Topstek TC25A4V) and scaled to the range 0-3V through signal conditioning circuit. The conditioned signal is fed to inbuilt analog to digital conversion (ADC) for further processing. Further, control strategy is digitally implemented using MPLABX IDE tool and appropriate gate signal is obtained from the digital to analog converter (DAC). The generated pulse is given to gate driver circuit, where

gate pulse is scaled to the range of 0-12V using TLP250 opto-coupler circuit.

Dynamic performance of the intelligent hybrid controller implemented using Cuk converter is examined for the step change in input voltage and load. The Fig. 4.12 and 4.13 shows the dynamic response of the Cuk converter for the step increase in V_{in} from 48V to 100V and step decrease in V_{in} from 100V to 48V. Performance of Cuk converter with GA, PSO, GWO and MARCGA-assisted controller is shown in Fig. 4.14 and 4.15 which depicts that the 48V is maintained across the load with buck and boost operation when V_{in} is 100V and 40V receptively. The settling time of the system when Cuk converter with GA, PSO, GWO and MARCGA-assisted controller is subjected to step decrease in V_{in} are 32.5, 28.12, 15.625, and 12.5ms respectively. Similarly, the system is subjected to the step increase in V_{in} and observed that MARCGA-assisted controller has least settling time of 11.25ms with an overshoot of 42.40% among all the controllers.

Next, the performance of the system is analyzed for the step increase in the load upto 120W with load current of 2.5A and for step decrease in load upto 30W with load current of 0.625A which is presented in Fig. 4.14 and 4.15. The settling time of the system when Cuk converter with GA, PSO, GWO and MARCGA-assisted controller is subjected to step decrease in P_L are 38.75, 15, 13.2, and 12.5ms receptively. Similarly, the system is subjected to the step increase in P_L and observed that MARCGA-assisted controller has least settling time of 12.5ms with an overshoot of 9.1% among all the controllers. It is analyzed that the hardware results obtained with the proposed intelligent hybrid controller are in agreement with simulated results which validate the dynamic performance of the proposed controller.

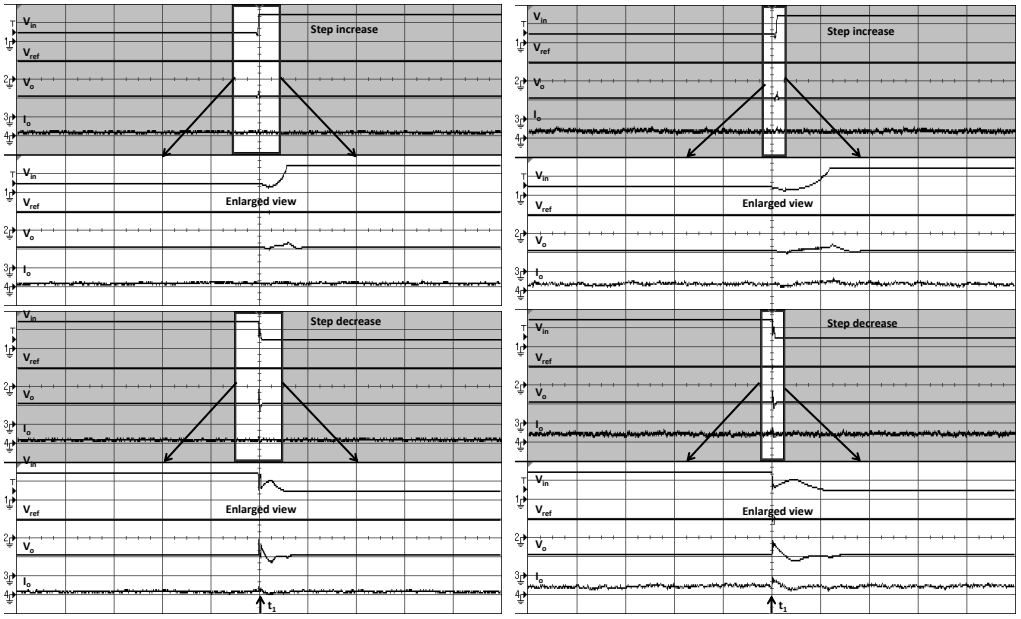

(a) (b)

Figure 4.12: Dynamic response of intelligent hybrid controller for input disturbance rejection. Controller assisted with (a) GA (b) PSO. Scale: channel1=80V/div, channel2=50V/div, channel3=45V/div, channel4=10A/div

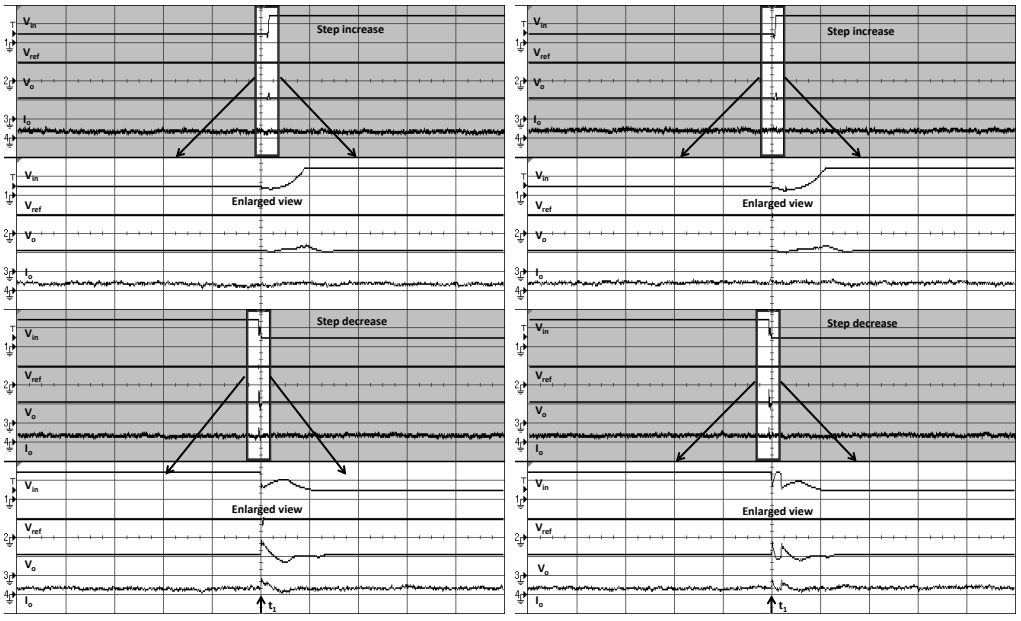

(a) GWO (b) MARCGA

Figure 4.13: Dynamic response of intelligent hybrid controller for input disturbance rejection. Controller assisted with (a) GWO (b) MARCGA. Scale: channel1=80V/div, channel2=50V/div, channel3=45V/div, channel4=10A/div

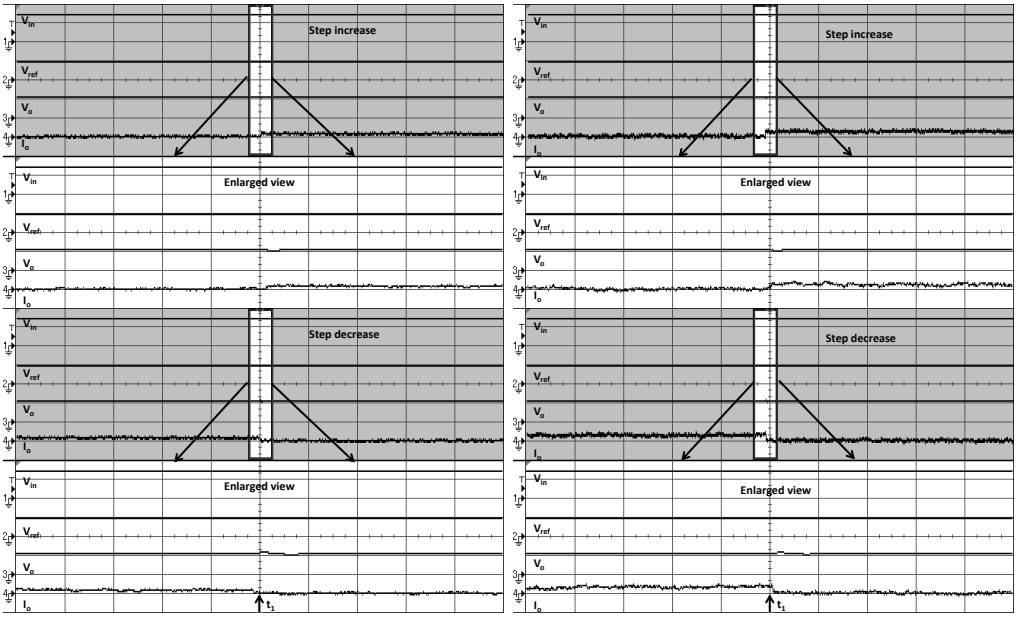

(a) GA (b) PSO

Figure 4.14: Dynamic response of intelligent hybrid controller for output disturbance rejection. Controller assisted with (a) GA (b) PSO. Scale: channel1=80V/div, channel2=50V/div, channel3=45V/div, channel4=10A/div

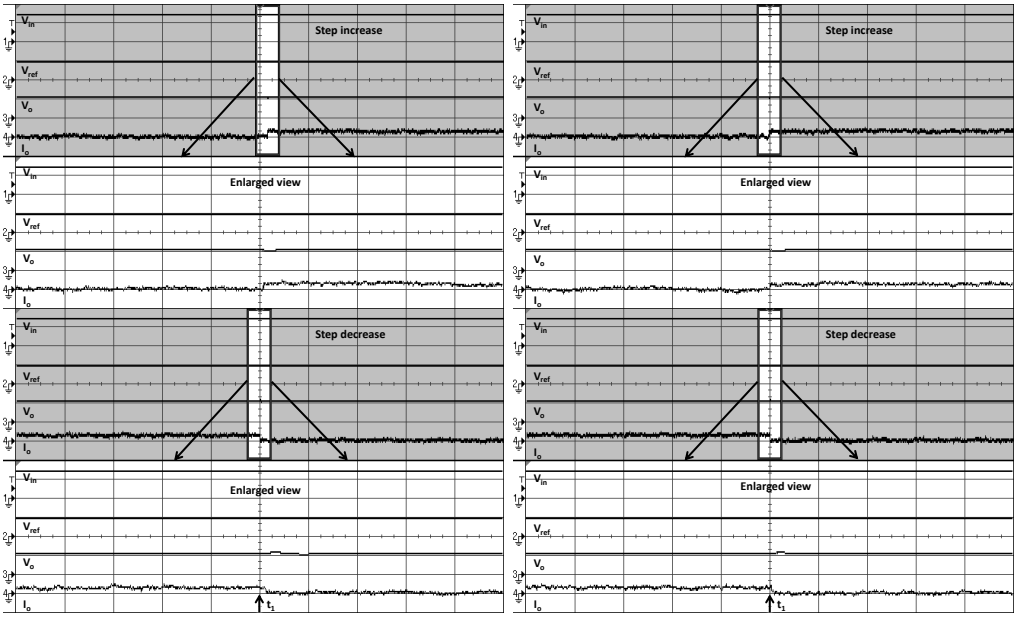

(a) GWO (b) MARCGA

Figure 4.15: Dynamic response of the intelligent hybrid controller for output disturbance rejection. Controller assisted with (a) GWO (b) MARCGA. Scale: channel1=80V/div, channel2=50V/div, channel3=45V/div, channel4=10A/div

4.10 Summary

The improved intelligent hybrid controller is proposed in the present chapter to regulate the DC distribution bus voltage of BS power supply architecture. The controller is a pre-tuned controller that has inherited the features from both linear controller and artificial intelligent controller i.e. meta-heuristic algorithms. In this study, the MARCGA has been proposed with enhanced diversity in the population and high accuracy due to proposed similarity check introduced in the real coded genetic algorithm. The potential of proposed MARCGA algorithm to tune the PID controller for the interfacing converter is examined by comparing with binary GA, PSO and GWO. At first, enhanced intelligent hybrid controller is implemented to the boost converter in the PEMFC based BS power supply proposed in chapter 3. Performance of the controller is analyzed for the input disturbance rejection, output disturbance rejection and reference tracking capability.

Later, HRES based power supply has been proposed and integrated to green telecom towers in remote rural areas using Cuk converter based interfacing unit. The Cuk converter ensures the wide range of operation of renewable resources, ripple free input and output currents and compact size of the converter. The HRES supply consists of complementary natured solar and wind energy resources which supply the load and charge the batteries. The requisite of telecom power supply are reliability, quality and tight voltage regulation at DC distribution bus. However, the terminal voltage of renewable resources is function of ambient conditions which are temperature and wind speed. Hence, the improved intelligent hybrid controller is implemented using Cuk converter for HRES based power supply for BS. The proposed controller maintains regulated voltage at the DC bus under the fluctuating terminal voltage of renewable resources, and unsteady traffic signals which result in the frequent switching of telecom load. It has been found that MARCGA-assisted intelligent hybrid controller outperforms when tested for the source and load disturbance rejection capability. Further, laboratory prototype of the interfacing converter is developed and the proposed intelligent hybrid controller performance is verified. Thus, hybrid power supply architecture with proposed controller will facilitate the industry's expansion while addressing the issues regarding conventional power supply and renewable resource integration.

Chapter 5

Optimal sizing of HRES

5.1 Introduction

A PV-wind energy based HRES with battery bank for BS in remote/rural areas where grid extension is not viable has been proposed in chapter 4. Integration of battery as energy storage system offers higher flexibility and reliability for storing surplus energy and managing deficit whenever needed. In HRES based supply, if renewable resources and battery bank are oversized; it will result in higher initial investment and underutilization of the resources. On the other hand, the undersized system would result in an energy deficit and less reliable system. Consequently, the quality of network and services to the subscribers degrade. Therefore, to have economical, practically viable, reliable and environment friendly alternative to the existing DGset based power supply, the proposed HRES supply should be an optimal mix of the renewable resources and storage. Furthermore, the power supply should enhance system mobility at lesser life cycle cost. During an emergency like natural disaster or wartime, the HRES based towers can be easily installed and relocated to ensure reliable communication.

The studies have been carried out for the sizing of stand-alone HRES considering economic, reliability, environment, and sensitivity analysis. Reliability studies involve LPSP, which is a measure of the probability of imbalance between electricity generation and consumption. Economic analysis is done with the objec-

tive to minimize the cost of the electricity consisting of capital cost, replacement cost, operation, and maintenance cost. Several methodologies has been adopted in the literature for sizing of HRES such as analytical methods, iterative methods, probabilistic approach, available software tools (e.g. HOMER) and optimization techniques. Further, optimization techniques could be conventional optimization or computational intelligence search techniques such as artificial neural network based, fuzzy logic based or meta-heuristic algorithm based optimization. Meta-heuristic techniques such as GA and PSO are especially attractive for multi-objective component sizing. The multiple objective might be conflicting in nature (e.g. COE minimization, system availability, efficiency maximization, and carbon emission minimization).

The optimum size of the power supply considering different scenarios which are only PV, only wind, and both PV and wind is calculated using iterative process [117]. The objective of the iterative process is to minimize the total annual cost of electricity to the customer and balancing demand-generation averaged over 24 hours. However, power quality, reliability, protection, ability to start motor has not been taken into constraints. In [81], Yang et al. have presented a GA based method for a hybrid PV-wind-batteries system that minimizes the ACS for LPSP less than 2%. The optimal sizing considers various parameters such as orientation (slope angle) of PV modules, MPPT factor, tower height of the wind turbine and capacity of batteries. In [118], Yang and Nehorai carried out the economic analysis for multiple renewable resources and storage optimization jointly under the assumption that the load and the renewable resources are perfectly forecasted. The objective is to minimize the capital, operation and maintenance cost of an isolated micro-grid having a small carbon footprint and high penetration of renewable resources. In [88], Nikhil et. al. have carried the optimal design analysis to ensure 100% reliability of PV-battery stand-alone system using adaptive feedback iteration technique. Further, the effect of disconnecting the battery during overcharge and low voltage state of PV with the reduction in component size has been studied. However, reduction in minimum SoC (SoC_{min}) would degrade the life cycle of the battery thus cost saving achieved by a reduction in component would be countered by increased replacement and maintenance cost of batteries.

In [29], Kaldellis used the available experimental probability density function to

predict the minimum acceptable nominal power of the wind turbine. In [80], Singh et. al. have suggested that detailed mathematical modeling of the system is inevitable to study comprehensive cost analysis. The above research has been carried out for grid connected PV-biomass hybrid energy system to provide uninterrupted supply to a village.

From the above literature, it is evident that the optimal size calculation of HRES is a complicated due to the involvement of multiple sources and battery energy storage. Therefore, a thorough analysis is required with detailed modelling of the components, and choosing the appropriate optimization technique. The 'average month' technique may not fulfill the load demand in certain periods in a real-world scenario. At the same time, the 'worst month' method may lead to an oversized system which would be costlier.

It is evident from the literature that HRES recommendation for the stand-alone system is based on a year-long analysis, but it is important to validate the proposal by a long-term analysis i.e. equivalent to the lifespan of the battery and the same has been proposed in this study. From the thorough literature review, the optimal sizing problem is formulated for the minimization of COE along with LPSP and EE. However, the nature of the objective of minimizing the COE and LPSP is contradictory in nature because enhancement of reliability will result in an increase in excess energy that would increase the cost. Therefore a multi-objective algorithm called NSGA-II is implemented to achieve a trade-off among the objectives. Since telecom towers are in remote, isolated areas, the excess energy could not be utilized effectively to benefit the telecom operators. Therefore, in this chapter, multi-objective optimal sizing problem is proposed with the objectives to reduce the COE of the system and 100% reliability that ensure minimal EE. The proposed HRES based telecom tower supply after optimal sizing reduces the OPEX of telecom companies and enables the towers to become 'green towers' i.e. environmental friendly.

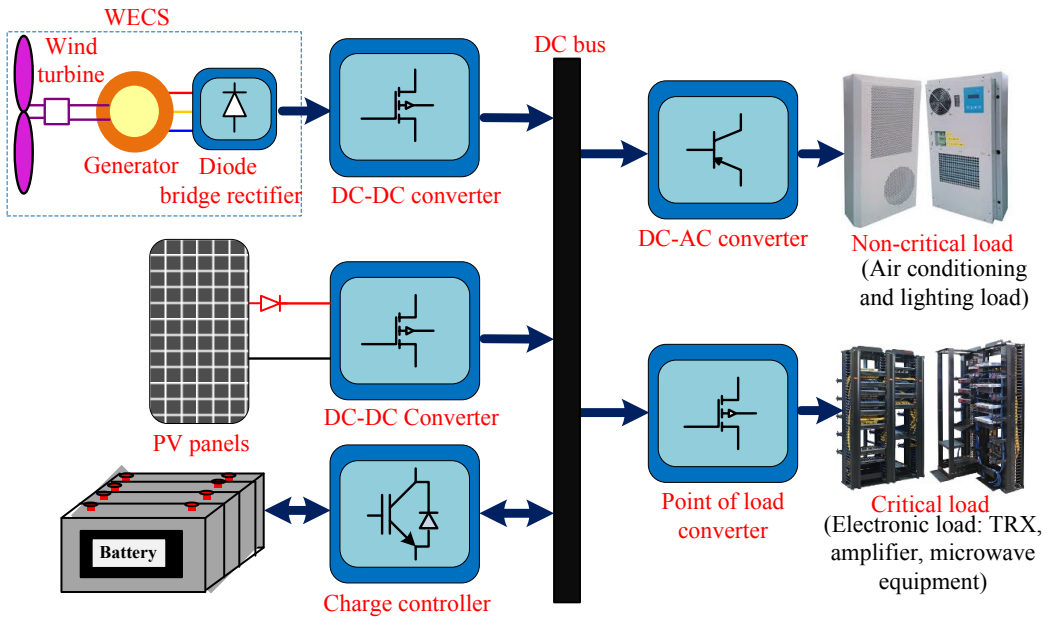

Figure 5.1: Architecture of the HRES for powering telecom tower

5.2 Hybrid renewable energy system based power supply

The HRES based power supply consists of WECS and PV panel with DC-DC converters as renewable energy generators, a battery energy storage system along with charge controller to buffer the intermittency in wind and solar energy. The battery voltage level of 400V is selected to reduce the size of conductors as the telecom power supply is a low voltage high current system. Thus, a bidirectional buck-boost charge controller is employed. A DC bus with 48V supplies power to different loads in the BS such as microwave unit, amplifier, and transceivers at a voltage level in the range of 12V-1.1V using POL converters. The architecture of the proposed wind-PV based HRES for telecom tower is shown in Fig.5.1.

5.2.1 Modelling of photovoltaic

It is assumed that the PV panel along with DC-DC converter to track maximum power is installed at the site. The power generation from PV panels is a function of ambient temperature and irradiation. The solar irradiation data of a site near

Jaipur, India is taken from the website of National Renewable Energy Laboratory, U.S. Department of Energy [119]. Therefore, power generated by PV panels is modeled in (5.1) and (5.2) considering the conversion efficiency, MPPT factor and de-rating factor.

$$P_{pv} = P_{pr}\frac{g}{g_{ref}}\left[1 + K_t(T_a + 0.0256g) - T_{ref}\right] \tag{5.1}$$

$$P_p = \eta_{pv}\eta_{MPPT}\eta_{dr}P_{pv} \tag{5.2}$$

5.2.2 Wind energy conversion system modelling

The WECS consists of a variable wind turbine, electric generator and converters for AC-DC conversion and MPPT tracking. The power output of WECS can be approximated in (3).

$$P_{wt} = \begin{cases} 0, & \text{if } v_{cin} < v, v > v_{cout} \\ v^3\frac{P_r}{v^3 - v_{cin}^3} - P_r\frac{v_{cin}^3}{v^3 - v_{cin}^3}, & \text{if } v_{cin} < v < v_r \\ P_r, & \text{if } v_r < v < v_{cout} \end{cases}$$

$$P_w = n_{wt}\eta_{wt}\eta_{dr}P_{wt} \tag{5.3}$$

5.2.3 Modelling of battery

The maximum battery capacity required for a given load is as follows,

$$E_{bmax} = \frac{P_Lad}{DoD\eta_{conv}\eta b} \tag{5.4}$$

Charging of the battery takes place when energy generated by the renewable resources is in surplus after meeting the load demand, i.e. $(P_{p,t} + P_{w,t} - P_{L,t} > 0)$. Charging happens only if $SoC_t < SoC_{max}$ and the SoC is given by

$$SoC_{t+1} = (1 - d)SoC_t + \eta_s(P_{p,t} + P_{w,t} - P_{L,t})t \tag{5.5}$$

where, $SoC_{max} = E_{bmax}$.It is assumed that each step of simulation is equivalent to one hour.

Discharging of the battery takes place when energy generated by the renewable is incapable of meeting the load demand, i.e.$(P_{p,t} + P_{w,t} - P_{L,t} < 0)$. Also discharging happens only if $Soc_t > SoC_{min}$ and the SoC is given by

$$SoC_{t+1} = (1 - d)SoC_t + \eta_s(P_{p,t} + P_{w,t} - P_{L,t})t \tag{5.6}$$

where, $SoC_{min} = (1 - DoD)E_{bmax}$ and to ensure the healthy and long lifespan of battery, the depth of discharge (DoD) is taken as 50%.

5.3 Optimal sizing

The optimal sizing of the HRES is done by performing the reliability, economic and EE generation analysis. The optimal sizing of the system will ensure the reliability of the proposed telecom power supply at a minimum COE. Since, conventional telecom tower supply uses lead acid battery for back-up. Therefore, lead acid battery storage is considered in the present study and SoC_{min} (50%) need to be maintained to enhance the lifespan of the battery as the battery is the most expensive component in HRES.

Table 5.1: Input parameters for optimal sizing of HRES

Capital cost of PV($/kW)	1200	Lifespan of PV,WECS,project	25
Capital cost of WECS($/kW)	1988	Lifespan of battery	3
Capital cost of battery($/kWh)	182	Lifespan of converter	15
Capital cost of converter($/kW)	127	Rating of PV panel(kW)	0.2
Maintenance cost of battery	10%	Rating of PV WECS(kW)	0.3
Real interest(p.a.)	6%	η_{conv}, η_b (%)	94, 85

5.3.1 Economic analysis

The COE (i.e. cost per unit of electricity) is the economic profitability of the renewable based hybrid telecom power supply. It is calculated as

$$COE = \frac{\text{total present cost}(\$)}{\sum_{t=0}^{3} \text{annual load}(kWh)} CRF \tag{5.7}$$

where, $CRF = \frac{i(1+i)^n}{(1+i)^n - 1}$

Net present cost is the sum of the capital cost, replacement cost, maintenance and operating cost of the PV panels, WECS, converters, and battery for the project lifetime i.e. 25 years. The cost of different components is presented in table 5.1.

5.3.2 Reliability analysis

Reliability analysis is necessary considering the intermittent nature of power generated by renewable resources. LPSP is a statistical term that defines the probability of insufficient power supplied to the load demand by the renewable based telecom power supply. LPSP is calculated when the load is not met by the power generated and based on the accumulative energy effect on the battery energy storage system.

$$LPSP_t = \frac{\sum P_{L,t} - P_{p,t} - P_{w,t} + P_{SoC_{min}}(\$)}{\sum P_{L,t}} \tag{5.8}$$

5.3.3 Excess energy

To ensure 100% reliability, the system is usually oversized and results in increased installation cost. Therefore, the EE is calculated under the condition that energy generated from renewable resources is greater than the load demand and battery is fully charged. The EE is minimized in the process of optimization and is given by

$$EE_t = P_{p,t} + P_{w,t} - P_{L,t} \text{ only when } SoC_t = SoC_{max} \tag{5.9}$$

5.4 Problem formulation

The HRES is proposed for the off-grid telecom tower which is more environment friendly than the diesel generator based power supply. An uninterrupted and economical power supply is the pre-requisite of the telecom tower. The feasibility of the HRES is analysed in this chapter by formulating a multi-objective optimal sizing problem having three objective functions namely, minimization of COE, LPSP, and EE. The objectives depend on the capacity of PV panels (P_{pr}), WECS (P_{wr}) and battery (E_{bmax}) installed at the site. 100% reliable system tends to be oversized and vice-versa. It is noteworthy that the objective functions are not commensurable. Therefore, conventional approaches such as weighted sum strategy or ϵ-constraint modeling are not efficient enough to solve multiple-objective optimal sizing problem as the effect of anyone objective might influence the solution in a higher proportion. Hence, NSGA-II is implemented in the proposed study which ranks the population by non-dominant sorting and all the objectives are minimized simultaneously giving a Pareto-optimal solution set. The optimal analysis is simulated for a time equivalent to the lifespan of battery i.e. three years with the step size of one hour.

$$\underset{\text{minimize}}{F_1} = \sum_{t=0}^{26280} COE, \underset{\text{minimize}}{F_2} = \sum_{t=0}^{26280} LPSP, \underset{\text{minimize}}{F_3} = \sum_{t=0}^{26280} EE \tag{5.10}$$

5.4.1 Optimization process

Objective functions are function of the P_{pr}, P_{wr} and ad which becomes the decision variable in the optimization process. The NSGA-II algorithm is implemented to minimize the objective functions (COE, LPSP and EE) and generates the optimal Pareto-front of the decision variables (P_{pr}, P_{wr} and ad). Every solution in the Pareto-front can be chosen by the user as per the requirement without worsening any of the objectives. An algorithm has two requirements: fast convergence and widespread. The elitism boosts the rate of convergence to obtain the Pareto-optimal fronts. The adoption of crowding parameter and non-dominant sorting guarantees the uniform spread along with diversity in the population. Moreover, the NSGA-II has low computational complexity, parameterless diversity preservation, and real valued representation, which is usually used to solve the problems with continuous search space.

The flowchart in Fig. 5.2a presents stepwise procedure of the optimization. Firstly, initial population of the decision variables (P_{pr}, P_{wr} and ad) is generated within the upper and lower limits of each decision variable. The weather data for three year (g_t and v_t) is loaded for the long term analysis of the HRES operation. Each step of simulation is considered equivalent to one hour and thus the variable t incremented from 0 to 26280 hours (3 years). The long term analysis is carried for each population member. For each hour the power generated by PV panels and wind corresponding to the current population member (decision variable: P_{pr} and P_{wr}) is calculated based on (5.1)-(5.3). The rated capacity of battery is calculated using (5.4) corresponding to ad in the current population member. For each hour, decision is taken to discharge or charge the battery during the deficit or excess of renewable power generated. The amount of energy discharged from battery is given by (5.6). If the renewable power as well as battery power fails to meet the load demand, the hourly $LPSP_t$ is calculated by (5.8). On the other end, the amount of battery charged is given by (5.5). If excess renewable energy is available after meeting the load demand and charging the battery to its full capacity, hourly EE_t calculations are done using (5.9). At the end of three years (t=26280 hours), net LPSP=sum($LPSP_t$) and EE=sum(EE_t). The COE is calculated using (5.7). Similarly, fitness of all the population member are evaluated by calculating the objective function value through the long term evaluation analysis.

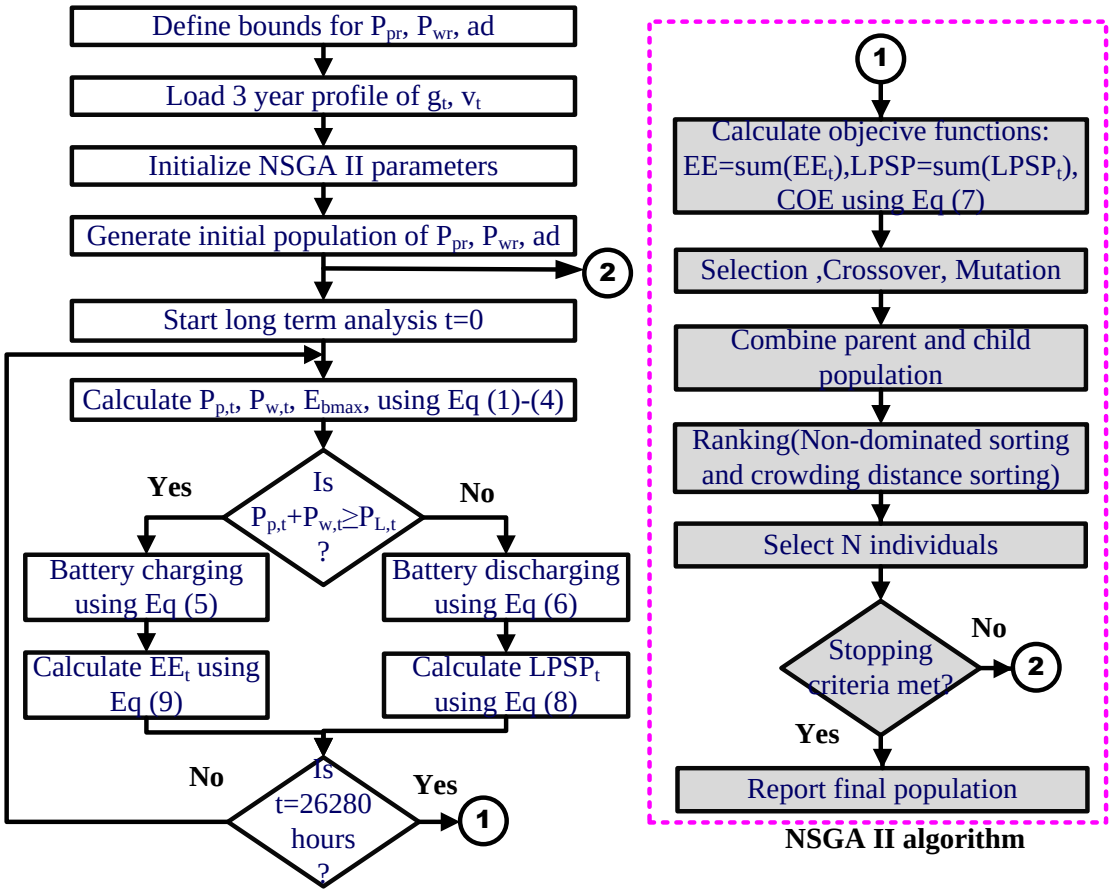

(a)

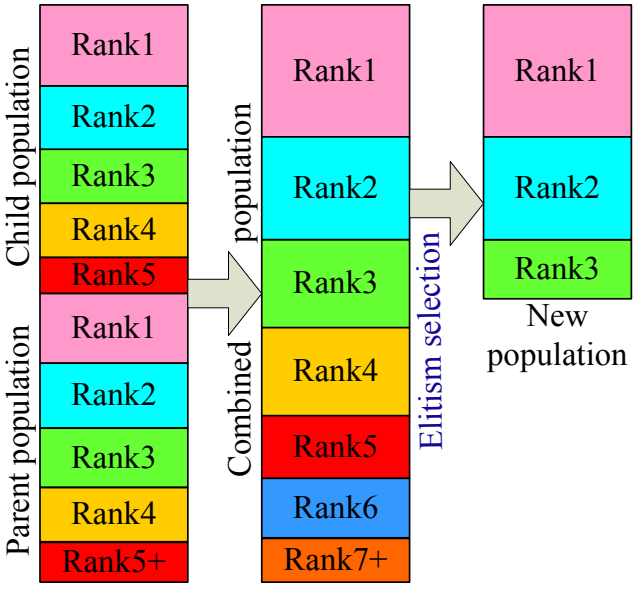

(b)

Figure 5.2: Optimization process based on NSGA-II (a) Flowchart (b) Offspring population selection in NSGA-II

Then offspring population is reproduced by following NSGA-II algorithm [91]. In NSGA-II, the parent population of size 'N' reproduces the offspring population. The non-dominated fronts are found from combined parent and child population by comparing each with every other solution in the population to find if it is dominated, as shown in Fig.5.2b. All fronts that could not be accommodated are deleted. To maintain the population size, the last front is sorted using the crowded-comparison operator so that the population slot filled by least crowded solutions and comprehensive uniform spread is maintained in the algorithm. Then parent population is selected by tournament selection based on crowding operator and offspring are reproduced by crossover and mutation. The flowchart shown in Fig.5.2a gives the step-wise description of NSGA II algorithm.

5.5 Results and discussions

The HRES for the 3.5kW telecom tower load has been proposed in this chapter which is reliable, sustainable and environment-friendly power supply. A dedicated program is developed in MATLAB to implement NSGA-II algorithm to carry out the optimal sizing of the proposed HRES. The program is simulated for 500 generations to find the optimal size of WECS, PV panels and battery size for minimizing LPSP, COE, and EE. The optimization is carried out for the long term analysis i.e. for three years equivalent to the lifetime of battery considering the 50% DoD as the lower limit so that battery bank would have long life cycles. The optimal Pareto solution obtained is shown in Fig. 5.3. The best solution based on the user defined conditions can be obtained from the Pareto-solution without worsening any of the objectives. Three solutions are obtained based on three different conditions namely, fully reliable system having LPSP=0.0, the cheapest system having LPSP=0.2 and system having COE as per the grid supply with LPSP =0.038. The case study for the three scenarios is carried out for long term. Further, the performance analysis of HRES supplying the telecom load is validated for two months i.e. January and July. The solar irradiation and wind speed data is taken from website of National Renewable Energy Laboratory, Department of U.S. Energy for the year 2010 to 2012 as presented in Fig.5.4a and Fig.5.4b.

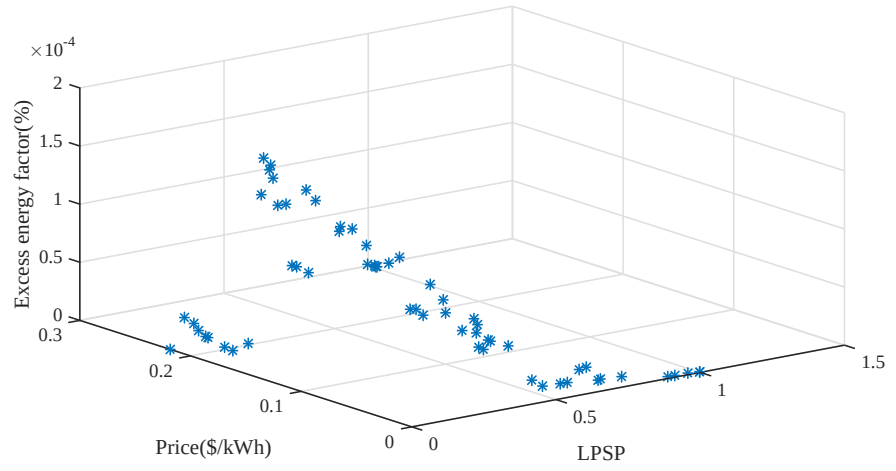

Figure 5.3: Pareto-optimal solutions of NSGA-II after 500 generations

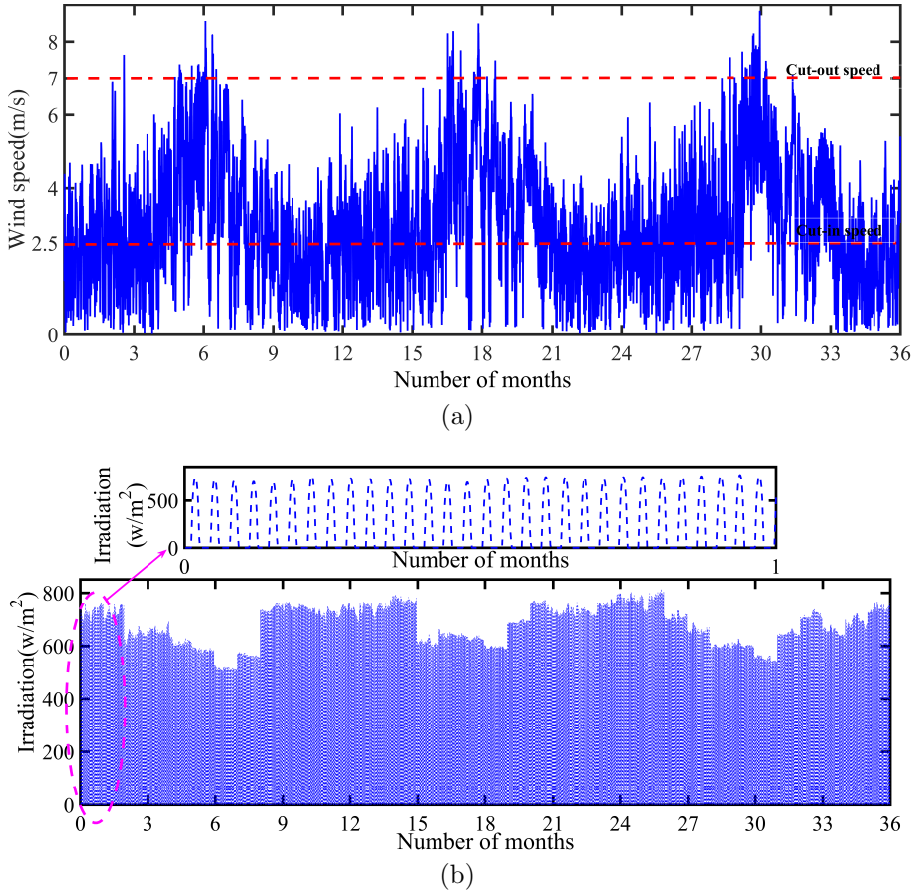

Figure 5.4: Data for the time period of long term analysis (a) Wind speed (b) Solar irradiation

5.5.1 Scenario 1: HRES configuration with LPSP=0

The size of 100% reliable HRES for telecom power supply obtained from the simulating the optimization process is 26.44 kW_p of PV plant with 106 PV panels each of 0.25kW_p, 9kW of WECS, and 400V, 306.63Ah battery energy storage considering 14 hours back-up. The cost of electricity of the obtained HRES configuration is Rs.13.08 ($0.218), and LPSP is 0.0. Fig.5.5a shows the long-term analysis of renewable power generated by HRES and battery SoC level. It is evident from the Fig.5.5a that the battery SoC level is maintained above 50% while supplying the load when renewable power (P_R) is not available. Further, the size of renewable resources is appropriate which generates sufficient energy that charges the battery after supplying the load demand. Fig.5.5b shows the frequency of DoD level achieved by the battery in three years. The battery discharge reaches to 50% of DoD level for only 3.8% of the total time which ensures long life cycle of the battery.

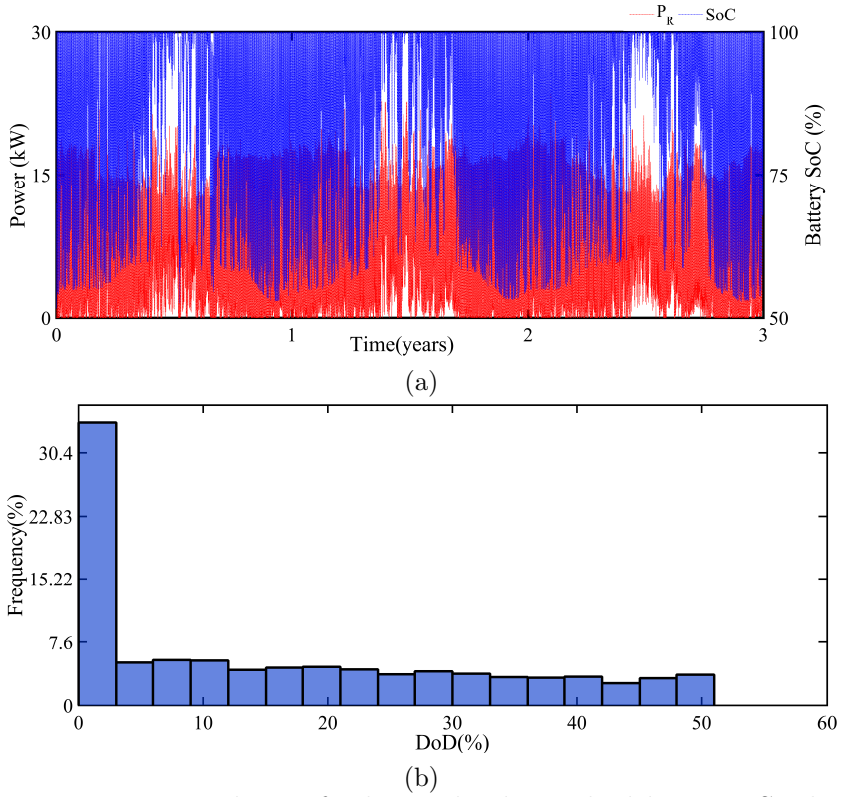

Figure 5.5: Long term analysis of telecom load supplied by HRES when sizing is done by taking LPSP=0 (a) Renewable power generated and SoC (b) Frequency of DoD of the battery

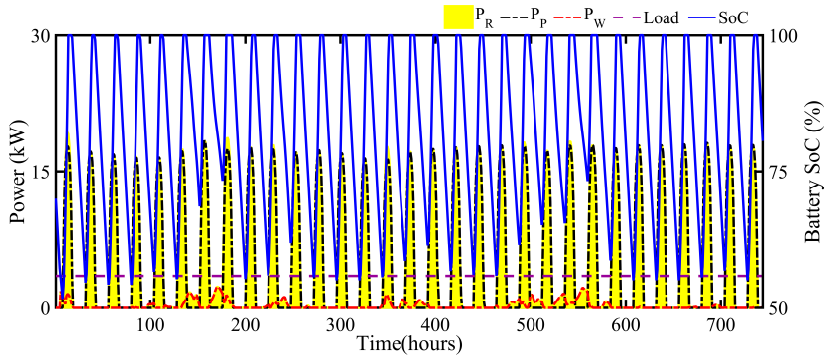

(a)

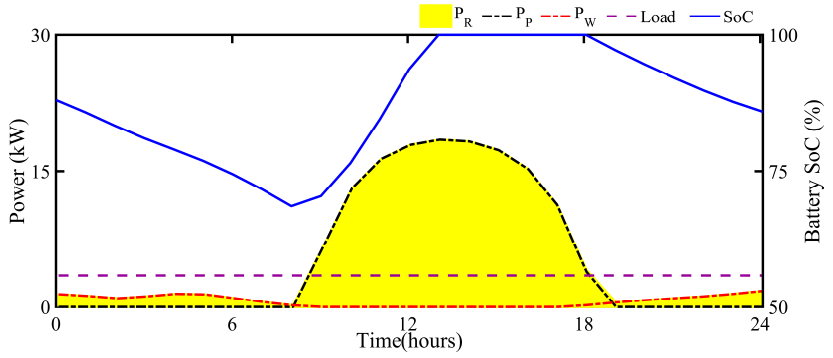

(b)

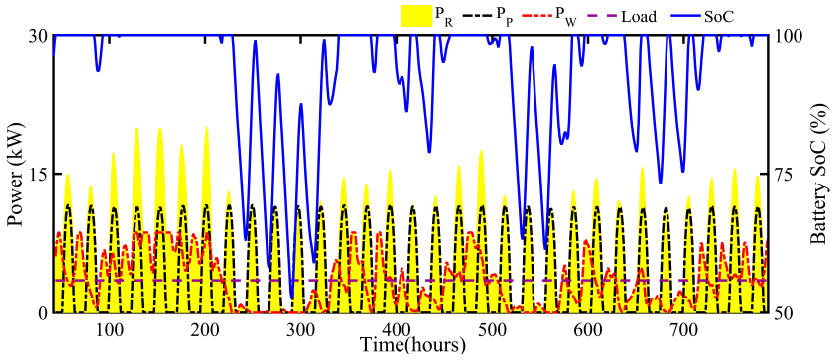

(c)

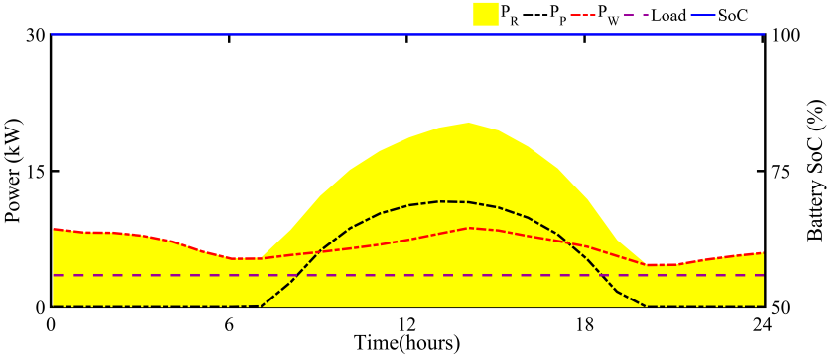

(d)

Figure 5.6: Performance of the renewable supplied telecom load for scenario 1 (a) January (b) A random day of January (c) July (d) A random day of July

The power generated by PV and WECS to meet 3.5kW of telecom load for the month of January and a random day of January is shown in Fig.5.6a and Fig.5.6b respectively. The PV panel generates power for 11 hours of the day i.e. from 8 a.m. to 7 p.m. with a peak power of 18.44kW. WECS generates the peak power of 1.78 kW, but no power from 8 a.m. to 5 p.m. as the wind speed is below the cut-in speed. As renewable energy is not sufficient to meet load demand, the battery discharges till 8 a.m. reaching a minimum SoC level of 68.59% of the day. The battery start getting charged as surplus solar energy is available during the day and reaches 100% SoC level at 1 p.m. and discharges after 6 p.m. Similarly, the renewable power generation and battery charge-discharge cycle for the month of July and a random day in July is shown in Fig.5.6c and Fig.5.6d. The power generated by PV is available for 13 hours of the day with peak power of 11.56kW. The wind is available throughout the day, so the power generated by WECS in the range of 4.6kW-8.7kW. Thus, the battery remains fully charged throughout the day.

5.5.2 Scenario 2: HRES configuration with LPSP=0.038

The optimal size of the HRES corresponding to LPSP=0.038 is 24 PV panels each of $0.25kW_p$, 6.3kW wind turbine and 400V, 247.1Ah battery providing 11.28 hours back-up. The COE of HRES is Rs.10.74 ($0.179). Fig.5.7a shows the long-term analysis of renewable power generated by HRES and battery SoC level. It is evident from the Fig.5.7a that the battery SoC level is maintained above 50% while supplying the load when renewable power (P_R) is not available. Further, the size of renewable resources is appropriate which generates sufficient energy that charges the battery after supplying the load demand.

Fig.5.7b shows the frequency of DoD level achieved by the battery in three years. The battery discharges up to 3% for 27.63% of total time and reaches to 50% of DoD level for 5.4% of the total time. The power generated by PV and WECS to meet 3.5kW of telecom load for the month of January and a random day of January is shown in Fig.5.8a and 5.8b respectively. The PV generates power for 11 hours of the day i.e. from 8 a.m. to 7 p.m. with a peak power of 16.66kW. WECS generates the peak power of 1.25 kW, but no power from 8 a.m. to 5 p.m.

as the wind speed is below the cut-in speed. As renewable energy is not sufficient to meet load demand, the battery discharges till 8 a.m. reaching a minimum SoC level of 56.85% of the day. The battery start getting charged as surplus solar energy is available during the day and reaches 100% SoC level at 2 p.m. and discharges after 6 p.m. Similarly, the renewable power generation and battery charge-discharge cycle for the month of July and a random day in July is shown in Fig.5.8c and 5.8d. The power generated by PV is available for 13 hours of the day with peak power of 10.52kW. The wind is available throughout the day, so the power generated by WECS in the range of 3.5 kW-6.09kW. Thus, battery remains fully charged throughout the day except for 2% discharge for 4 hours in the night.

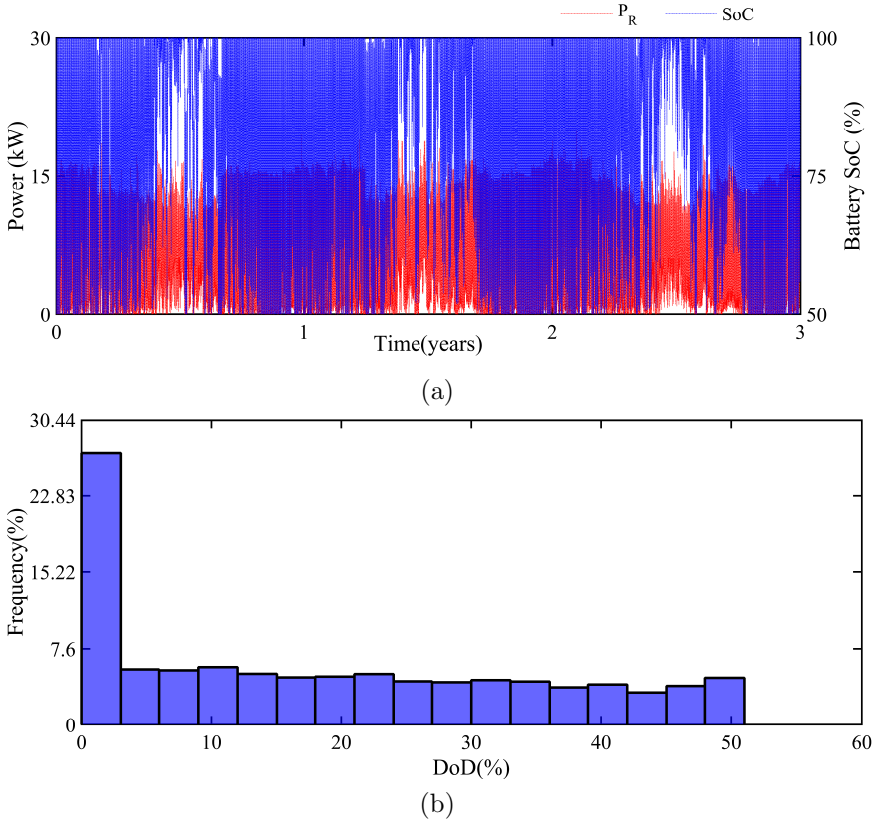

Figure 5.7: Long term analysis of telecom load supplied by HRES when sizing is done by taking LPSP=0.038 (a) Renewable power generated and SoC (b) Frequency of DoD of the battery

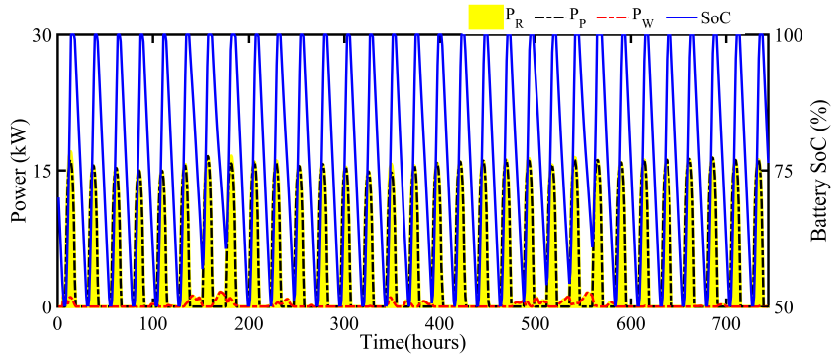

(a)

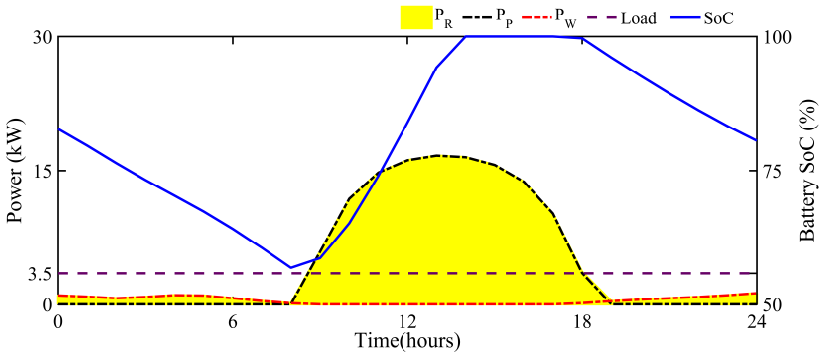

(b)

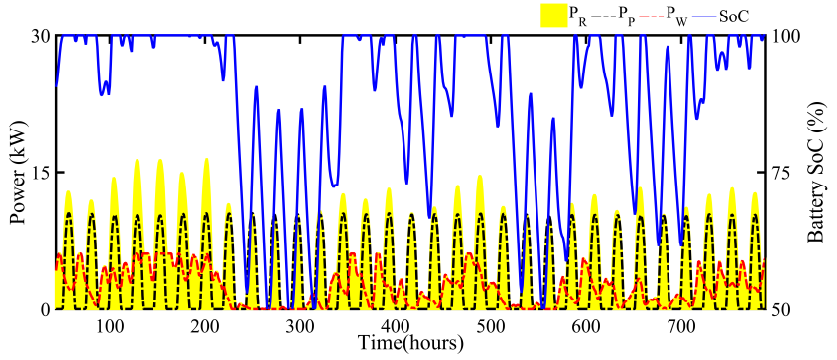

(c)

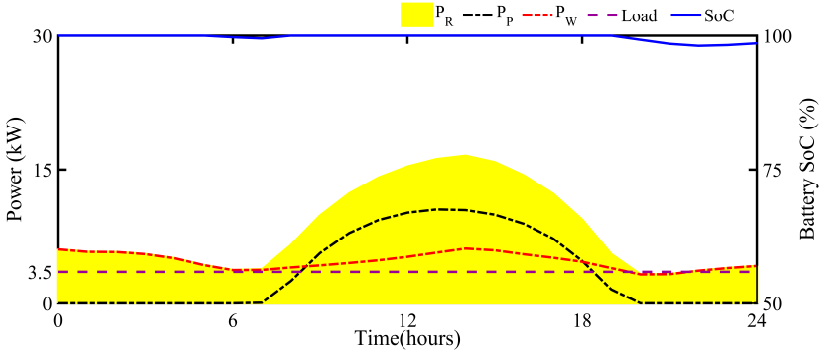

(d)

Figure 5.8: Performance of the renewable supplied telecom load for scenario 2 a) January (b) A random day of January (c) July (d) A random day of July

5.5.3 Scenario 3: HRES configuration with LPSP=0.2

The optimal size of HRES corresponding to COE (Rs. 5.34 or $0.089) lower than grid electricity price (Rs.7-9) is $11.72kW_p$ PV plant with 47 PV panels each of $0.25kW_p$, 30.8kW WECS and 400V, 189.3Ah battery with 8.64 hours back-up. The HRES with this configuration has large LPSP of 0.2. Fig.5.9a shows the long-term analysis of renewable power generated by HRES and battery SoC level. It is evident from the Fig.5.9a that the battery SoC level is maintained above 50% while supplying the load when (P_R) is not available. Further, the size of renewable resources is appropriate which generates sufficient energy that charges the battery after supplying the load demand though may be inefficient to supply the load for 20% times because of large value of LPSP (0.2). Fig.5.9b shows the frequency of DoD level achieved by the battery in three years. The battery discharges reach to 50% of DoD level for 27.4% of the total time which leads to reduced life cycles of the battery.

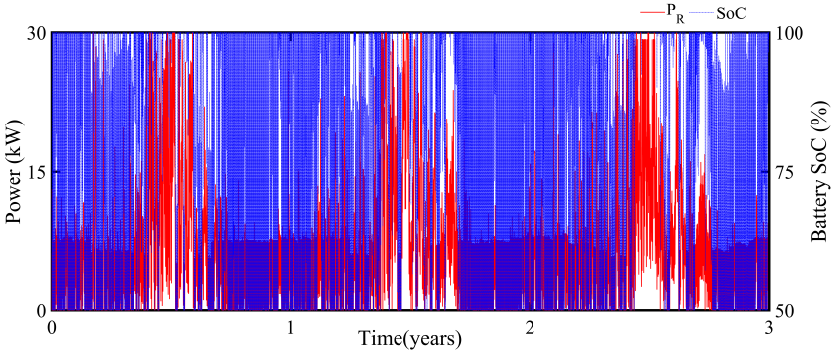

(a)

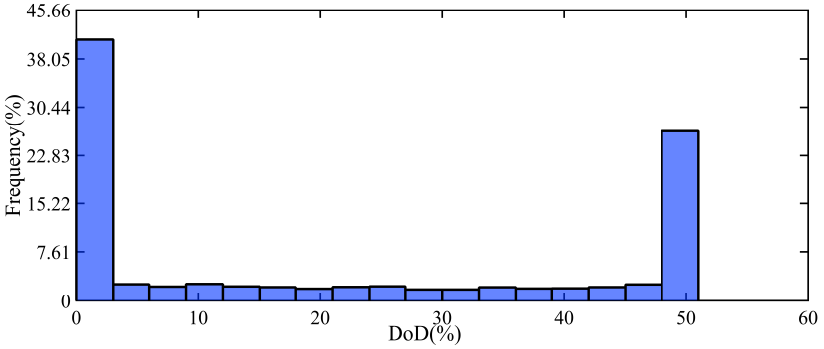

(b)

Figure 5.9: Long term analysis of telecom load supplied by HRES when sizing is done by taking LPSP=0.2 (a) Renewable power generated and SoC (b) Frequency of DoD of the battery

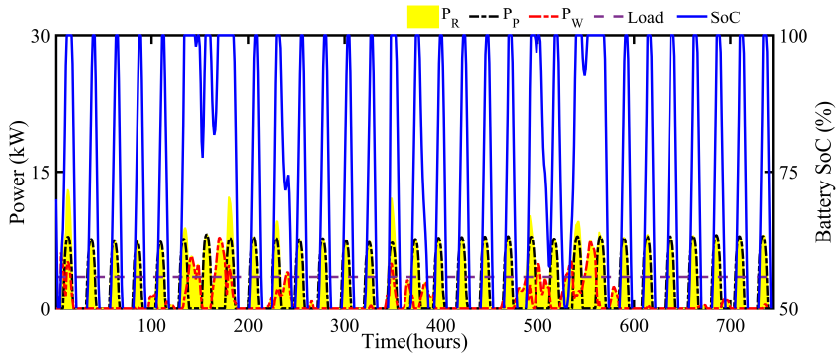

(a)

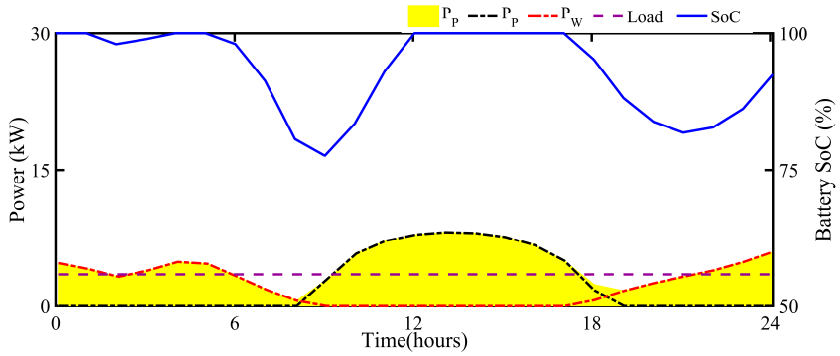

(b)

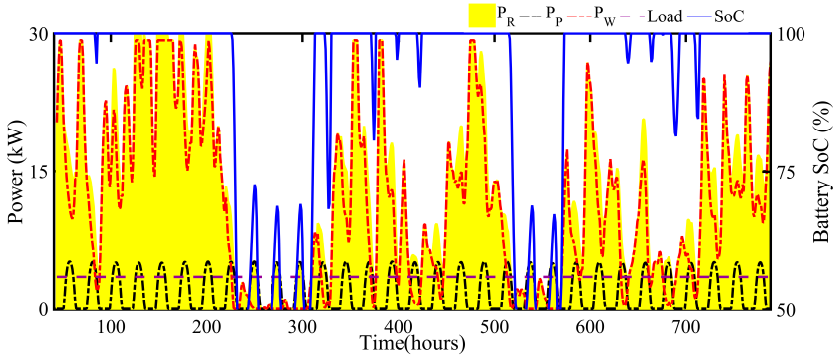

(c)

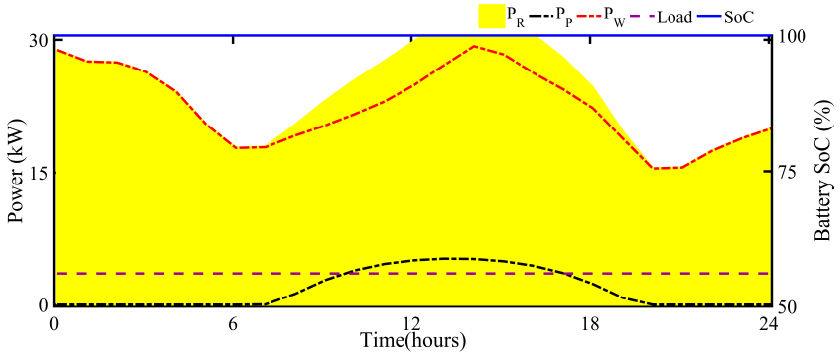

(d)

Figure 5.10: Performance of the renewable supplied telecom load for scenario 3 a) January (b) A random day of January (c) July (d) A random day of July

Table 5.2: Summary of optimal solution for techno-economic analysis of HRES

LPSP	0.0	0.038	0.2
Load	3.5kW	3.5kW	3.5kW
COE	0.2180$(Rs.13.08)	0.179$,(Rs.10.74)	0.089$,(Rs.5.34)
P_{pv}	26.44kW	23.89kW	11.72kW
P_{wt}	9.174kW	6.411kW	30.81kW
P_{batt}	400V, 306.63Ah	400V, 247.1Ah	400V, 189.3Ah
Back-up	14hrs	11.28hrs	8.64hrs

The power generated by PV and WECS to meet 3.5kW of telecom load for the month of January and a random day of January is shown in Fig.5.10a and 5.10b respectively. The PV generates power for 11 hours of the day with a peak power of 6kW. WECS generates the peak power of 8.173kW but no power from 9 a.m. to 5 p.m. As renewable energy is not sufficient to meet load demand, the battery discharges till 8 a.m. reaching a minimum SoC level of 56.85% of the day. Similarly, the renewable power generation and battery charge-discharge cycle for the month of July and a random day in July is shown in Fig.5.10c and 5.10b. The power generated by PV is available for 13 hours of the day with peak power of 5.16kW. The wind is available throughout the day, so the power generated by WECS in the range of 153.5kW-29.27kW. Thus, battery remains fully charged throughout the day.

Summary of optimal solution for techno-economic analysis of HRES is presented in table 5.2.

5.6 Summary

The HRES is proposed for new telecom towers that are to be installed in off-grid or bad grid areas to ensure economical, clean and green operation. NSGA-II, a multi-objective optimization technique has been successfully implemented to minimize the LPSP, excess energy and COE for techno-economic feasibility of the proposed HRES. Hourly solar irradiation and wind speed data profile are used for long term analysis equivalent to the lifespan of the battery. The modeling of

renewable resources is carried out with consideration of the de-rating factor and MPPT factor. The simulation study has been performed for different scenarios to analyze the feasibility the proposed HRES to supply telecom towers. It was observed from the simulations that, for 100% reliable system the COE is Rs 13 i.e., 35% lower than conventional diesel-generator system. If the 3.6% risk is allowed then the COE reduces to Rs.10.74 and further increasing the LPSP to 20% results in Rs 5.34 i.e., lower than the COE from the grid power supply (Rs 6-7). It is noteworthy that the procedure developed for optimal sizing in the present chapter should be carried out for each tower to get the number of PV panel, size of wind systems and battery requirements. Tower to tower, renewable energy potential can change depending on the geographical location.

Chapter 6

Optimal sizing of HRES considering uncertainty in source and load

6.1 Introduction

In this thesis, HRES consisting of complementary natured PV and wind energy resources along with battery back-up is proposed for the BS in remote/rural areas. The optimal sizing analysis is essential to find the optimal mix of renewable resources and storage for economic and reliable power supply, to mitigate the non-linearity and intermittency of renewable resources. The over-sized HRES results in higher reliability, but at higher capital expenditure and the undersized HRES gives economical system at the stake of reduced reliability of power supply. In previous chapter, the optimal sizing of the HRES based power supply for BS in remote/rural areas as proposed in chapter 4 is attempted by formulating multi-objective optimization problem. Three objectives are formulated viz. LPSP, COE and EE which ensure reliable and cost effective configuration. A well known NSGA-II algorithm is implemented for the long term analysis of the system to find the Pareto optimal front of the solution candidates. In NSGA-II based optimal sizing technique renewable resources are modelled without uncertainties and constant load equivalent to the peak load is considered which may lead to system

oversizing. Also, the rated wind capacity variable is taken as positive real number (continuous variable). Further, the architecture of HRES consists of lead acid batteries for the storage, and a maximum limit of 50% is imposed on the DoD to have enhanced lifespan of the batteries.

In the present chapter, detailed mathematical modelling of HRES to reflect the near practical behavior of the renewable is developed for the comprehensive cost analysis for optimal sizing. The BS load is modelled based on the long term evaluation model and the telecom traffic is modelled using poison PDF [120]. The uncertainty in the renewable resources is incorporated using PDF in the optimal sizing optimization. The uncertainties in wind speed and solar irradiation are incorporated using Weibull and Beta PDFs. In previous chapter, capacity of wind turbine is approximated to continuous variable. As commercially available sizes of wind turbines are discrete in nature and continuous variable based optimization leads to a suboptimal solution. Since, single objective approach is not always practical, as all the criteria cannot be converted to same unit as of cost. The conventional approaches such as weighted sum strategy or ϵ-constraint modeling are not efficient enough to solve multiple-objective optimal sizing problem. The effect of one objective might influence the optimization solution in a higher proportion. A multi-objective approach is presented to consider different criteria without the need of conversion for the unified unit to define the optimal sizing share between PV and wind power generations. The LCOE is considered for cost analysis of HRES which account for the capital, replacement, operation and maintenance costs. Reliability studies are based on balancing the HRES power generation and load demand. Reliability studies are based on whether the generation can meet the demand which is represented in terms of LPSP However, it is equally essential for a standalone HRES to keep a check for excess power generation after meeting the load demand, as excess energy can not be sold to the grid. Therefore, an additional reliability index based on excess energy generated, along with LPSP, is introduced in this thesis for optimal sizing analysis of standalone HRES for BS.

NSGA-II is implemented to get the optimal configuration of the renewable based power supply. The NSGA-II employs the fast non-dominated sorting and parameterless niching operator to group the individuals in the population after selection, recombination and mutation [91]. MPSO is also implemented for optimal sizing.

However, the fast convergence of the algorithm may leads to the local minimum stagnation and results in a pseudo Pareto front (sub-optimal solution). Thus, DMGWO is proposed in this chapter. DMGWO utilizes the concept of the external archive to store the non dominated sorted solutions which enhances the convergence rate similar to MPSO. However, the leader selection mechanism of DMGWO prevents premature termination of the algorithm. Further, a corrective algorithm is embedded in DMGWO to handle the discrete variable (capacity of wind turbine). The DMGWO finds the optimal energy mix of the proposed PV-wind based HRES by minimizing the three objective viz. LPSP, LCOE and EE.

In the following section of the chapter, modelling of the HRES, problem formulation and DMGWO description is given. Further, analysis of the optimal configuration of the HRES from DMGWO based optimal sizing optimization is discussed in section 6.4.

6.2 HRES modelling

The proposed HRES for the BS of telecom tower consists of the PV-panels and single unit of wind generator installed at the top of telecom tower. Further, a

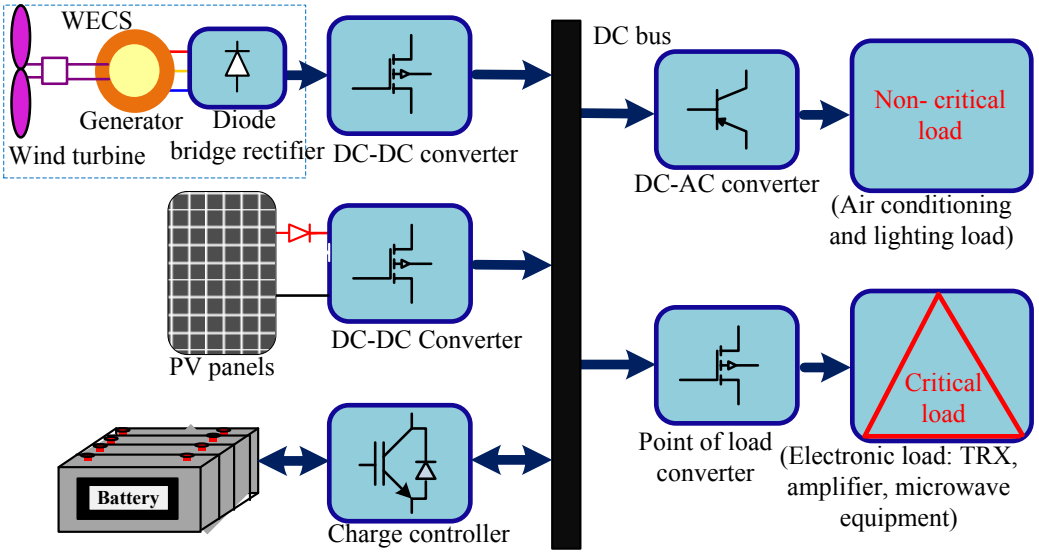

Figure 6.1: Architecture of the proposed PV-wind HRES for BS

battery storage system buffers the intermittency in renewable energy generation. A bidirectional buck-boost charge controller is employed to match the voltage level of battery bank rated voltage of 400V with the DC distribution bus voltage (48V). Distribution bus supplies power to critical loads (electronic components, transceiver, amplifier) and non critical loads (lighting and air conditioning load). The architecture of the proposed PV-wind based HRES for BS is shown in Fig.6.1.

6.2.1 BS load modelling

Generally, macro BS are installed along the highways and remote areas. The traffic load at BS is quantified in terms of power consumed by air conditioners and losses in feeders as fixed load, and instantaneous traffic of communication signal forming the variable load. The power consumption at the LTE macro BS is given by (6.1) [120] and is shown in Fig. 6.2a for one week.

$$P_{L,t} = N_{trx}(P_o + \Delta K(t) P_{max}), \quad 0 \leq K(t) \leq 1 \tag{6.1}$$

It is observed from the Fig. 6.2a that the traffic load follows diurnal patterns owing to peak loads during the day and low traffic during the night. Also, the overall load on weekends is lesser than the weekdays.

6.2.2 PV modelling

The solar irradiation data is characterized by the bimodal distribution function. The solar data is divided into two groups for the same hour over the number of days and each group has unimodal distribution. The unimodal function that match best to the considered solar data is beta distribution [121]. The beta distribution parameters for historical hourly irradiation data are estimated using maximum-likelihood method in curve fitting toolbox of MATLAB. The estimated beta PDF fit for solar irradiation is shown in Fig. 6.2b.

$$f(g_t) = \frac{\Gamma(a+b)}{\Gamma(a)+\Gamma(b)} g_t^{(a-1)}(1-g_t)^{(b-1)} \tag{6.2}$$

Then, the PV output power is calculated for each hour. A_p for 1kW PV panel is 1.75 m^2.

$$P_{p,t} = \eta_p \eta_{dr} A_p g_t \tag{6.3}$$

6.2.3 Wind energy conversion system modelling

The wind speed follows the Weibull PDF based on the historical data analysis. The two parameter Weibull PDF for the wind speed is given by (6.4) and (6.5). The estimated beta PDF fit for solar irradiation is shown in Fig. 6.2c.

$$f(v_t) = \frac{k}{C}\left(\frac{v_t}{C}\right)^{k-1} exp\left[-\left(\frac{v_t}{C}\right)^{k}\right] \tag{6.4}$$

The cumulative distribution function of Weibull distribution given by

$$F(v_t) = exp\left[-\left(\frac{v_t}{C}\right)^{k}\right] \tag{6.5}$$

The power output of the WECS for each hour is given by:

$$P_{w,t} = \begin{cases} 0, & \text{if } v_{ci} < v_t > v_{co} \\ v_t^3 \frac{C_w}{v_t^3 - v_{ci}^3} - C_w \frac{v_{ci}^3}{v_t^3 - v_{ci}^3}, & \text{if } v_{ci} < v_t < v_r \\ C_w, & \text{if } v_r < v_t < v_{co} \end{cases}$$

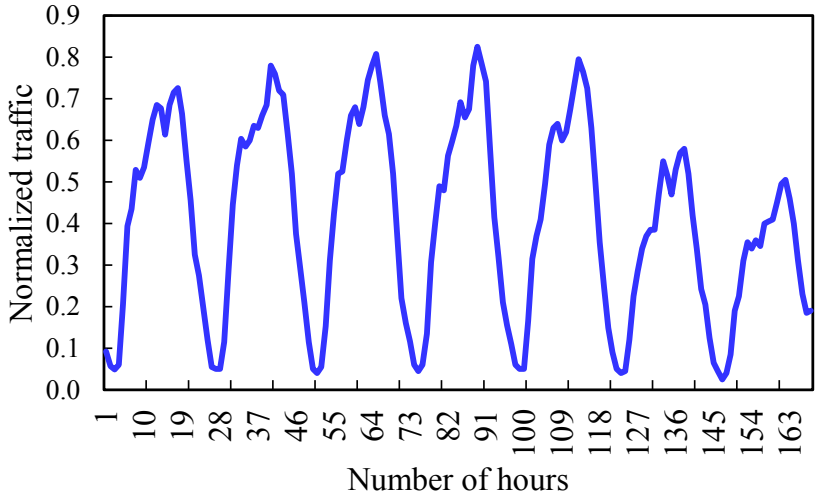

(a)

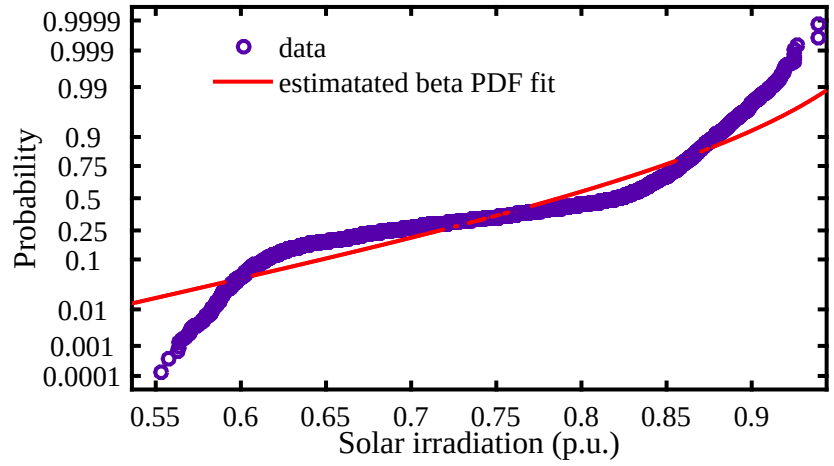

(b)

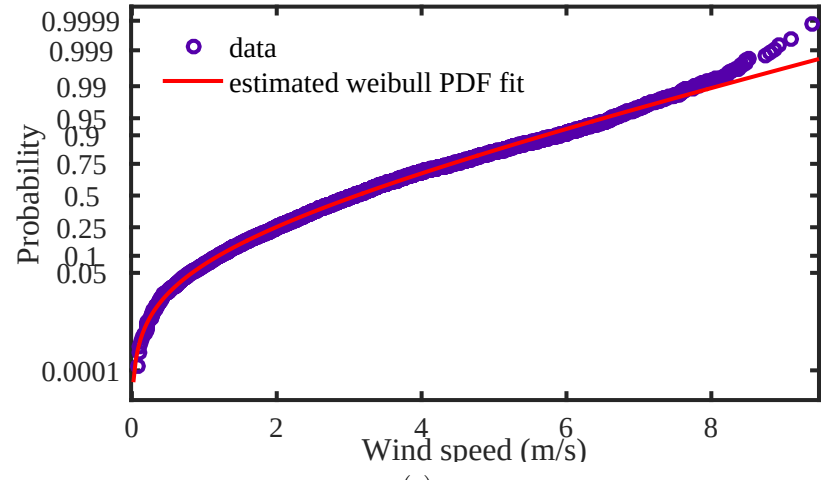

(c)

Figure 6.2: Data representation(a) normalized telecom traffic over a period of one week (b) Estimated Beta PDF fit for solar irradiation (c) Estimated Weibull PDF fit for wind speed

6.2.4 Battery modelling

The maximum battery capacity required for telecom load is as follows,

$$E_{b,max} = \frac{P_{L,avg} ad}{DoD \eta_{co} \eta_b} \tag{6.6}$$

Charging of the battery takes place when energy generated by the renewable resources is in surplus after meeting the load demand, i.e. $(P_{p,t} + P_{w,t} - P_{L,t} > 0)$. Charging happens only if $E_{b,t} < E_{b,max}$ and the $E_{b,t}$ is given by

$$E_{b,t+1} = E_{b,t} + \eta_s (P_{p,t} + P_{w,t} - P_{L,t}) t \tag{6.7}$$

It is assumed that each step of simulation is equivalent to one hour.

Discharging of the battery takes place when energy generated by the renewable is incapable of meeting the load demand, i.e.$(P_{p,t} + P_{w,t} - P_{L,t} < 0)$. Also discharging happens only if $E_{b,t} > E_{b,min}$ and the $E_{b,t}$ is given by

$$E_{b,t+1} = E_{b,t} + \eta_s (P_{p,t} + P_{w,t} - P_{L,t}) t \tag{6.8}$$

where, $E_{b,min} = (1 - DoD) E_{b,max}$ and the DoD is taken as 80%.

6.3 Optimal sizing

The configuration of the proposed PV-wind HRES should be such that it supplies reliable and economical power to the BS in remote/rural areas. Both cost and reliability are significant criteria which are incommensurate, therefore multi-objective

mixed integer optimal sizing problem is formulated. LCOE is calculated for HRES to analyze the system economy. An EE index is developed to keep check on excess energy generation along with LPSP which evaluates the system reliability. A corrective algorithm is developed to handle discrete capacity of the wind turbines in the optimization process. The optimal analysis is simulated for whole year with the step size of one hour.

6.3.1 Discrete multi-objective grey wolf optimization algorithm

A multi-objective grey wolf optimizer is proposed in [122] for continuous variable optimization problems. In this chapter, a DMGWO is proposed to solve the multi-objective mixed integer optimal sizing of the PV-wind HRES for the BS of telecom tower.

DMGWO simulates the hunting mechanism and leadership hierarchy in apex predators of food chain i.e. a pack of grey wolves. There are four types of wolves in the pack, alpha (α) the leader, beta (β) the subordinator, omega (ω) the scapegoats and the remaining are delta (δ). The pack of wolves perform the three steps of hunting, encircling and attacking the prey. The encircling is modeled for iteration k_{th} as

$$\vec{D_{dis}} = \left|\vec{C}\vec{X_p}(k) - \vec{X(k)}\right| \tag{6.9a}$$

$$\vec{X}(k+1) = \left|\vec{X_p}(k) - \vec{A}\vec{D_{dis}}\right| \tag{6.9b}$$

where, $\vec{A} = 2\vec{a}r_1 - \vec{a}$, $\vec{C} = 2r_2$, $\vec{a}$ varies linearly from 2 to 0. r_1 and r_2 are random variables in the range [0,1]. The search agents explore by diverging from the prey when $\vec{A} > 1$ and exploit the search space by converging to the prey when $\vec{A} < 1$. The GWO is modified to solve the multi-objective optimization by employing archive concept similar to MPSO. External archive stores the non-dominated Pareto-optimal solutions obtained so far and aids the sorting. If the archive is full, the grid mechanism is followed to accommodate more non-dominated solutions. The grid mechanism suggests that the non-dominated solutions which are in the

most crowded zone are omitted to accommodate the new non-dominated solutions. Further, α, β and δ solutions are selected from the archive for the hunting process. The leader selected from the least crowded area of solution search space which ensures coverage and diversity of solution across the search space among all solutions. In the conventional MGWO[122], all the variables are continuous. A corrective algorithm is proposed in this chapter to handle with discrete wind turbine capacity variable. The corrective algorithm is embodied in the MGWO to transform it to discrete MGWO. Fig. 6.3 presents the flowchart of DMGWO. There are three solution variables: C_w (discrete variable), N_{pv} and ad. Initial population is randomly generated for each variable. During the process of updation of the position of each variable in the population based on the position of selected leaders (α, β and ω), C_w also get converted to continuous variable. Then, the corrective algorithm generates the two possible integers for the C_w. Also takes the

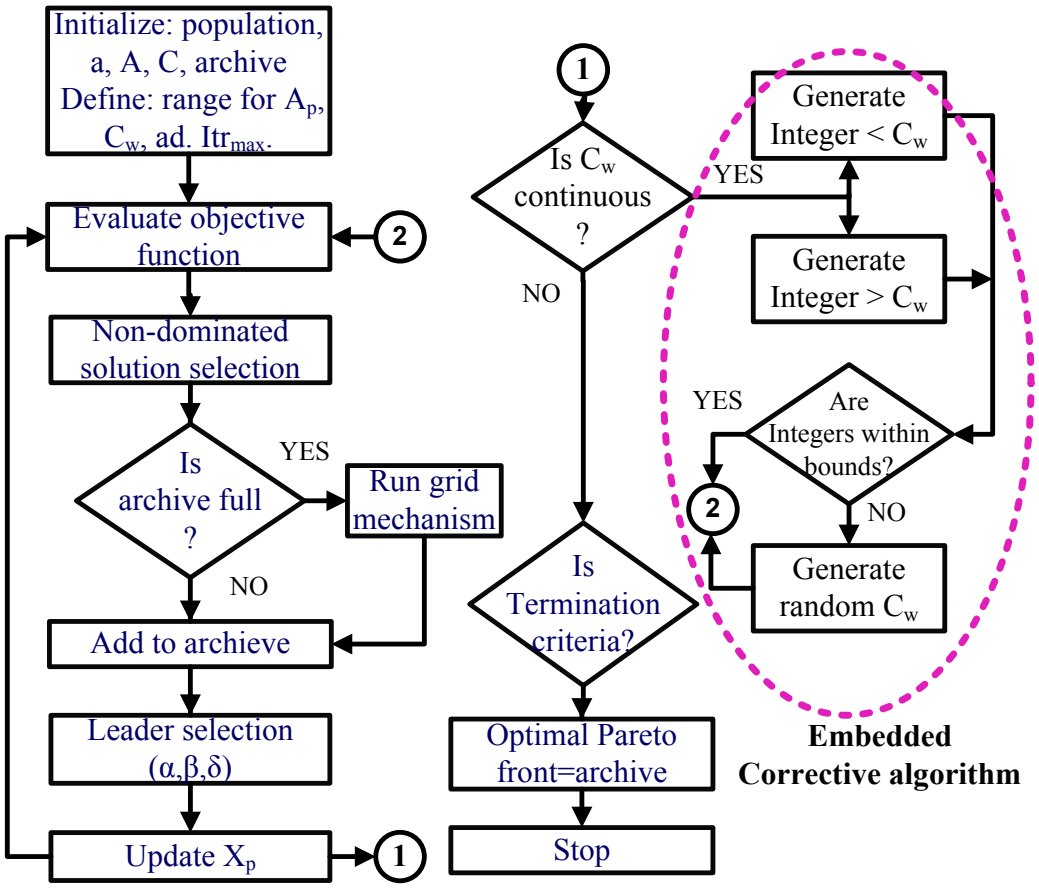

Figure 6.3: DMGWO with embedded corrective algorithm

corrective action if C_w violates the predefined boundary limits by replacing it with a new random integer.

6.3.2 Objective functions

6.3.2.1 Economic analysis

The economical analysis of the HRES includes cost analysis of each component (PV panel, wind turbine, converters and battery). The present worth (PW) of the cost (investment, replacement, operation and maintenance cost) for each component is calculated using (6.10). Then, LCC is summation of the PW of all costs (investment, replacement, operation and maintenance cost) for each component. LCOE is calculated by annualized LCC from (6.11).

$$PW = y\ Cost,\ PW_c = \frac{1-y^n}{1-y},\ where\ y = \left(\frac{1+r_i}{1+r_d}\right)^n \tag{6.10}$$

$$ALCC = \frac{LCC}{yPW_c},\ LCOE = \frac{ALCC}{\text{Total energy gerneration}} \tag{6.11}$$

6.3.2.2 Reliability analysis

Reliability analysis is necessary considering the intermittent nature of power generated by renewable resources. LPSP is a statistical term that defines the probability of insufficient power supplied by the HRES to the load demand. LPSP obtained as 0 is best, indicating 100% reliable system, whereas, value 1 indicates the worst reliability.

$$LPSP_t = \frac{P_{L,t} - P_{p,t} - P_{w,t} + E_{b,min}t}{P_{L,t}} \tag{6.12}$$

6.3.2.3 Excess energy

The reliability of the HRES improves as the system size increases. Similarly, the generation cost comes down for large scale installation of the renewable resources. However, the over-sized renewable installation is beneficial to the telecom operator only if the HRES is grid connected as excess energy is sold to the grid. However, the BS considered here is off-grid, therefore excess energy has to dissipate in dump loads. Optimizing the energy mix for standalone system using only two criteria which are LPSP and LCOE leads to an over-sized system. Therefore for a standalone BS, the optimal sizing of the HRES necessitates the consideration of the EE criteria along with LPSP and LCOE. The EE is calculated under the condition that energy generated from renewable resources is greater than the load demand and battery is fully charged. The EE is minimized in the process of optimization and is given by

$$EE_t = \frac{P_{p,t} + P_{w,t} - P_{L,t}}{P_{p,t} + P_{w,t}} \text{ only when } E_{b,t} = E_{b,max} \tag{6.13}$$

6.4 Optimal configuration analysis

The PV-wind based HRES is proposed to supply reliable, sustainable and environment friendly power to off-grid BS of the telecom tower in the remote/rural areas. A dedicated program is developed in Matlab to implement DMGWO to optimize the size of HRES by achieving the trade-off among the three objective viz. LCOE, LPSP and EE.

The historical data of solar irradiation and wind speed is taken from national renewable energy laboratory (NREL), USA website [119]. Then the data is modelled

Table 6.1: Optimal Configuration of HRES

A_p	$C_w(kW)$	$E_b(kWh)$	$LCOE(\$)$	$LPSP$	EE
21	02	10.64	0.12	0.07	0.21

through PDF as explained in section 6.2. The mean and variance of normalized solar irradiation are 0.775 and 0.009, and that of wind speed are 3.313 and 3.0643 respectively. Beta PDF is estimated for solar irradiation with parameters a and b as 14.1742 and 4.080 respectively. Similarly, wind speed follows the Weibull PDF with C and k values as 3.737 and 1.976 respectively. Based on the estimated PDFs, the one year data profiles are generated for solar irradiation and wind speed as shown in Fig. 6.4a and 6.4b. The one year BS load (power consumption) based on the LTE model discussed in section 6.2 is shown in Fig. 6.4c. The objective functions are evaluated after one year performance analysis of the HRES.

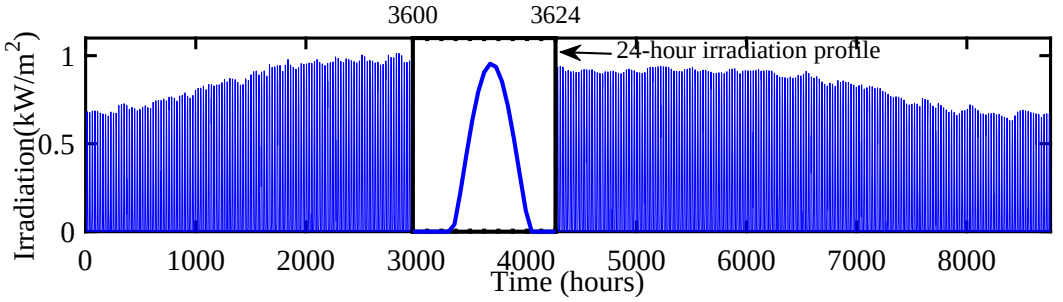

(a)

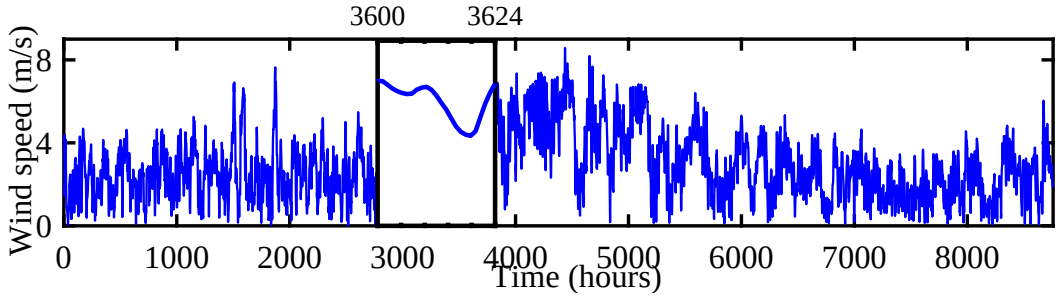

(b)

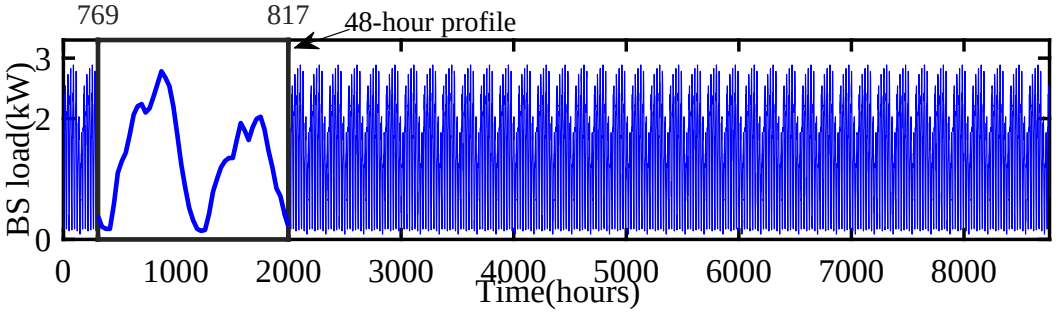

(c)

Figure 6.4: One year profile of data (a)Solar irradiation (b) wind speed (c) BS load

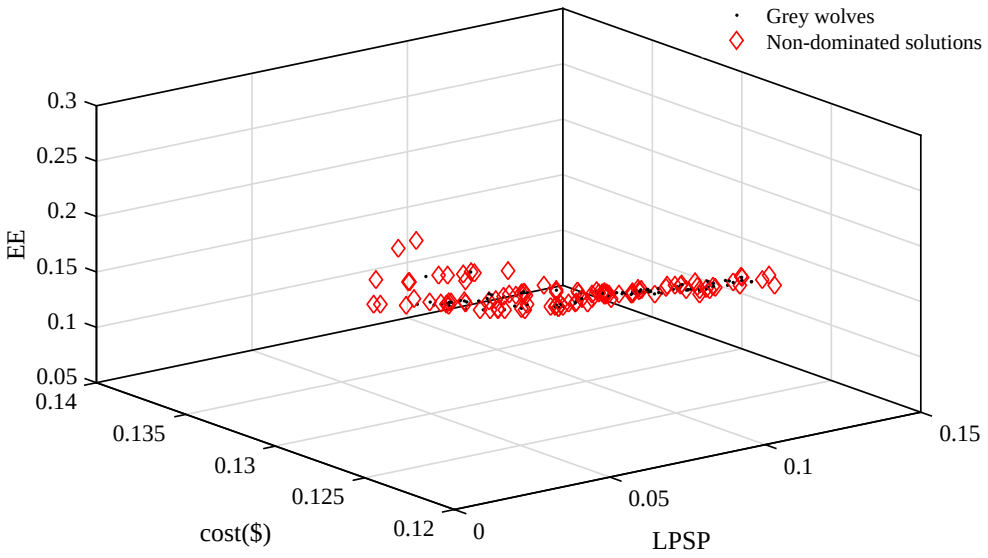

Figure 6.5: Pareto optimal front of the DMGWO

The DMGWO generates the optimal Pareto front as shown in Fig.6.5 after 500 iterations or when there is no further improvement in the fitness of the solution candidates. All solutions in the Pareto front are non-dominated and any solution could be selected without worsening any of the objectives. The wide spread of the solutions in the Pareto front provides flexibility to the user (telecom operator) to choose the suitable solution as per the user defined conditions. Here, Euclidean distance based method is implemented for decision making from the Pareto front and the optimal configuration of HRES so obtained is presented in table 6.1.

6.4.1 Power balance analysis

The A_p required to install PV panels is $21m^2$ which can accommodate PV panels of $6kW_p$ capacity. The rating of single unit wind turbine to be installed on the tower calculated by the DMGWO is 2kW as the DMGWO is embedded with corrective algorithm to handle discrete variable. The battery bank capacity is 10.64 kWh with 5.04 autonomous hours. The optimal configuration of proposed PV-wind HRES supplies BS at LCOE of \$0.12 (Rs 7.20). Conventionally, telecom operator bears the LCOE of \$0.33 (Rs 20) when DGset are used to supply same BS in remote/rural areas. The LPSP obtained is 0.07 indicating that supply reliability is good. Further, the EE value for system is 0.21 indicating that excess energy

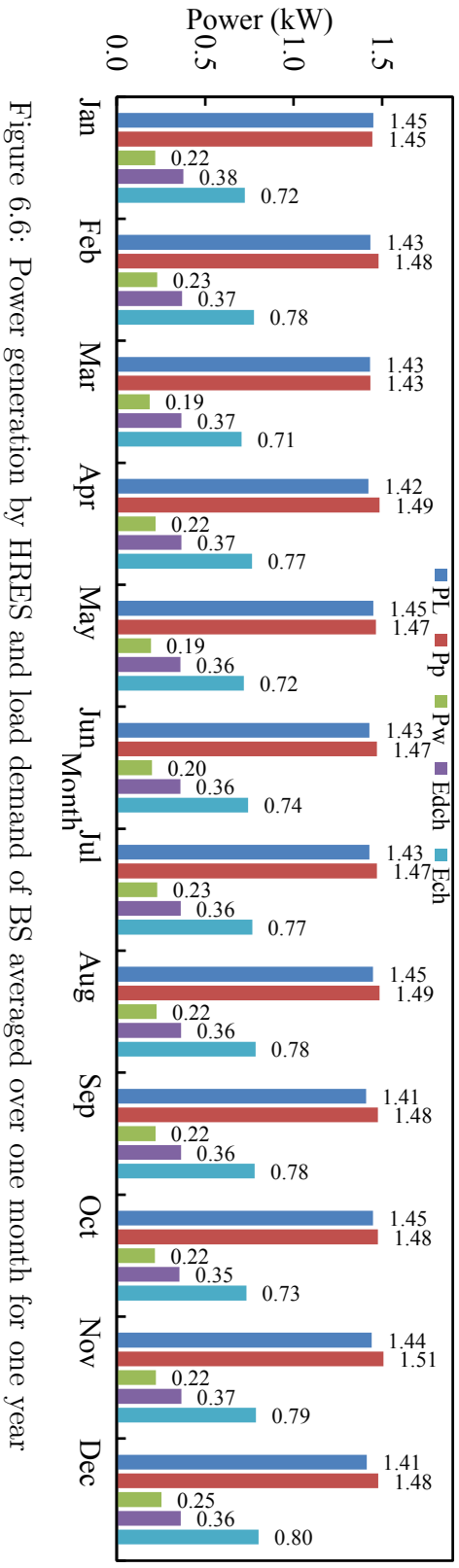

Figure 6.6: Power generation by HRES and load demand of BS averaged over one month for one year

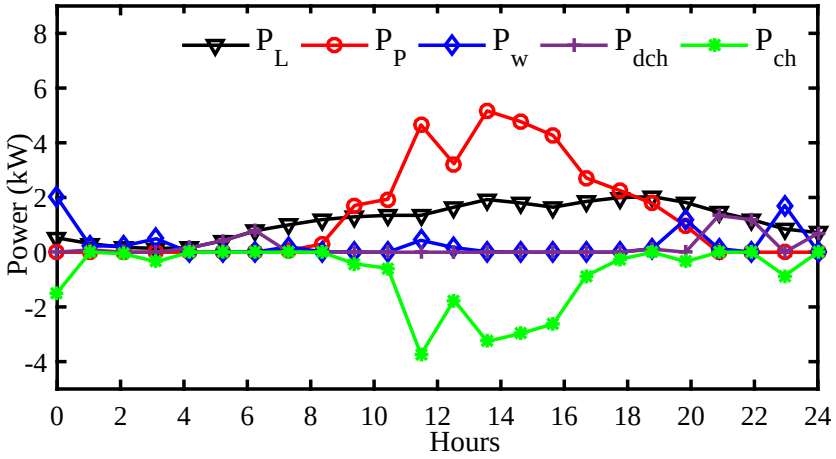

(a)

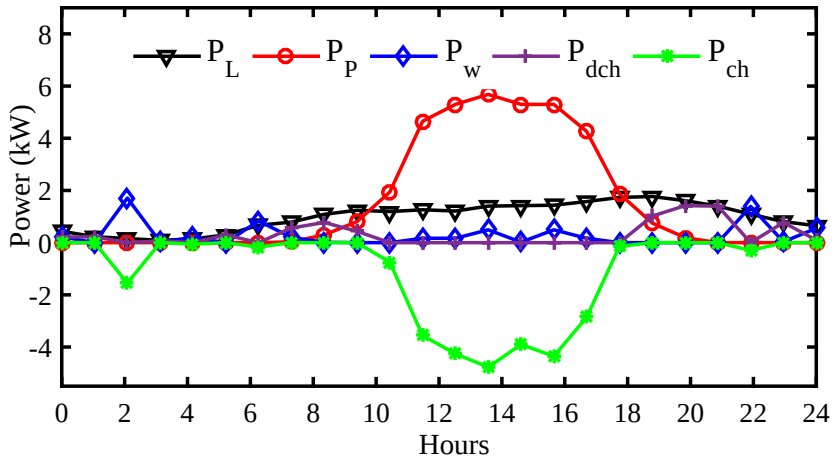

(b)

Figure 6.7: 24-hour profile for power balance for the load demand of BS (a) Weekday (b) Weekend

generation is under check. Figure 6.6 presents the monthly analysis over the whole year of the load met by the PV-wind HRES. Each month is represented by one day which is average power generated and load over the month. It is observed that battery discharges each month to mitigate the intermittency in renewable sources and get charged from the renewable power exceeds the load demand.

As the weekday load is higher than weekends as shown in Fig. 6.4c, therefore, one weekday and weekend 24-hour profile analysis is done separately. The random weekday and weekend 24-hour profile showing the pattern of load, renewable power generation, charging and discharging of battery is shown in Fig. 6.7. Figure 6.7a presents the weekday power balance analysis. The peak load demand for the

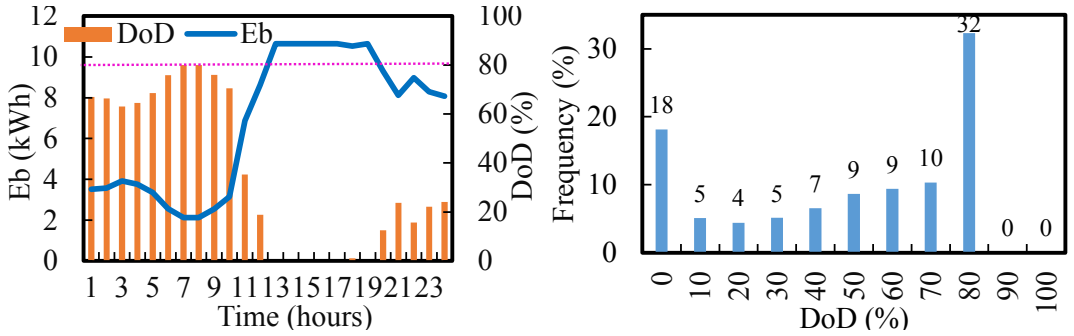

(a) (b)

Figure 6.8: Battery profile and DoD analysis (a)24 hour analysis (b) Complete year analysis

weekday is 2.03kW at 19:00 hours. The P_p is available from 7:00 to 19:00 hours with maximum power generation of 5.17kW at 13:00 hours. During daytime, excess energy generated by PV charges the battery from 9:00 to 17:00 hours. When power from PV is not available, load demand is met by WECS during the night from 22:00 to 03:00 hours. Battery also supplies the load demand along with renewable resources when the $P_{p,t} + P_{w,t} < P_{L,t}$. Figure 6.8a shows the status of battery energy available throughout the day and DoD level. It is observed that the DoD of the battery doesn't exceed the limit of 80% and minimum energy of 2.13kWh is maintained. Battery remains above the 50% of DoD for 14 hours in the day. Similarly, the weekend analysis is shown in Fig. 6.7b. The peak load demand is 1.77 kW at 19:00 hour lesser than weekdays and least load demand of 0.088 kW at 04:00 hour. As observed from the Fig. 6.7b, the excess power is available from PV panels between 10:00 to 17:00 hour. The battery charges from the wind power between 1:00 to 3:00 hour. The battery DoD remains above 50% throughout the day. In the same way, the battery charging and discharging profile is analyzed for the complete year. The minimum energy of 2.13kWh (DoD above 80%) is well maintained as evident from the Fig. 6.8b. The DoD above 50% is maintained for 48% time of the one year.

6.4.2 Assessment of the optimal configuration of the proposed HRES for BS

In the proposed PV-wind HRES, the contributions from different resources is assessed as the ratio of power generated by the resource to total power generated. The calculated fraction of PV (f_p) and wind(f_w) is 0.8716 and 0.1284 respectively. Then coverage of load by each resource is quantified as the ratio of total power generated by resource to the load power demand over the whole year. Coverage of load by PV (COL_p) is 1.0271 and that by WECS (COL_w) is 0.1513. Finally the energy to load ratio (ELR) is obtained as 1.1784.

6.5 Sensitivity analysis

The effect of design variable of the optimization (A_p, C_w and ad) on the three objective functions viz. LCOE, LPSP and EE is studied. Firstly, the optimal HRES configuration calculated by the proposed DMGWO based optimal sizing procedure (A_p=21m^2, C_w=2kW and ad=5.04 hours) is considered. The effect A_p on objective functions is studied by increasing P_p from 0kW to 100kW while keeping the other two variables to their respective optimal values. Then, C_w is varied from 0kW to 100kW while keeping the value of A_p and ad fixed. In the same way, E_b which is a function of ad is varied in the range 0kWh-100kWh.

As stated in subsection 6.3.2.3, large scale installation of renewable resources lead to lower LCOE, which is depicted by the Fig. 6.9a. LCOE reduces non-linearly (exponentially) by increasing the P_p. It is noteworthy that LCOE reduces by 13% and 23% with increment of 30% and 100% in the P_p beyond the optimal size of PV panels(P_p=6kW_p, A_p=21m^2). However, increasing the C_w beyond the optimal value (2kW) has negligible effect as LCOE reduces by only 2% with an increase of 50% in C_w. This happens because the WECS has higher capital cost than the PV panels. As discussed in section 6.1, increasing E_b in the HRES lead to higher LCOE is verified in Fig. 6.9a. LCOE increases linearly with increase in ad. LCOE increases by 33% with doubling the E_b in HRES.

The impact of parameter variation on LPSP and EE is studied in similar way

as LCOE is presented in Fig. 6.9b and 6.9c. In spite of higher capital cost of WECS than PV panels, PV-wind based HRES for telecom towers is proposed in this chapter. Because, increasing the C_w in HRES leads to lowering the LPSP index resulting in the more reliable system without additional E_b. It is observed from Fig. 6.9b and 6.9c, 100% increment in P_p beyond the optimal size results in 30% enhancement in reliability but the EE increases by 171%. Whereas,the 100% increase in C_w beyond the optimal size, reduces the LPSP by 41% with increase of EE by 30% only. This happens because the solar energy is available only during the day time as shown in Fig. 6.4a. Once the battery is charged during daytime, it discharges during the night time only. The wind availability is complementary to the solar irradiation as shown in the Fig. 6.4b. Hence, at night time load demand is met by the wind as well as battery is charged thus lesser value of EE index than that of PV.

Increasing the E_b in the HRES, enhances the reliability which is verified from the Fig. 6.9b. With E_b more than 32kWh HRES system has LPSP as 0 (theoretically 100% reliable) but with LCOE of \$0.2 which is 60% higher than the optimal configuration LCOE i.e.\$0.12. As the size of battery is increased, more EE is absorbed in the battery hence, the EE index reduces with increasing size of battery.

The sensitivity analysis shows that the design variables has non-linear relationships with the objectives as well as correlated to each other. Thus, the choice of multi-objective optimal sizing approach with three objectives is justified. The proposed DMGWO algorithm has given the non-dominated optimal Pareto front of solutions by achieving the trade off among the objectives and satisfying the constraints of the PV-wind HRES optimal sizing for BS.

6.5.1 Oversizing the renewable resources

As observed from the sensitivity analysis, the LCOE decreases exponentially with increase in the size of PV panels; due to the lower capital cost of PV panels compared to WECS. The LCOE decrement (13%) is significant only upto 30% increase in Pp beyond the optimal value and is shown using x_1 to x_2 in the zoomed-in window of Fig. 6.9a.

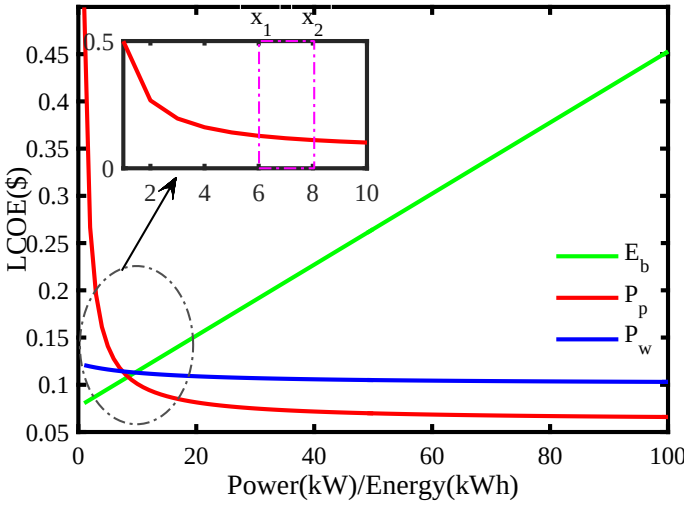

(a)

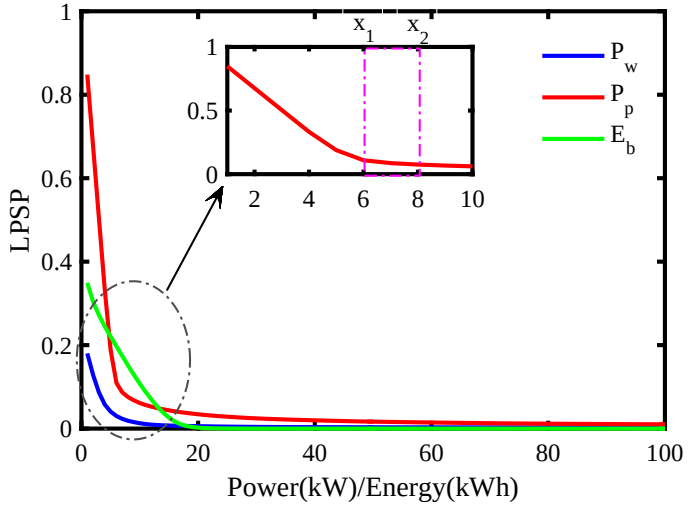

(b)

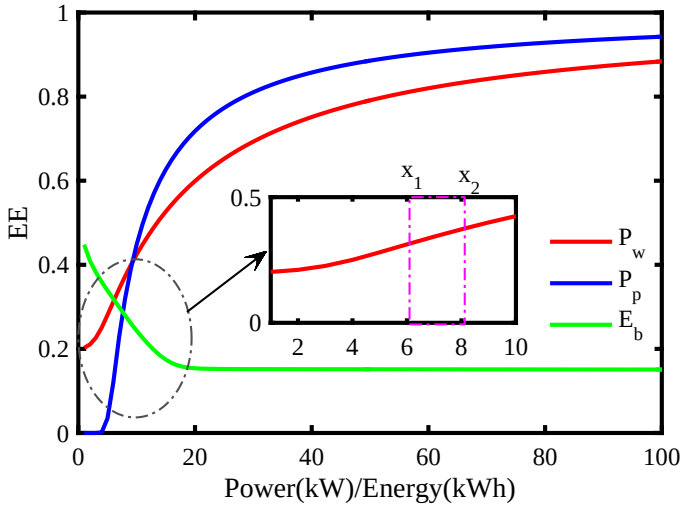

(c)

Figure 6.9: Effect on objective functions by the variation P_p, P_w and E_b (a) LCOE (b) LPSP (c) EE

At the same time, the LPSP index reduces by 14% which represents enhanced HRES reliability but the EE index increases from 0.21 to 0.39 indicating the increase in excess renewable energy and is presented in the zoomed-in window of Fig. 6.9b and 6.9c. Based on the detailed analysis presented in this chapter, upto 30% oversizing of PV panels above the optimal size without changing the rating of the converters would increase economic benefits and reliability. The solar irradiation is variable throughout the day and peak irradiation is available only for 1-2 hours/day, hence, the PV inverters can operate in non-MPPT mode during the excess energy generation which would allow maximum utilization of the converters and overall system.

6.6 Summary

The PV-wind HRES is proposed for off-grid telecom tower in remote/rural areas to provide reliable, economic, environment friendly, and higher resistance to disasters. The intermittent nature of solar irradiation is incorporated through Beta PDF and that of wind is modelled using Weibull PDF. The telecom traffic is modelled through LTE modelled and one year profile is generated. The detailed economic and reliability analysis is done to formulate three objectives viz. LCOE, LPSP and EE which are correlated and incommensurate. The EE is a index developed in the present chapter to keep check on the excess energy generation as surplus energy cannot be sold to the grid. The sensitivity analysis is performed to observe the effect of design parameter (A_p, C_w and ad) on the three objective functions. Thus, DMGWO is developed and implemented to find the trade-off among the three objective to find the optimal Pareto front. Also, the corrective algorithm is developed and embedded in the DMGWO to handle the discrete wind capacity variable. Each solution in the Pareto front is a non-dominated solution. The Pareto front provides a wide range to the telecom operator to choose the desired configuration of HRES. Here, euclidean distance is used for decision making to select the optimal configuration of PV-wind HRES. Also, based on the sensitivity analysis, the 30% oversizing of the PV panels is recommended such that maximum utilization of converter capacity is achieved with enhanced reliability and reduced cost of electricity generation.

Chapter 7

Energy management using virtual energy storage concept in PV-battery powered BS

7.1 Introduction

There is drastic growth in telecom traffic and multimedia communication which has resulted in increased energy demand by cellular networks. The load demand and carbon emissions of an individual telecom tower is not large in global terms. But the collective energy demand of more than 3 billion towers worldwide becomes considerable large energy demand contributing to 3% of the global energy consumption. Similarly, the telecom towers are responsible for more than 170 metric tons of global carbon emission. Therefore, environment-friendly HRES based BS power supply for remote/rural telecom towers is proposed in chapter 4 which is otherwise powered by conventional DGset based supply. Also, WECS and PV panels integration to BS supply architecture is achieved in the chapter 4. It is estimated that 15% more towers will be installed in the remote/rural areas. Therefore, energy efficiency has become one of the most significant requirements for future telecom industry. Thus, energy management of HRES supplied remote/rural telecom towers is proposed in this chapter to ensure high energy efficiency, reduced OPEX and enhanced reliability. Energy consumption optimization in a BS in-

cludes three approaches: energy optimization of the network and radio frequency connection, energy optimization of the site sheltering the BS, and optimization of energy consumption of BS. One way for energy optimization of the site sheltering the BS can be obtained by adopting distributed architecture. Another way is to optimally place the equipments near to each other which minimizes the losses in cable but the overall temperature of BS increases. Therefore, BS requires proper cooling to ensure the temperature within the limits as closely placed electronic equipment are sensitive to temperature rise. The distribution of power consumption averages of the various components of BSs is recapitulated in Fig. 7.1 [92]. Among all the components of BS, air conditioning consumes 17.5% of power. The power consumption in air conditioning is commonly reduced by the installation of additional elements. The additional elements which facilitate in lowering the operational temperature of BS are heat exchangers, membrane filters, and smart fans [98].

Unlike conventional power supply to telecom towers consisting grid and DGset, HRES supply is intermittent and random in nature due to dependence on weather and geographical location of site. Hence, the energy saving techniques implemented in conventional BS supply architecture could not be effective in the futuristic HRES supplied BS in remote/rural areas. The offline energy management techniques are effective when the renewable energy information is available ahead

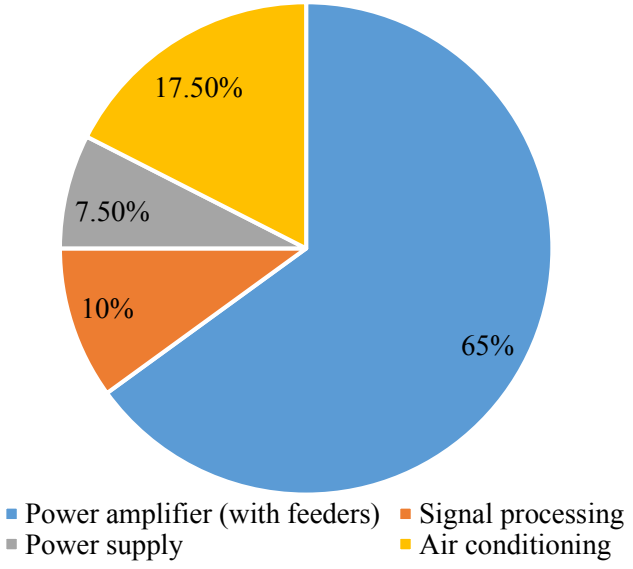

Figure 7.1: Distribution of power consumption in BS

of time. In real-time scenario, exact renewable energy profile determination in advance is difficult to acquire [123]. Therefore, energy management of HRES based BS power supply in the environment of time varying and random renewable energy is a critical issue .

Power consumption in the BS components is reduced by implementing the concept of DRM. In DRM algorithms, interruptible loads are shed based on market conditions and demand limits to modify the instantaneous power demand during periods of peak demand [99]. The interruptible load in BS are the air conditioners which are non critical load for BS with time constant above 30 minutes. In literature, the air conditioners are modelled as constant power loads operating at the rated power without any cycling or variations. However, air conditioners and refrigerators have a distinct cyclic turn on period and turn off period [104]. Therefore, in the present chapter, DRM concept is implemented by modelling the air conditioners as analogous to batteries to create VES. Similar to batteries, the VES also buffers the intermittency in the solar energy and enhances the reliability. The modelling of air conditioner does consider the cyclic turn on and off patterns along with the stochastic nature of the HRES. The VES based DRM enhances the life of BESS without installation of additional equipments to save energy in air conditioners.

The chapter is organized as follow: modelling of the air conditioner is presented in section 7.2 followed by VES based DRM algorithm for the PV-battery based BS power supply. Performance analysis of the proposed VES based DRM algorithm is demonstrated in section 7.4 and finally chapter is summarized in section 7.5.

7.2 PV-battery based BS power supply modelling

In the present chapter, the PV-battery based power supply for BS in remote/rural areas is considered. The BS architecture consists of non-critical loads which are lighting and air conditioner load. The PV panels are the main source of BS power supply with battery bank as back up supply to buffer the intermittency of the PV panels. Similar to the HRES based power supply architecture explained in the chapter 4, PV-battery based power supply in this chapter is integrated to the DC

bus using Cuk converter. The Cuk converter ensures the voltage regulation under source and load disturbances and POL converters ensures that all electronic load are supplied at the required voltage level. The centralized hierarchical control is implemented for the BS power supply which is low power rating, low voltage and high current supply (3.5kW, 48V bus voltage). The hierarchical control consists of three levels of control viz. primary, secondary and tertiary control. The local voltage and current flow is maintained within the set limits using switches and individual SMPC with each source and load. Further, secondary control is carried out by the Cuk converter which maintains the DC bus voltage and the voltage controller technique (intelligent hybrid controller) has already been proposed in the chapter 3 and 4. In this chapter the tertiary control which aims at optimizing the power consumption of the BS power supply architecture is proposed. The VES based algorithm is proposed which implements the DRM concept in the BS supply architecture in the environment of renewable resources.

The optimal configuration of the PV-battery BS power supply is obtained from the optimization technique proposed in chapter 6. The telecom traffic model presented in chapter 6, is used here to model the load of the telecom tower.

7.2.1 Air conditioner modelling

The batteries store energy in the form of chemical energy and amount of energy available is represented in terms of state of charge (SoC). Similarly, the air conditioner store thermal energy and represented in terms of kWh. The energy stored in batteries is dissipated through the internal resistance whereas in case of air conditioner, it is lost through heat gain from atmosphere. Hence, air conditioner are analogous to batteries as shown in Fig. 7.2. The BS load consists of one air conditioner of 1.2kW. The air conditioner is modelled with cyclic turn on and off pattern which maintains the room temperature (T_{room}) in the range 19-25^oC. Normally, the air conditioner is turned on for 15 minutes with power consumption of 1.2kW and turned off for next 45 minutes during that period there is no power consumption. The change in T_{room} due the effect of the outside (ambient) temperature (T_{out}) and the temperature of the air conditioner coil (T_{coil}) is given

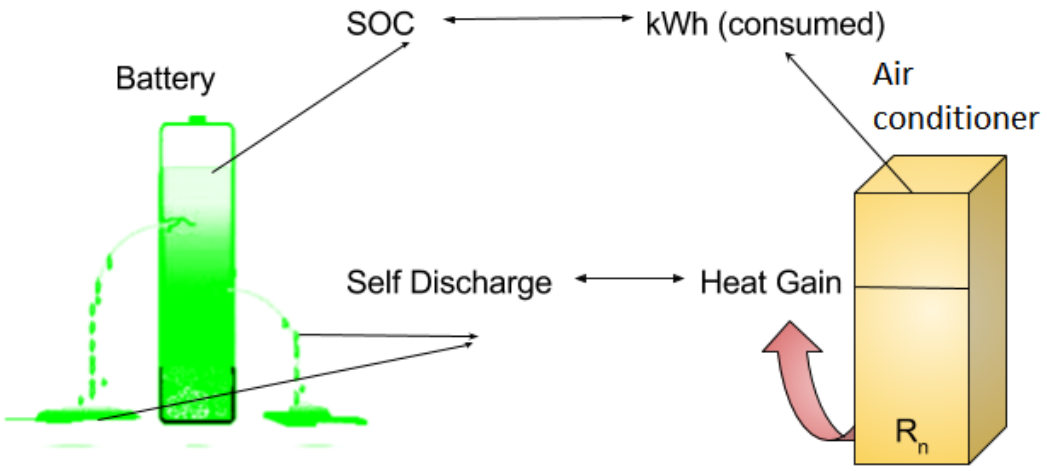

Figure 7.2: Analogy of air conditioner as electro-chemical battery

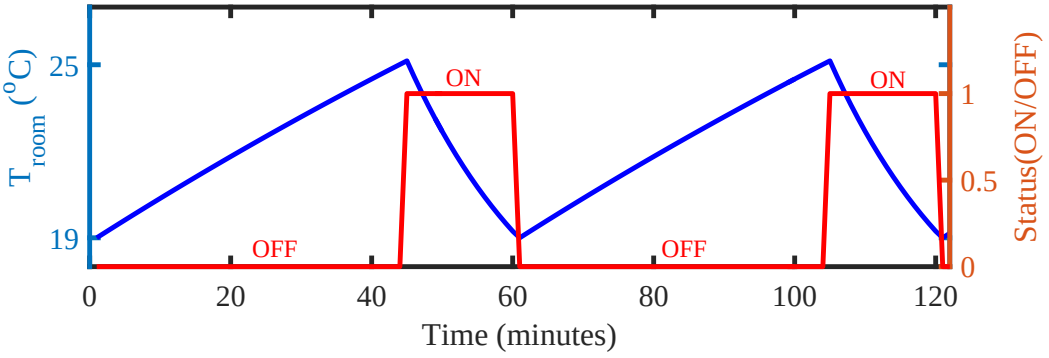

Figure 7.3: Room temperature profile with air conditioner

by

$$\frac{dT_{room}}{dt} = k(T_{out} - T_{room}) + k_{ac}(T_{coil} - Troom) \tag{7.1}$$

where, k and k_{ac} are positive constant called as cooling coefficient and cooling coefficient of air conditioner coil receptively. The Fig. 7.3 shows the change in T_{room} in accordance to (7.1). It is observed that air conditioner is turned on as soon as the T_{room} exceeds the upper limit i.e. 25^oC and automatically turned off when the lower limit i.e. 19^oC.

7.3 Virtual energy storage based energy management algorithm

In general, DRM algorithms sheds the interruptible loads based on market conditions and demand limits to modify the instantaneous power demand during periods of peak demand. The BS supply architecture is off-grid system with PV panels are primary sources and battery banks act as the back up supply. The required battery power to buffer the power deficit in PV power ($P_{P,t}$) and load demand ($P_{L,t}$) is calculated by

$$P_{b,t} = P_{L,t} - P_{P,t} \tag{7.2}$$

The proposed algorithm synchronizes the air conditioner load which is flexible with a time constant of 30 minutes, with that of the solar power generation. The algorithm allows air conditioners to turn on ($T_{on,t}$) for extended time when excess renewable power is present and extends the off period ($T_{off,t}$) during energy deficit hours. The upper ($T_{on,max}$) and lower ($T_{on,min}$) temperature limits of the room temperature are maintained by the algorithm. Considering the analogy of the air conditioner and battery, the air conditioner consumes 1.2kW which is equivalent to the battery charging process during turn on time duration. During the turn off period of the air conditioner, it is equivalent to discharging process of battery considering the 30 minutes time constant of the air conditioner. Therefore, a virtual storage capacity (VSC) is created by the air conditioner which stores electrical energy in the form of thermal energy. The process of achieving and utilizing the VSC (discharging and charging powers) is governed by the following equations and summarized in the flowchart shown in Fig. 7.4.

Priority values for turning off the air conditioner:

$$\sigma_{off,t} = 1 - \frac{T_{on,max} - T_{off,t}}{T_{on,max}} \tag{7.3}$$

where, $T_{on,t} \geq T_{on,max}$

Priority values for turning on the air conditioner:

$$\sigma_{on,t} = 1 - \frac{T_{off,max} - T_{off,t}}{T_{off,max}} \tag{7.4}$$

where, $T_{off,t} \geq T_{off,max}$

Virtual power that can be generated by switching off the appliances at any interval can be calculated as:

$$P_{vsc,t} = P_{ac} \quad \text{where,} T_{on,t} \geq T_{on,max} \tag{7.5}$$

Virtual power that can be consumed by switching on the appliances is calculated as:

$$P_{vsc,t} = 0 - P_{ac} \quad \text{where, } T_{off,t} \geq T_{off,max} \tag{7.6}$$

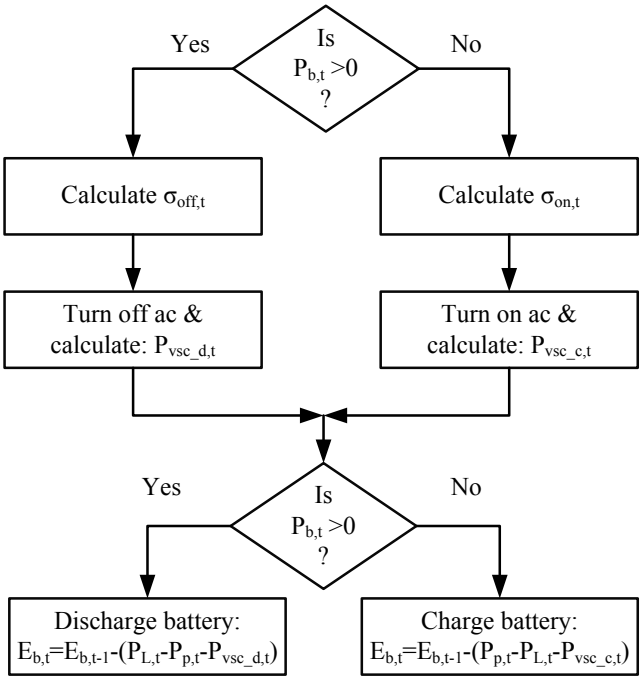

Figure 7.4: Priority-based strategic control for VES

7.4 Performance analysis of the virtual energy storage based energy management algorithm

A macrocell BS with peak load demand of 3.5kW is powered by PV panels and battery banks. The optimal configuration of PV panels and battery size for the BS power supply are $6.9kW_P$ and 400V, 15.1Ah respectively. The proposed VES based DRM algorithm is developed and implemented for PV-battery based BS power supply to analyze its performance. The time interval 't' is considered as 1 minute for the performance analysis. On a typical day PV power generation, load demand by the BS and the power deficit required from battery is shown in the Fig. 7.5. It is also observed that the excess renewable power is also available during the daytime after meeting the load demand. In the proposed VES based DRM algorithm, the operation of the air conditioner is synchronized with PV power generation. The impact of the proposed VES based power management algorithm on PV-battery based power supply is shown in Fig. 7.6 for a typical day. Strategically turning on the air conditioner allows utilization of excess renewable energy from 10:00 am to 4:00 pm. The negative sign of power due to virtual stored capacity ($P_{vsc,t}$) depicts the analogy of battery charging process as power is consumed by the air conditioner. When the air conditioner is strategically turned off during power deficit condition, which virtually generates $P_{vsc,t}$ which is shown by positive sign in the Fig. 7.6. The proposed VES based DRM algorithm doesn't change the frequency of switching, rather only changes the duration of turning on and off of the air conditioner. Hence, the proposed algorithm doesn't degrade the

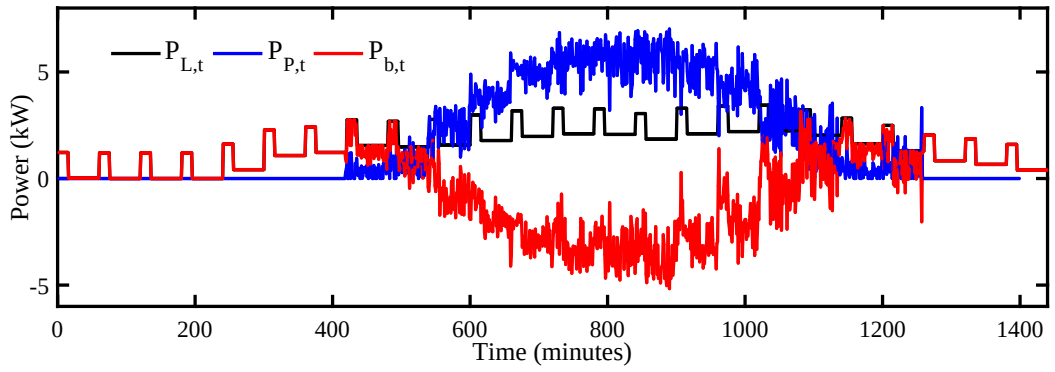

Figure 7.5: Load, PV power and power requirement on a typical day

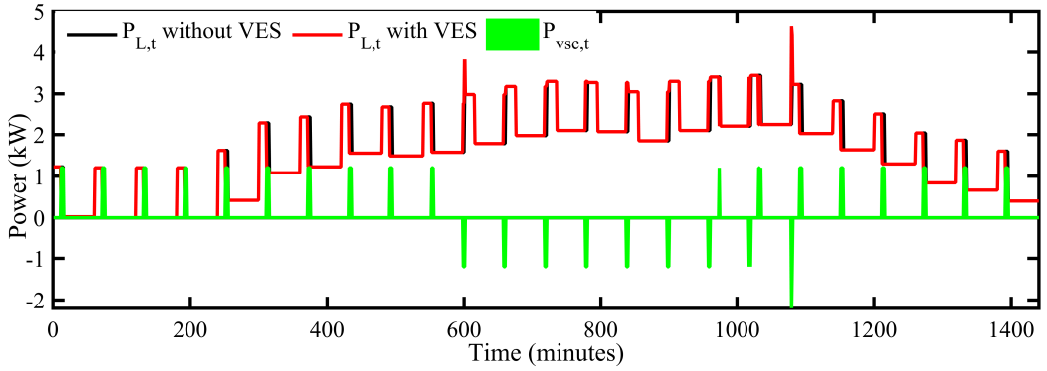

Figure 7.6: Impact of proposed controller on a typical day

Table 7.1: Configuration of PV-battery based BS power supply

	A_p	$ad(hours)$	$LCOE(\$)$	$LPSP$	EE
Without VES	24	6.8	0.1302	0.0832	0.197
With VES	24	6.8	0.1302	0.041	0.138

air conditioning system.

Further, the operation of the PV-battery based power supply with proposed VES based DRM algorithm is analyzed for one year. The strategically changing the turn on and off duration according to the VES based DRM algorithm improves the reliability of the overall system. The cost of electricity, reliability and excess energy generation are highly correlated for the renewable based off-grid power supplies as explained in previous chapter. To enhance the reliability, system tends to be oversized leading to increased LCOE due to higher capital cost and converter ratings. Also the oversized system has under utilized resources resulting in higher value for the excess energy generation index. Table 7.1 shows the that implementation of the energy management algorithm reduces the LPSP index accounting the reliability of the power supply to 0.041 from 0.0832 when the system is without the proposed algorithm. Also, the resource utilization has increased as excess energy index has decreased from the 0.197 to 0.138. Thus, the reliability of the renewable based off-grid power supply with proposed power management algorithm is enhanced by 50% in comparison to the system without energy management. At the same time, utilization of resources due to the implementation of the algorithm is increased by 30% with LCOE of \$0.1302.

7.5 Summary

The predicted expansion of the telecom towers in the remote/rural areas would lead to the installation of more renewable resource powered BS as initiative for 'green telecom towers'. The DRM concept prevailing in smart grids need to be introduced in the renewable powered BS to perform energy management. The DRM concept has been implemented using the air conditioning load of BS which has large time constant. An algorithm is proposed which considers the analogy of the air conditioners with battery charging and discharging process. The proposed algorithm considers the air conditioner as the virtual storage capacity due its thermal inertia and acts virtual energy storage. The VES based algorithm models cyclic turning on and off pattern of air conditioner. The VES based algorithm synchronizes the working of the air conditioners with that of excess renewable power generation similar to the DRM concept in the smart grids. Simulation studies are done to analyze the performance of the system with the implementation of the VES based DRM algorithm. It was observed that the proposed algorithm was capable of reducing the energy required from battery storage without changing the switching frequency of air conditioner. The VES based DRM algorithm has enhanced the reliability and utilization of resources without increment in the LOCE. Thus, utilizing the VES generated from the air conditioners partially level the intermittent output from renewable resource (PV panels).

Chapter 8

Conclusion and future scope

8.1 Conclusion

The issues in the conventional power supply for the BS on remote/rural areas is discussed. Thus, potential of alternative resources for the BS power supply in off-grid mode is explored. The PEMFC and HRES based power supplies are proposed which are environment friendly alternatives for the BS. However, the integration of these resources to the DC distribution bus pose challenge to voltage regulation of the DC distribution bus of the BS power supply architecture. Since, the terminal voltage of the fuel cell depends on the load and ambient conditions such as humidity, pressure and temperature therefore, boost converter based interfacing unit is proposed. Similarly, the terminal voltage of renewable resources is variable with changing ambient temperature and wind speed, the Cuk converter based interfacing unit is proposed. The Cuk converter allows the wide rang of operation of the renewable resource, ripple free input and output current and compactness in size. Since, the SMPC are time variant and non linear system with RHP zero, therefore, the open loop dynamic response of the SMPC is characterized by overshoots, multiple zero crossing and large settling time. Hence, the intelligent hybrid controller is proposed for SMPC based interfacing unit. The controller has inherited the best features of the linear and intelligent controllers. Like PID controllers, it is simple, inexpensive implementation, fairly robust performance and fixed frequency operation. It is known that designing the parameters for the continuous time model of

the converter would be best tuned. Meta-heuristic algorithms tune the parameters of PID considering the overall system in continuous time model, and incorporates the non-linearity, switching and time varying behavior of the converter. The trade-off among different performance specifications of the dynamic response of the interfacing converter with PID controller are satisfied by using improved objective function for the meta-heuristic techniques. Moreover, MARCGA is proposed for the intelligent hybrid controller with similarity check and enhanced diversity in the population. The performance of the MARCGA-assisted hybrid controller is compared with GA, PSO and GWO for input disturbance rejection, output disturbance rejection and reference tracking capability. A laboratory prototype of the interfacing converter is developed and the proposed intelligent hybrid controller performance is verified. Further, optimal sizing analysis is essential to find the configuration of renewable resources and battery storage for economic and reliable power supply. The multi-objective optimal sizing problem is formulated considering cost, reliability and excess energy generation as the objective functions. The renewable resources are modelled while considering the intermittent nature using the probability distribution function. The telecom load is also modelled to consider variability and randomness using poison's ratio. To make the HRES system modelling more practical, the capacity of WECS is taken as discrete variable. Thus, a multi-objective DMGWO algorithm is proposed which has an embedded corrective algorithm to handle discrete and continuous variable simultaneously. The system operation is analyzed for long term which considers the battery energy management algorithm. The performance of the optimal configuration so obtained is analyzed for different case scenarios through simulations. The sensitivity analysis is also performed to observe the effect of the decision variables on the three objective functions which are LCOE, LPSP and EE. Lastly, to enhance the energy efficiency of renewable supplied BS a VES based DRM algorithm is proposed. The proposed algorithm enhances the reliability of the system without additional cost and keeping the switching frequency of the air conditioners.

The major contributions of the thesis are following:

- The issues in the conventional telecom power supply are studied and detailed literature survey is carried for the different alternative resources and storage for the telecom power supply. Hence, a PV-wind based HRES having battery

bank as back-up is proposed for BS of telecom towers in remote/rural areas.

- Different SMPC are designed and implemented for voltage regulation of DC bus of the telecom power supply in the environment of renewable resources.

- Intelligent hybrid controller is developed for voltage regulation. Different meta-heuristic algorithm (GA, PSO, GWO and MARCGA) are implemented for the tuning of the PID parameters. MARCGA has been proposed with enhanced diversity in the population and high accuracy due to proposed similarity check introduced in the real coded genetic algorithm.

- The controller performance is validated under different test conditions (input an output disturbance rejection, reference tracking capability) through rigorous simulations.

- Laboratory prototype of the interfacing converter is developed and the performance of proposed intelligent hybrid controller is validated.

- The detailed economic and reliability analysis is done to formulate three objectives viz. LCOE, LPSP and EEG which are correlated and incommensurate. The EEG is a index developed to keep check on the excess energy generation as surplus energy cannot be sold to the grid.

- A multi-objective problem is formulated to obtain the optimal configuration of PV-wind based power supply to ensure economical, reliable and green operation of the off-grid telecom towers.

- The intermittent nature of solar irradiation is incorporated through Beta PDF and that of wind is modelled using Weibull PDF. The telecom traffic is modelled through LTE model and one year profile is generated.

- The corrective algorithm is developed and embedded in the DMGWO to handle the discrete wind capacity variable. DMGWO is implemented to find the optimal Pareto front which provides wide range of solution to the telecom operator to choose the desired configuration of HRES.

- The sensitivity analysis is performed to observe the effect of design parameter (A_p, C_w and ad) on the three objective functions. It supports the choice of multi-objective optimal sizing problem formulation.

8.2 Future scope

In this thesis, the renewable based topology of BS power supply is proposed for the off-grid towers. The renewable based power supply can be extended for bad grid towers (grid connected towers having power outages more than 8 hours). The optimal sizing problem formulation proposed in this thesis can be redrafted for bidirectional flow of the power to the grid.

The VES based DRM algorithm for energy management is implemented for the PV-battery system which has enhanced the reliability of the system. The extension of the proposed energy management scheme in this thesis to the PV-wind-battery system would give scope for the future work.

Bibliography

[1] D. Feng, C. Jiang, G. Lim, L. J. Cimini, G. Feng, and G. Y. Li, "A survey of energy-efficient wireless communications," *IEEE Communications Surveys Tutorials*, vol. 15, no. 1, pp. 167–178, 2013.

[2] H. Smertnik *et al.*, "Green power for mobile bi-annual report," *GSM Association, August*, 2014.

[3] M. H. Alsharif, J. Kim, and J. H. Kim, "Green and sustainable cellular base stations: An overview and future research directions," *Energies*, vol. 10, no. 5, p. 587, 2017.

[4] V. Chamola and B. Sikdar, "Solar powered cellular base stations: current scenario, issues and proposed solutions," *IEEE Communications Magazine*, vol. 54, no. 5, pp. 108–114, May 2016.

[5] Digital india-power to empower. [Online]. Available: http://digitalindia.gov.in/content/about-programme

[6] D. of Telecommunications. (2012) National telecom policy - 2012. [Online]. Available: http://www.trai.gov.in/WriteReadData/userfiles/file/NTP2012.pdf

[7] G. Auer, V. Giannini, C. Desset, I. Godor, P. Skillermark, M. Olsson, M. A. Imran, D. Sabella, M. J. Gonzalez, O. Blume, and A. Fehske, "How much energy is needed to run a wireless network?" *IEEE Wireless Communications*, vol. 18, no. 5, pp. 40–49, 2011.

[8] M. Deruyck, W. Joseph, and L. Martens, "Power consumption model for macrocell and microcell base stations," *Transactions on Emerging Telecommunications Technologies*, vol. 25, no. 3, pp. 320–333, 2014.

[9] M. Fraisse and L. Buchsbaum, "Environment friendly high quality, high availability telecom power plant architecture," in *Proceedings of IEEE 24th Annual International Telecommunications Energy Conference (INTELEC)*, 2002, pp. 463–469.

[10] O. C. Onar, O. H. A. Shirazi, and A. Khaligh, "Grid interaction operation of a telecommunications power system with a novel topology for multiple-input buck-boost converter," *IEEE Transactions on Power Delivery*, vol. 25, no. 4, pp. 2633–2645, 2010.

[11] W. Allen and S. V. Natale, "Achieving ultra-high system availability in a battery-less -48v dc power plant," in *Proceedings of IEEE 24th Annual International Telecommunications Energy Conference (INTELEC)*, 2002, pp. 287–294.

[12] M. Trifkovic, M. Sheikhzadeh, K. Nigim, and P. Daoutidis, "Modeling and control of a renewable hybrid energy system with hydrogen storage," *IEEE Transactions on Control Systems Technology*, vol. 22, no. 1, pp. 169–179, 2014.

[13] T. Han and N. Ansari, "Powering mobile networks with green energy," *IEEE Wireless Communications*, vol. 21, no. 1, pp. 90–96, 2014.

[14] Central electricity authority of india. [Online]. Available: http://www.cea.nic.in/

[15] Microtuines: A distruptive technology. [Online]. Available: http://www.retailenergy.com/articles/microturbines.htm

[16] J. Hag and D. Bernstein, "Nonminimum-phase zeros-much to do about nothing-classical control-revisited part ii," *IEEE Control Systems Magazine*, vol. 3, no. 27, pp. 45–57, 2007.

[17] A. Balestrino, D. Corsanini, A. Landi, and L. Sani, "Circle-based criteria for performance evaluation of controlled dc–dc switching converters," *IEEE Transactions on Industrial Electronics*, vol. 53, no. 6, pp. 1862–1869, 2006.

[18] O. C. Onar, O. H. A. Shirazi, and A. Khaligh, "Grid interaction operation of a telecommunications power system with a novel topology for multiple-input

buck-boost converter," *IEEE Transactions on Power Delivery*, vol. 25, no. 4, pp. 2633–2645, Oct 2010.

[19] A. Payman, S. Pierfederici, and F. Meibody-Tabar, "Energy control of supercapacitor/fuel cell hybrid power source," *Energy conversion and management*, vol. 49, no. 6, pp. 1637–1644, 2008.

[20] A. Massardo, C. Mcdonald, and T. Korakianitis, "Microturbine/fuel-cell coupling for high-efficiency electrical-power generation," *Journal of engineering for gas turbines and power*, vol. 124, no. 1, pp. 110–116, 2002.

[21] K. Rajashekara, "Hybrid fuel-cell strategies for clean power generation," *IEEE Transactions on Industry Applications*, vol. 41, no. 3, pp. 682–689, May 2005.

[22] M. L. Perry and S. Kotso, "A back-up power solution with no batteries," in *Proceedings of IEEE 26th Annual International Telecommunications Energy Conference (INTELEC)*, Sept 2004, pp. 210–217.

[23] H. Wen and B. Su, "Hybrid-mode interleaved boost converter design for fuel cell electric vehicles," *Energy conversion and management*, vol. 122, pp. 477–487, 2016.

[24] M. F. Serincan, "Reliability considerations of a fuel cell backup power system for telecom applications," *Journal of Power Sources*, vol. 309, pp. 66–75, 2016.

[25] D. Scamman, M. Newborough, and H. Bustamante, "Hybrid hydrogen-battery systems for renewable off-grid telecom power," *International Journal of Hydrogen Energy*, vol. 40, no. 40, pp. 13 876–13 887, 2015.

[26] D. of telecommunication, "Annual report 2014-15," New Delhi, Tech. Rep. [Online]. Available: http://www.dot.gov.in/sites/default/files/u10/EnglishAR2015.pdf

[27] S. Liu, R. Dougal, and E. Solodovnik, "Design of autonomous photovoltaic power plant for telecommunication relay station," *IEE Proceedings-Generation, Transmission and Distribution*, vol. 152, no. 6, pp. 745–754, 2005.

[28] A. S. Satpathy, N. K. Kishore, D. Kastha, and N. C. Sahoo, "Control scheme for a stand-alone wind energy conversion system," *IEEE Transactions on Energy Conversion*, vol. 29, no. 2, pp. 418–425, June 2014.

[29] J. Kaldellis and I. Ninou, "Energy balance analysis of combined photovoltaic–diesel powered telecommunication stations," *International Journal of Electrical Power & Energy Systems*, vol. 33, no. 10, pp. 1739–1749, 2011.

[30] P. Nema, S. Rangnekar, and R. K. Nema, "Pre-feasibility study of pv-solar/ wind hybrid energy system for gsm type mobile telephony base station in central india," in *Proceedings of 2nd International Conference on Computer and Automation Engineering (ICCAE)*, vol. 5, Feb 2010, pp. 152–156.

[31] M. A. Johnson and P. D. Smith, "Eco priority source dc micro-grids in telecom sites," in *Proceedings of IEEE First International Conference on DC Microgrids (ICDCM)*, June 2015, pp. 165–170.

[32] M. Zahran, A. Dmowski, B. Kras, P. Biczel, and J. Drazkiewicz, "Pv battery wind-turbine public-grid hybrid power supply for telecom.-equipment, system management and control," in *Collection of Technical Papers. 35th Intersociety Energy Conversion Engineering Conference and Exhibit (IECEC) (Cat. No.00CH37022)*, 2000, pp. 1252–1260 vol.2.

[33] A. Balestrino, D. Corsanini, A. Landi, and L. Sani, "Circle-Based Criteria for Performance Evaluation of Controlled DC–DC Switching Converters," *IEEE Transactions on Industrial Electronics*, vol. 53, no. 6, pp. 1862–1869, 2006.

[34] P. García, C. A. García, L. M. Fernández, F. Llorens, and F. Jurado, "ANFIS-Based control of a grid-connected hybrid system integrating renewable energies, hydrogen and batteries," *IEEE Transactions on Industrial Informatics*, vol. 10, no. 2, pp. 1107–1117, 2014.

[35] M. Taghvaee, M. Radzi, S. Moosavain, H. Hizam, and M. H. Marhaban, "A current and future study on non-isolated dc–dc converters for photovoltaic applications," *Renewable and sustainable energy reviews*, vol. 17, pp. 216–227, 2013.

[36] S. B. Kjaer, J. K. Pedersen, and F. Blaabjerg, "A review of single-phase grid-connected inverters for photovoltaic modules," *IEEE transactions on industry applications*, vol. 41, no. 5, pp. 1292–1306, 2005.

[37] D. M. Sable, B. H. Cho, and R. B. Ridley, "Use of leading-edge modulation to transform boost and flyback converters into minimum-phase-zero systems," *Power Electronics, IEEE Transactions on*, vol. 6, no. 4, pp. 704–711, 1991.

[38] P. Cominos and N. Munro, "Pid controllers: recent tuning methods and design to specification," *IEE Proceedings-Control Theory and Applications*, vol. 149, no. 1, pp. 46–53, 2002.

[39] L. Guo, J. Y. Hung, and R. Nelms, "Digital controller design for buck and boost converters using root locus techniques," in *Industrial Electronics Society, 2003. IECON'03. The 29th Annual Conference of the IEEE*, vol. 2. IEEE, 2003, pp. 1864–1869.

[40] A. Balestrino, D. Corsanini, A. Landi, and L. Sani, "Circle-based criteria for performance evaluation of controlled dc–dc switching converters," *Industrial Electronics, IEEE Transactions on*, vol. 53, no. 6, pp. 1862–1869, 2006.

[41] J. Y. Hung, W. Gao, and J. C. Hung, "Variable structure control: a survey," *Industrial Electronics, IEEE Transactions on*, vol. 40, no. 1, pp. 2–22, 1993.

[42] E. Figueres, G. Garcerá, J. M. Benavent, M. Pascual, J. Martínez *et al.*, "Adaptive two-loop voltage-mode control of dc-dc switching converters," *Industrial Electronics, IEEE Transactions on*, vol. 53, no. 1, pp. 239–253, 2006.

[43] R. Middlebrook and S. Cuk, "A general unified approach to modelling switching-converter power stages," in *Power Electronics Specialists Conference, 1970 IEEE*. IEEE, 1970, pp. 18–34.

[44] V. Vorpérian, "Simplified analysis of pwm converters using model of pwm switch. ii. discontinuous conduction mode," *Aerospace and Electronic Systems, IEEE Transactions on*, vol. 26, no. 3, pp. 497–505, 1990.

[45] V. Canalli, J. Cobos, J. Oliver, and J. Uceda, "Behavioral large signal averaged model for dc/dc switching power converters," in *Power Electronics*

Specialists Conference, 1996. PESC'96 Record., 27th Annual IEEE, vol. 2. IEEE, 1996, pp. 1675–1681.

[46] R. W. Erickson, S. Cuk, and R. D. Middlebrook, "Large-signal modeling and analysis of switching regulators," in *IEEE power electronics specialists conference records*, 1982, pp. 240–250.

[47] R. W. Erickson and D. Maksimovic, *Fundamentals of power electronics*. Springer Science & Business Media, 2007.

[48] Y.-F. Liu and P. C. Sen, "A general unified large signal model for current programmed dc-to-dc converters," *Power Electronics, IEEE Transactions on*, vol. 9, no. 4, pp. 414–424, 1994.

[49] R. Middlebrook, "Small-signal modeling of pulse-width modulated switched-mode power converters," *Proceedings of the IEEE*, vol. 76, no. 4, pp. 343–354, 1988.

[50] S. Bibian and H. Jin, "High performance predictive dead-beat digital controller for dc power supplies," *IEEE Transactions on Power Electronics*, vol. 17, no. 3, pp. 420–427, 2002.

[51] J. Chen, A. Prodic, R. W. Erickson, and D. Maksimovic, "Predictive digital current programmed control," *IEEE Transactions on Power Electronics*, vol. 18, no. 1, pp. 411–419, 2003.

[52] G. C. Verghese, C. Bruzos, K. N. Mahabir *et al.*, "Averaged and sampled-data models for current mode control: a re-examination," in *Power Electronics Specialists Conference, 1989. PESC'89 Record., 20th Annual IEEE*. IEEE, 1989, pp. 484–491.

[53] K. Ogata and Y. Yang, *Modern control engineering*. Prentice-Hall Englewood Cliffs, NJ, 1970.

[54] W.-C. Wu, R. M. Bass, and J. R. Yeargan, "Eliminating the effects of the right-half plane zero in fixed frequency boost converters," in *Power Electronics Specialists Conference, 1998. PESC 98 Record. 29th Annual IEEE*, vol. 1. IEEE, 1998, pp. 362–366.

[55] Y. T. Chang and Y. S. Lai, "Online parameter tuning technique for predictive current-mode control operating in boundary conduction mode," *IEEE Transactions on Industrial Electronics*, vol. 56, no. 8, pp. 3214–3221, 2009.

[56] F. Himmelstoss, J. W. Kolar, F. C. Zach *et al.*, "Analysis of a smith-predictor-based-control concept eliminating the right-half plane zero of continuous mode boost and buck-boost dc/dc converters," in *Industrial Electronics, Control and Instrumentation, 1991. Proceedings. IECON'91., 1991 International Conference on.* IEEE, 1991, pp. 423–428.

[57] I. D. Nanov, "Large signal analysis of switching regulators employing adaptive gain current injected control," *Industrial Electronics, IEEE Transactions on*, vol. 41, no. 3, pp. 339–343, 1994.

[58] Z.-Y. Zhao, M. Tomizuka, and S. Isaka, "Fuzzy gain scheduling of pid controllers," in *Control Applications, 1992., First IEEE Conference on.* IEEE, 1992, pp. 698–703.

[59] M. Elmore and V. Skormin, "Adaptive model following control of switching regulators," in *Industry Applications Conference, 2003. 38th IAS Annual Meeting. Conference Record of the*, vol. 3. IEEE, 2003, pp. 1750–1757.

[60] P. Mattavelli, L. Rossetto, G. Spiazzi, and P. Tenti, "General-purpose sliding-mode controller for dc/dc converter applications," in *Power Electronics Specialists Conference, 1993. PESC'93 Record., 24th Annual IEEE.* IEEE, 1993, pp. 609–615.

[61] P. Mattavelli, L. Rossetto, and G. Spiazzi, "Small-signal analysis of dc-dc converters with sliding mode control," *Power Electronics, IEEE Transactions on*, vol. 12, no. 1, pp. 96–102, 1997.

[62] V. Raviraj and P. C. Sen, "Comparative study of proportional-integral, sliding mode, and fuzzy logic controllers for power converters," *IEEE Transactions on Industry Applications*, vol. 33, no. 2, pp. 518–524, 1997.

[63] R. Naim, G. Weiss, and S. Ben-Yaakov, "H control applied to boost power converters," *Power Electronics, IEEE Transactions on*, vol. 12, no. 4, pp. 677–683, 1997.

[64] E. Vidal-Idiarte, L. Martinez-Salamero, H. Valderrama-Blavi, F. Guinjoan, and J. Maixe, "Analysis and design of h control of nonminimum phase-switching converters," *Circuits and Systems I: Fundamental Theory and Applications, IEEE Transactions on*, vol. 50, no. 10, pp. 1316–1323, 2003.

[65] A. Balestrino, A. Landi, and L. Sani, "Cuk converter global control via fuzzy logic and scaling factors," *Industry Applications, IEEE Transactions on*, vol. 38, no. 2, pp. 406–413, 2002.

[66] T. Gupta, R. Boudreaux, R. Nelms, and J. Y. Hung, "Implementation of a fuzzy controller for dc-dc converters using an inexpensive 8-b microcontroller," *Industrial Electronics, IEEE Transactions on*, vol. 44, no. 5, pp. 661–669, 1997.

[67] W.-C. So, C. K. Tse, and Y.-S. Lee, "Development of a fuzzy logic controller for dc/dc converters: design, computer simulation, and experimental evaluation," *Power Electronics, IEEE Transactions on*, vol. 11, no. 1, pp. 24–32, 1996.

[68] K. Viswanathan, D. Srinivasan, and R. Oruganti, "A universal fuzzy controller for a non-linear power electronic converter," in *Fuzzy Systems, 2002. FUZZ-IEEE'02. Proceedings of the 2002 IEEE International Conference on*, vol. 1. IEEE, 2002, pp. 46–51.

[69] J. H. Holland, "Genetic algorithms," *Scientific american*, vol. 267, no. 1, pp. 66–72, 1992.

[70] C. Akachukwu, A. Aibinu, M. Nwohu, and B. Salau, "A decade survey of engineering applications of genetic algorithm in power system optimization," in *Fifth international conference on intelligent systems, modelling and simulation*, 2014, pp. 38–42.

[71] I. BoussaïD, J. Lepagnot, and P. Siarry, "A survey on optimization metaheuristics," *Information Sciences*, vol. 237, pp. 82–117, 2013.

[72] S. E. De León-Aldaco, H. Calleja, and J. A. Alquicira, "Metaheuristic optimization methods applied to power converters: A review," *IEEE Transactions on Power Electronics*, vol. 30, no. 12, pp. 6791–6803, 2015.

[73] J. Fermeiro, J. Pombo, M. Calado, and S. Mariano, "Evaluation of a particle swarm optimization controller for dc-dc boost converters," in *Compatibility and Power Electronics (CPE), 2015 9th International Conference on*. IEEE, 2015, pp. 179–184.

[74] K. Sundareswaran, S. Sankar, and P. S. R. Nayak, "Feedback controller design for a buck-boost converter through evolutionary algorithms," in *Power Electronics, Drives and Energy Systems (PEDES), 2012 IEEE International Conference on*. IEEE, 2012, pp. 1–7.

[75] K. Sundareswaran and V. Sreedevi, "Boost converter controller design using queen-bee-assisted ga," *IEEE Transactions on industrial electronics*, vol. 3, no. 56, pp. 778–783, 2009.

[76] X. Li, M. Chen, and Y. Tsutomu, "A method of searching pid controller's optimized coefficients for buck converter using particle swarm optimization," in *2013 IEEE 10th International Conference on Power Electronics and Drive Systems (PEDS),*. IEEE, 2013, pp. 238–243.

[77] O. Altinoz and H. Erdem, "Evaluation function comparison of particle swarm optimization for buck converter," in *International Symposium on Power Electronics Electrical Drives Automation and Motion (SPEEDAM), 2010*. IEEE, 2010, pp. 798–802.

[78] T. Han and N. Ansari, "On optimizing green energy utilization for cellular networks with hybrid energy supplies," *IEEE Transactions on Wireless Communications*, vol. 12, no. 8, pp. 3872–3882, 2013.

[79] B. Zhou, D. Xu, C. Li, Y. Cao, K. W. Chan, Y. Xu, and M. Cao, "Multi-objective generation portfolio of hybrid energy generating station for mobile emergency power supplies," *IEEE Transactions on Smart Grid*, 2017.

[80] S. Singh and S. C. Kaushik, "Optimal sizing of grid integrated hybrid pv-biomass energy system using artificial bee colony algorithm," *IET Renewable Power Generation*, vol. 10, no. 5, pp. 642–650, 2016.

[81] H. Yang, W. Zhou, L. Lu, and Z. Fang, "Optimal sizing method for stand-alone hybrid solar–wind system with lpsp technology by using genetic algorithm," *Solar energy*, vol. 82, no. 4, pp. 354–367, 2008.

[82] Y.-Y. Hong and R.-C. Lian, "Optimal sizing of hybrid wind/pv/diesel generation in a stand-alone power system using markov-based genetic algorithm," *IEEE Transactions on Power Delivery*, vol. 27, no. 2, pp. 640–647, 2012.

[83] S. Salinas, M. Li, and P. Li, "Multi-objective optimal energy consumption scheduling in smart grids," *IEEE Transactions on Smart Grid*, vol. 4, no. 1, pp. 341–348, 2013.

[84] P. P. Vergara, J. M. Rey, L. C. P. da Silva, and G. Ordóñez, "Comparative analysis of design criteria for hybrid photovoltaic/wind/battery systems," *IET Renewable Power Generation*, vol. 11, no. 3, pp. 253–261, 2016.

[85] M. B. Shadmand and R. S. Balog, "Multi-objective optimization and design of photovoltaic-wind hybrid system for community smart dc microgrid," *IEEE Transactions on Smart Grid*, vol. 5, no. 5, pp. 2635–2643, 2014.

[86] R. Atia and N. Yamada, "Sizing and analysis of renewable energy and battery systems in residential microgrids," *IEEE Transactions on Smart Grid*, vol. 7, no. 3, pp. 1204–1213, 2016.

[87] M. Bhuiyan and M. A. Asgar, "Sizing of a stand-alone photovoltaic power system at dhaka," *Renewable Energy*, vol. 28, no. 6, pp. 929–938, 2003.

[88] P. Nikhil and D. Subhakar, "Sizing and parametric analysis of a stand-alone photovoltaic power plant," *IEEE journal of photovoltaics*, vol. 3, no. 2, pp. 776–784, 2013.

[89] H. Borhanazad, S. Mekhilef, V. G. Ganapathy, M. Modiri-Delshad, and A. Mirtaheri, "Optimization of micro-grid system using mopso," *Renewable Energy*, vol. 71, pp. 295–306, 2014.

[90] L. Wang and C. Singh, "Multicriteria design of hybrid power generation systems based on a modified particle swarm optimization algorithm," *IEEE Transactions on Energy Conversion*, vol. 24, no. 1, pp. 163–172, 2009.

[91] K. Deb, A. Pratap, S. Agarwal, and T. Meyarivan, "A fast and elitist multiobjective genetic algorithm: Nsga-ii," *IEEE Transactions on Evolutionary Computation*, vol. 6, no. 2, pp. 182–197, Apr 2002.

[92] A. Ayang, P.-S. Ngohe-Ekam, B. Videme, and J. Temga, "Power consumption: Base stations of telecommunication in sahel zone of cameroon: Typology based on the power consumptionmodel and energy savings," *Journal of Energy*, vol. 2016, 2016.

[93] A. Conte, A. Feki, L. Chiaraviglio, D. Ciullo, M. Meo, and M. A. Marsan, "Cell wilting and blossoming for energy efficiency," *IEEE Wireless Communications*, vol. 18, no. 5, 2011.

[94] O. Blume, H. Eckhardt, S. Klein, E. Kuehn, and W. M. Wajda, "Energy savings in mobile networks based on adaptation to traffic statistics," *Bell Labs Technical Journal*, vol. 15, no. 2, pp. 77–94, 2010.

[95] M. Etoh, T. Ohya, and Y. Nakayama, "Energy consumption issues on mobile network systems," in *Applications and the Internet, 2008. SAINT 2008. International Symposium on.* IEEE, 2008, pp. 365–368.

[96] A. Ayang, P.-S. Ngohe-Ekam, B. Videme, and J. Temga, "Power consumption: Base stations of telecommunication in sahel zone of cameroon: Typology based on the power consumptionmodel and energy savings," *Journal of Energy*, vol. 2016, 2016.

[97] S. Zoican, "The role of programmable digital signal processors (dsp) for 3 g mobile communication systems," *ACTA Tech. Napoc*, vol. 49, pp. 49–56, 2008.

[98] S. N. Roy, "Energy logic: A road map to reducing energy consumption in telecom munications networks," in *Proceedings of 2008 IEEE 30th International Telecommunications Energy Conference (INTELEC)*, Sept 2008, pp. 1–9.

[99] P. Yi, X. Dong, A. Iwayemi, C. Zhou, and S. Li, "Real-time opportunistic scheduling for residential demand response," *IEEE Transactions on smart grid*, vol. 4, no. 1, pp. 227–234, 2013.

[100] S. A. Husen, A. Pandharipande, L. Tolhuizen, Y. Wang, and M. Zhao, "Lighting systems control for demand response," in *Innovative Smart Grid Technologies (ISGT), 2012 IEEE PES.* IEEE, 2012, pp. 1–6.

[101] M. Pipattanasomporn, M. Kuzlu, and S. Rahman, "An algorithm for intelligent home energy management and demand response analysis," *IEEE Transactions on Smart Grid*, vol. 3, no. 4, pp. 2166–2173, 2012.

[102] G. Hug-Glanzmann, "A hybrid approach to balance the variability and intermittency of renewable generation," in *PowerTech, 2011 IEEE Trondheim*. IEEE, 2011, pp. 1–8.

[103] R. Wang, P. Wang, G. Xiao, and S. Gong, "Power demand and supply management in microgrids with uncertainties of renewable energies," *International Journal of Electrical Power & Energy Systems*, vol. 63, pp. 260–269, 2014.

[104] M. Pipattanasomporn, M. Kuzlu, S. Rahman, and Y. Teklu, "Load profiles of selected major household appliances and their demand response opportunities," *IEEE Transactions on Smart Grid*, vol. 5, no. 2, pp. 742–750, 2014.

[105] N. K. Kandasamy, K. J. Tseng, and S. Boon-Hee, "Virtual storage capacity using demand response management to overcome intermittency of solar pv generation," *IET Renewable Power Generation*, vol. 11, no. 14, pp. 1741–1748, 2017.

[106] D. Wang, K. Meng, X. Gao, J. Qiu, L. L. Lai, and Z. Dong, "Coordinated dispatch of virtual energy storage systems in lv grids for voltage regulation," *IEEE Transactions on Industrial Informatics*, 2017.

[107] K. Meng, Z. Y. Dong, Z. Xu, Y. Zheng, and D. J. Hill, "Coordinated dispatch of virtual energy storage systems in smart distribution networks for loading management," *IEEE Transactions on Systems, Man, and Cybernetics: Systems*, 2017.

[108] Z. Sun, N. Wang, Y. Bi, and D. Srinivasan, "Parameter identification of pemfc model based on hybrid adaptive differential evolution algorithm," *Energy*, vol. 90, pp. 1334–1341, 2015.

[109] U. K. Chakraborty, T. E. Abbott, and S. K. Das, "Pem fuel cell modeling using differential evolution," *Energy*, vol. 40, no. 1, pp. 387–399, 2012.

[110] P. García, C. A. García, L. M. Fernández, F. Llorens, and F. Jurado, "Anfis-based control of a grid-connected hybrid system integrating renewable energies, hydrogen and batteries," *IEEE Transactions on Industrial Informatics*, vol. 10, no. 2, pp. 1107–1117, 2014.

[111] J. Chen, A. Prodic, R. W. Erickson, and D. Maksimovic, "Predictive digital current programmed control," *IEEE Transactions on Power Electronics*, vol. 18, no. 1, pp. 411–419, 2003.

[112] S. E. De León-Aldaco, H. Calleja, and J. A. Alquicira, "Metaheuristic optimization methods applied to power converters: A review," *IEEE Transactions on Power Electronics*, vol. 30, no. 12, pp. 6791–6803, 2015.

[113] D. H. Wolpert and W. G. Macready, "No free lunch theorems for optimization," *IEEE transactions on evolutionary computation*, vol. 1, no. 1, pp. 67–82, 1997.

[114] R. L. Haupt and S. E. Haupt, *Practical genetic algorithms*. John Wiley & Sons, 2004.

[115] B. K. Sahu, S. Pati, and S. Panda, "Hybrid differential evolution particle swarm optimisation optimised fuzzy proportional–integral derivative controller for automatic generation control of interconnected power system," *IET Generation, Transmission & Distribution*, vol. 8, no. 11, pp. 1789–1800, 2014.

[116] S. Mirjalili, S. Saremi, S. M. Mirjalili, and L. d. S. Coelho, "Multi-objective grey wolf optimizer: a novel algorithm for multi-criterion optimization," *Expert Systems with Applications*, vol. 47, pp. 106–119, 2016.

[117] J. Kaldellis, D. Zafirakis, and E. Kondili, "Energy pay-back period analysis of stand-alone photovoltaic systems," *Renewable Energy*, vol. 35, no. 7, pp. 1444–1454, 2010.

[118] P. Yang and A. Nehorai, "Joint optimization of hybrid energy storage and generation capacity with renewable energy," *IEEE Transactions on Smart Grid*, vol. 5, no. 4, pp. 1566–1574, 2014.

[119] Nsrdb - the national solar radiation database. [Online]. Available: https://maps.nrel.gov/nsrdb-viewer/

[120] V. Chamola and B. Sikdar, "A multistate markov model for dimensioning solar powered cellular base stations," *IEEE Transactions on Sustainable Energy*, vol. 6, no. 4, pp. 1650–1652, 2015.

[121] M. R. Singaravel and S. A. Daniel, "Studies on battery storage requirement of pv fed wind-driven induction generators," *Energy conversion and management*, vol. 67, pp. 34–43, 2013.

[122] S. Mirjalili, S. Saremi, S. M. Mirjalili, and L. d. S. Coelho, "Multi-objective grey wolf optimizer: a novel algorithm for multi-criterion optimization," *Expert Systems with Applications*, vol. 47, pp. 106–119, 2016.

[123] M. Sheng, D. Zhai, X. Wang, Y. Li, Y. Shi, and J. Li, "Intelligent energy and traffic coordination for green cellular networks with hybrid energy supply," *IEEE Transactions on Vehicular Technology*, vol. 66, no. 2, pp. 1631–1646, 2017.

List of Publications

Journal Publications

1. Rajvir Kaur, et.al.,"A novel proton exchange membrane fuel cell based power conversion system for telecom supply with genetic algorithm assisted intelligent interfacing converter." Energy conversion and management 136 (2017): 173-183.

2. Rajvir Kaur, Vijayakumar Krishnasamy, and Nandha Kumar Kandasamy. "Optimal sizing of windPV-based DC microgrid for telecom power supply in remote areas." IET Renewable Power Generation 12, no. 7: 859-866.

3. Rajvir Kaur, Vijayakumar K, Nandha Kumar Kandasamy, and Saurabh Kumar. "Discrete multi-objective grey wolf algorithm based optimal sizing and sensitivity analysis of PV-wind energy system for remote/rural telecom towers." IEEE Systems Journal. [Under Review]

4. Rajvir Kaur, Vijayakumar K, and Periasamy C. "Performance enhancement of intelligent hybrid power conversion controller for fuel cell powered standalone telecom loads." International Journal of Electrical Power and Energy Systems. [Submitted]

International Conference Publications

1. Rajvir Kaur, Saurabh Kumar, Vijayakumar K. "Artificial intelligence based controller for PV-based telecom power supply." International Conference cum Exhibition on renewable and sustainable energy (ICRSE 2017), Coimbatore, 2017.